

**COMMUNICATION FREE CHARGING
MANAGEMENT OF ELECTRIC VEHICLES
UNDER GRID CONSTRAINTS**

BY

GHOUS MUHAMMAD ASIM AKHTAR

A Thesis Presented to the
DEANSHIP OF GRADUATE STUDIES

KING FAHD UNIVERSITY OF PETROLEUM & MINERALS

DHAHRAN, SAUDI ARABIA

In Partial Fulfillment of the
Requirements for the Degree of

MASTER OF SCIENCE

In

ELECTRICAL ENGINEERING

December, 2013

KING FAHD UNIVERSITY OF PETROLEUM & MINERALS

DHAHRAN- 31261, SAUDI ARABIA

DEANSHIP OF GRADUATE STUDIES

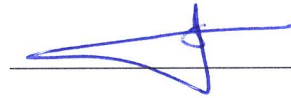
This thesis, written by **GHOUS MUHAMMAD ASIM AKHTAR** under the direction his thesis advisor and approved by his thesis committee, has been presented and accepted by the Dean of Graduate Studies, in partial fulfillment of the requirements for the degree of **MASTER OF SCIENCE IN ELECTRICAL ENGINEERING**.



Dr. Ali Ahmad Al-Shaikhi
Department Chairman



Dr. Salam A. Zummo
Dean of Graduate Studies



Dr. Ali Taleb Al-Awami
(Advisor)



Dr. Mohammad Ali Abido
(Member)



Dr. Eric Sortomme
(Member)

Date

28/12/13



© Ghous Muhammad Asim Akhtar

2013

*This thesis is dedicated to my beloved parents, my fiancée,
my brothers and my passion.*

ACKNOWLEDGMENTS

I humbly thank to Almighty ALLAH for His shower of blessings and for making me able to complete this research successfully.

I want to acknowledge the role of my family including my parents who prayed for me and made me enable to reach this height of my career, my dear fiancée whose continuous moral support gave me confidence to achieve my goal and my lovely brothers who always remain a source of affection for me.

I want to express my gratitude to my thesis advisor Dr. Ali Taleb Al-Awami for his continual support, insight and guidance throughout this work. He has helped me overcome numerous problems and obstacles that came during the journey of this work. I would also like to thank the committee members Dr. Abido and Dr. Eric Sortomme for their visionary suggestions and recommendations, which has made this project possible.

I want to acknowledge my friends in KFUPM who have always supported me and have made my stay in the university memorable. I want to particularly mention Waqar Ahmed, Haider Ali, Saad Mehmood, Arbab Latif, Asrar-ur-Rehman Omer Qureshi, Mustafa Sweti and Abdul Hafeez Ansari for their encouragement and help in all aspects.

I would like to thank all my teachers from my school to this level of professional education, because all of them have their contribution in my success of this Masters degree.

TABLE OF CONTENTS

ACKNOWLEDGMENTS	V
TABLE OF CONTENTS.....	VI
LIST OF TABLES	X
LIST OF FIGURES	XI
LIST OF ABBREVIATIONS.....	XVII
ABSTRACT.....	XVIII
ملخص الرسالة	XX
CHAPTER 1 INTRODUCTION	1
1.1 Background	1
1.2 Literature Review.....	2
1.2.1 Centralized Charging Control	3
1.2.2 Decentralized Charging Control	6
1.2.3 Autonomous Charging Control	7
1.3 Outcome of Literature Review.....	9
1.4 Thesis Objectives and Contributions.....	10
1.5 Thesis Outline	11
CHAPTER 2 OVERVIEW OF ELECTRIC VEHICLES	13
2.1 Types of Electric Vehicles.....	14
2.2 Important Facts and Figures	15
2.3 Technological Impacts of Electric Vehicles	17
2.3.1 Potential Benefits.....	18

2.3.2 Problems	18
CHAPTER 3 VOLTAGE FEEDBACK CONTROL STRATEGY	19
3.1 Voltage Droop Characteristics – Proportional Control	22
3.2 Charging “Fairness”	24
3.3 Voltage Point Selection	25
3.4 Charging as a Function of State of Charge	27
3.5 Preferred End-of-Charge Time (ECT).....	28
CHAPTER 4 DESCRIPTION OF TEST SYSTEM.....	30
4.1 Radial Distribution System.....	30
4.2 Assumptions and Specifications for Electric Vehicles	33
4.3 Assumptions for EV Plug-in / Plug-off Time	33
4.4 Types of Charging Schemes	34
4.4.1 Opportunistic Charging	34
4.4.2 Basic Proportional Control Charging.....	34
4.4.3 Fair, SOC-Dependent Proportional Control Charging	34
CHAPTER 5 SIMULATION RESULTS FOR EV CHARGING MANEGEMENT	36
5.1 Same Plug-In Time for all EVs.....	36
5.1.1 Opportunistic Charging	36
5.1.2 Basic Proportional Control Charging and Flat V-reference	39
5.1.3 Fair, SOC-Dependent Charging	42
5.2 Variable Plug-in Time for all EVs	48
5.2.1 Opportunistic Charging	48
5.2.2 Basic Proportional Control Charging and Flat V-reference	51
5.2.3 Fair, SOC-Dependent Charging	54

CHAPTER 6 PERFORMANCE ANALYSIS OF PROPOSED CONTROL	61
6.1 EV Penetration Level Test	61
6.2 System Reconfiguration Test	62
6.3 End of Charge Time Preference Test.....	62
6.4 Voltage Sag Test.....	64
6.5 Moving Average Test	65
CHAPTER 7 COORDINATION WITH VOLTAGE CONTROL DEVICES.....	67
7.1 Voltage Control with Voltage Regulator	67
7.1.1 Simulation Results.....	69
7.2 Voltage Control with Shunt Capacitors.....	81
7.2.1 Simulation Results.....	82
CHAPTER 8 IMPLEMENTATION OF PROPOSED CHARGING STRATEGY OVER RTDS PLATFORM	90
8.1 Real Time Digital Simulator (RTDS)	90
8.2 RTDS Hardware	91
8.3 RTDS Software	91
8.4 RTDS Applications	92
8.5 System Modeling	92
8.6 Simulation Results.....	95
8.6.1 Opportunistic Charging	97
8.6.2 Basic Proportional Charging.....	99
8.6.3 More Fair, SOC-dependent Charging	102
CHAPTER 9 PROGRAM TO INCENTIVIZE EV OWNER	107
CHAPTER 10 CONCLUSION AND RECOMMENDATIONS	111

REFERENCES	113
VITAE.....	120

LIST OF TABLES

Table 4-1	Distribution System Parameters	31
Table 4-2	Secondary Network Parameters	32
Table 5-1	Voltage Set Points for Fair Charging for Phases A, B and C.....	43
Table 5-2	Comparison in terms of average time to full charge	46
Table 5-3	Voltage Set Points for Fair Charging for Sample EVs at Node-2 and 6	55
Table 5-4	Comparison in terms of time to full charge – Basic vs. SOC-dependent Schemes.....	60
Table 6-1	Comparison in terms of time to full charge (in Hours) – SOC-dependent scheme at Different EV Penetration Levels	61
Table 6-2	Comparison in terms of time to full charge (in Hours) – SOC-dependent scheme after Disconnecting a Peripheral Node.....	62
Table 7-1	Comparison in terms of time to full charge (in Hours) – SOC-dependent scheme with Voltage Control Devices	89
Table 8-1	Voltage Set Points for Fair Charging for Phases A, B, and C - RTDS	96
Table 8-2	Comparison in terms of average time to full charge	105

LIST OF FIGURES

Figure 2-1 A plug in hybrid electric vehicle in Smart grid environment [52]	14
Figure 2-2 Different types of Electric Vehicles – A Comparison	15
Figure 2-3 Cumulative U.S. Plug-In Vehicles Sales (2011 – till date) [53]	16
Figure 2-4 Country wise Sales of World PHEV in 2012.....	17
Figure 2-5 Country wise Sales of World BEV in 2012	17
Figure 3-1 Block diagram for basic proportional control	20
Figure 3-2 Charging rate vs. voltage relationship.....	23
Figure 3-3 Shifting droop characteristics by increasing $V_{ref,i}$	25
Figure 3-4 Block diagram for SOC-dependent proportional control.....	27
Figure 3-5 Droop characteristics as a function of battery SOC	28
Figure 4-1 The distribution feeder test system. Load buses are 2-18.	30
Figure 4-2 Aggregated load profile for Day-15 [60]	31
Figure 4-3 Secondary distribution network topology	32
Figure 4-4 Distribution of EVs with respect to plug-in times	33
Figure 5-1 Total load at node 2, using opportunistic charging	37
Figure 5-2 Total load at node 6, using opportunistic charging	37
Figure 5-3 Voltage profile at node 2, using opportunistic charging	38
Figure 5-4 Voltage profile at node 6, using opportunistic charging	38
Figure 5-5 Average battery SOC at node 2, using opportunistic charging	39
Figure 5-6 Average battery SOC at node 6, using opportunistic charging	39
Figure 5-7 Total load at node 2, using basic proportional control & flat voltage set point	40

Figure 5-8	Total load at node 6, using basic proportional control & flat voltage set point	40
Figure 5-9	Voltage profile at node 2, using basic proportional control & flat voltage set points	41
Figure 5-10	Voltage profile at node 6, using basic proportional control & flat voltage set points	41
Figure 5-11	Average battery SOC at node 2, using basic proportional control & flat voltage set points	42
Figure 5-12	Average battery SOC at node 6, using basic proportional control & flat voltage set points	42
Figure 5-13	Total load at node 2 using fair, SOC-dependent proportional control	43
Figure 5-14	Total load at node 6 using fair, SOC-dependent proportional control	44
Figure 5-15	Voltage profile at node 2, using fair, SOC-dependent proportional control	44
Figure 5-16	Voltage profile at node 6, using fair, SOC-dependent proportional control	45
Figure 5-17	Average battery SOC at node 2, using fair, SOC-dependent proportional control	45
Figure 5-18	Average battery SOC at node 6, using fair, SOC-dependent proportional control	46
Figure 5-19	Aggregate EV charging load for the distribution system	47
Figure 5-20	Total load (EV + non-EV) for the distribution system	47
Figure 5-21	Total load at primary node 2 using opportunistic charging	48
Figure 5-22	Total load at primary node 6 using opportunistic charging	49
Figure 5-23	Voltage profile at Node-2 & 6 (phase-c), using opportunistic charging	50
Figure 5-24	Voltage profiles for POC-A & POC-B, using opportunistic charging	50
Figure 5-25	Battery SOC's for POC-A & POC-B, using opportunistic charging	51
Figure 5-26	Total load at primary node 2 using basic proportional charging	52

Figure 5-27	Total load at primary node 6 using basic proportional	52
Figure 5-28	Voltage profile at Node-2 & 6 (phase-c), using flat V-reference	53
Figure 5-29	Voltage profiles for POC-A & POC-B, using flat V-reference	53
Figure 5-30	Battery SOC's for POC-A & POC-B, using Flat V-reference.....	54
Figure 5-31	Total load at primary node 2-c using fair, SOC-dependent control.....	55
Figure 5-32	Total load at primary node 6-c using fair, SOC-dependent control.....	56
Figure 5-33	Voltage profiles at nodes 2-c and 6-c using fair, SOC-dependent control...	56
Figure 5-34	Voltage profiles for POCs A and B EVs using fair, SOC-dependent control	57
Figure 5-35	Battery SOC for POCs A's & B's EVs using fair, SOC-dependent control	58
Figure 5-36	Aggregate EV charging load for the distribution system.....	59
Figure 5-37	Total load (EV + non-EV) for the distribution system	59
Figure 6-1	Total load for distribution system at different percentages of ECT preference	63
Figure 6-2	Voltage profiles at nodes 2 & 6 at different percentages of EV owners with preferred ECT	63
Figure 6-3	Total EV load at node 6 during the voltage sag test	64
Figure 6-4	Voltages at node 6 during the voltage sag test.....	65
Figure 6-5	Vref profiles using moving averages constrained by 0.952, Node-2	66
Figure 6-6	Vref profiles using moving averages constrained by 0.952, Node-6	66
Figure 7-1	Basic circuit diagram for step voltage regulator [64].....	68
Figure 7-2	Controller for Step voltage regulator [65].....	68
Figure 7-3	Voltages at POC-A and B without voltage control devices.....	71
Figure 7-4	Power draw for EVs at POC-A & B without voltage control devices	71

Figure 7-5	Battery SOC for POCs A's & B's without voltage control devices	72
Figure 7-6	Voltages at POC-A and B, voltage regulator at Node-2	72
Figure 7-7	Taps for Voltage regulator at Node-2	73
Figure 7-8	Power draw for EVs at POC-A & B, voltage regulator at Node-2	74
Figure 7-9	Battery SOC for POCs A's & B's, voltage regulator at Node-2.....	74
Figure 7-10	Voltages at POC-A and B, voltage regulator at Node-5	75
Figure 7-11	Taps for Voltage regulator at Node-5	76
Figure 7-12	Power draw for EVs at POC-A & B, voltage regulator at Node-5	76
Figure 7-13	Battery SOC for POCs A's & B's, voltage regulator at Node-5.....	77
Figure 7-14	Voltages at POC-A and B, voltage regulator at Node-6	78
Figure 7-15	Taps for Voltage regulator at Node-6	78
Figure 7-16	Power draw for EVs at POC-A & B, voltage regulator at Node-6	79
Figure 7-17	Battery SOC for POCs A's & B's, voltage regulator at Node-6.....	79
Figure 7-18	EV load comparison with and without voltage regulators	80
Figure 7-19	Total (EV+Non EV) load comparison with and without voltage regulator .	80
Figure 7-20	Voltages at POC-A and B, shunt capacitors at Node-2	84
Figure 7-21	Shunt capacitor steps Node-2.....	84
Figure 7-22	Power draw for EVs at POC-A & B, shunt capacitor at Node-2	85
Figure 7-23	Battery SOC for POCs A's & B's, shunt capacitor at Node-2.....	85
Figure 7-24	Voltages at POC-A and B, shunt capacitors at Node-6	86
Figure 7-25	Shunt capacitor steps Node-6.....	86
Figure 7-26	Power draw for EVs at POC-A & B, shunt capacitor at Node-6	87
Figure 7-27	Battery SOC for POCs A's & B's, shunt capacitor at Node-6.....	87
Figure 7-28	EV load comparison with and without shunt capacitors	88

Figure 7-29	Total (EV+Non-EV) load comparison with and without shunt capacitors ..	88
Figure 8-1	Unbalanced loads	93
Figure 8-2	Balanced Loads	93
Figure 8-3	EV charging controller at nodes with unbalanced loads	95
Figure 8-4	EV charging controller at nodes with balanced loads	95
Figure 8-5	Voltage profile at node 2, using opportunistic charging	97
Figure 8-6	Voltage profile at node 6, using opportunistic charging	97
Figure 8-7	Total load at node 2, using opportunistic charging	98
Figure 8-8	Total load at node 2, using opportunistic charging	98
Figure 8-9	Voltage profile at node 2, using basic proportional control with flat voltage set points	99
Figure 8-10	Voltage profile at node 6, using basic proportional control with flat voltage set points	99
Figure 8-11	Total load at node 2, using basic proportional control with flat voltage set points	100
Figure 8-12	Total load at node 6, using basic proportional control with flat voltage set points	100
Figure 8-13	Average battery SOC at node 2, using basic proportional control with flat voltage ref	101
Figure 8-14	Average battery SOC at node 6, using basic proportional control with flat voltage ref	101
Figure 8-15	Voltage profile at node 2, using fair, SOC-dependent proportional control	102
Figure 8-16	Voltage profile at node 6, using fair, SOC-dependent proportional control	102
Figure 8-17	Total load at node 2 using fair, SOC-dependent proportional control	103
Figure 8-18	Total load at node 6 using fair, SOC-dependent proportional control	103

Figure 8-19 Average battery SOC at node 2, using fair, SOC-dependent proportional control	104
Figure 8-20 Average battery SOC at node 6, using fair, SOC-dependent proportional control	104
Figure 8-21 Aggregate EV charging load for the distribution system.....	106
Figure 8-22 Total load (EV + non-EV) for the distribution system	106
Figure 9-1 Voltages at Node-2 Phase-b for different ECT levels for all EVs	108
Figure 9-2 Voltages at Node-6 Phase-b for different ECT levels for all EVs	109

LIST OF ABBREVIATIONS

ICE	:	Internal Combustion Engine
EV	:	Electric Vehicles
PHEV	:	Plug-in Hybrid Electric Vehicles
HEV	:	Hybrid Electric Vehicles
SOC	:	State of Charge
POC	:	Point of Charge
PD	:	Power Draw
RES	:	Renewable Energy Resources
SAE	:	Society of Automotive Engineers
ECT	:	End of Charge Time
TOU	:	Time of Use
RTDS	:	Real Time Digital Simulator
RL	:	Rate Limiter
VR	:	Voltage Regulator
SC	:	Shunt Capacitor
ERCOT	:	Electric Reliability Council of Texas
pu	:	Per Unit

ABSTRACT

Full Name : Ghous Muhammad Asim Akhtar
Thesis Title : Communication Free Charging Management of Electric Vehicles
Under Grid Constraints
Major Field : Electrical Engineering
Date of Degree : December 2013

The concept of green environment, security of oil supply, and the increased use of renewable energy resources (RES) in power grids are all factors that are increasing the focus on Electric Vehicles (EVs). The charging of these EVs can be a relatively large load in the distribution grid. If the charging is not managed properly the distribution grid can be affected negatively. Therefore, charging EVs without any negative impacts on the distribution grid is important for their successful integration in large numbers.

This work is intended to develop a communication free i.e. an autonomous voltage feedback control structure, for EV charging. This control structure relies on the local voltage measurement at the point where EV is plugged in. It compares the system measured voltage at the point of charging with a predefined reference voltage. The EV charging is reduced as the system voltage approaches this reference. The reduced charging rate takes into account the EV battery state of charge (SOC) and the owner's end-of-charge time (ECT) preference. The proposed control structure has been simulated on an eighteen bus distribution system. The performance of the control strategy has been tested under the presence of voltage control devices. A contingency analysis was also performed to ensure the system's robustness. The simulation results show that this

method can successfully reduce EV charging to eliminate system voltage violations that would otherwise be caused from EV charging while ensuring fairness among the various EVs. In addition, these results demonstrate the effectiveness of the proposed approach in flattening the distribution feeder's load profile during periods of intense charging and robustness under certain contingencies. The proposed strategy is also tested on Real Time Digital Simulator (RTDS). A basic incentive program is also proposed for those EV owners who would participate in the proposed program.

ملخص الرسالة

الاسم الكامل: غوث محمد عاصم اختر

عنوان الرسالة: نظام اتصال مستقل لتنظيم عملية شحن المركبات الكهربائية الموصولة بالشبكات

التخصص: الهندسة الكهربائية

تاريخ الدرجة العلمية: كانون الأول 2013

مفهوم البيئة الخضراء والأمان في تزويد الوقود والزيادة في استخدام مصادر الطاقة المتجددة كلها عوامل من شأنها زيادة التركيز على المركبات الكهربائية (EVs). تُعد عملية شحن المركبات الكهربائية حمل كهربائي ثقيل نسبياً بالنسبة لشبكات التوزيع الكهربائي. عدم إدارة عملية الشحن على الأغلب سيؤثر سلباً على شبكات توزيع الكهرباء. من أجل ذلك، شحن المركبات الكهربائية بدون أي تأثير سلبي على شبكات توزيع الكهرباء يعد أمراً مهماً لنجاح تضمين عدد أكبر منها على هذه الشبكات.

في هذا العمل البحثي يتم تطوير هيكلية تحكم مستقلة، أي دون الحاجة لأي اتصال عن بعد، بالتغذية الراجعة للبولتية (فرق الجهد) لأجل لشحن المركبات الكهربائية. تعتمد هذه الهيكلية الخاصة بالتحكم على قياس الجهد المحلي على النقطة المربوطة عليها المركبة الكهربائية. تقوم عملية التحكم بمقارنة قيمة الجهد المُقاس في النقطة التي يتم الشحن منها مع القيمة المرجعية للجهد والتي تم تحديدها مسبقاً. يتم تقليل شحن المركبات الكهربائية حتى يصل الجهد للقيمة المرجعية. من أولويات نسبة التقليل في الشحن الأخذ بعين الاعتبار حالة الشحن لبطارية المركبة الكهربائية (كمية الطاقة المتوفرة في البطارية) و وقت الانتهاء المفضل لعملية الشحن بالنسبة لمستخدم هذه المركبة. يتم عمل محاكاة عن طريق هيكلية التحكم المقترحة على نظام توزيع كهربائي يحتوي على ثمانية عشر نقطة توزيع للكهرباء. يتم فحص أداء هيكلية التحكم في ظل وجود أجهزة التحكم بالجهد (الفولتية). يتم تمثيل تحليلات الحالات الطارئة وذلك من أجل ضمان الحفاظ على متانة النظام الكهربائي. تظهر النتائج الناجمة من عملية المحاكاة أن هذه الطريقة تستطيع تقليل عملية شحن المركبة الكهربائية على إزالة أي انتهاك للجهد التي قد تحدث بسبب عملية شحن نفس هذه المركبة بدون وجود أي طريقة للتحكم بشحنها مع ضمان عملية شحن المركبات بشكل عادل بين جميع المركبات الكهربائية المربوطة بالشبكة. بالإضافة إلى ذلك، هذه النتائج تشرح مدى فعالية الطريقة المطروحة في عملية تنعيم الحمل الكهربائي على طول خط التوزيع الواحد في فترات ذروة عملية الشحن وأيضاً توضح مدى متانة النظام في ظل وجود الحالات الطارئة (التغيرات الفجائية). أيضاً تم اختبار الاستراتيجية المقترحة على نظام المحاكاة الرقمية للوقت الحقيقي. بالإضافة لكل ذلك، يتم اقتراح برنامج تحفيزي أساسي لمالكي المركبات الكهربائية الراغبين في المشاركة في البرنامج المقترح.

CHAPTER 1

INTRODUCTION

1.1 Background

The concept of green environment, security of oil supply, and the increased use of renewable energy resources (RES) in power grids are all factors that are increasing the focus on electric vehicles (EVs). The charging of these EVs can be a relatively large load in the distribution grid. If the charging is not managed properly the distribution grid can be affected negatively. Therefore, charging EVs without any negative impacts on the distribution grid is important for their successful integration in large numbers. Various methods have been proposed to control EV charging to prevent negative impacts on the distribution system. These methods can be categorized into either centralized or decentralized charge control strategies. In general, centralized charge control strategies require developed communication infrastructure. The main advantages of decentralized control are that there is reduced communications infrastructure required and reduced computational burden.

In this work, a voltage-feedback-based control strategy is introduced to manage electric vehicle charging. This control strategy requires no communications from the utility as the controller's only input signal is the local nodal voltage at the charging point. It also ensures that the distribution feeder voltages will never vary outside of the voltage limits

set by the respective distribution system in the country of operation. Moreover, the said strategy will simplify the electricity market structure as it can be implemented even in the absence of aggregators.

This work will involve designing distributed voltage feedback controllers installed either at the EVs or at the charge stations. Each controller receives as an input the local nodal voltage at the charging point. Based on this input and on other considerations, the controller decides on the charging rate for the EV. The strategy will be tested on an eighteen bus distribution network.

1.2 Literature Review

Electric vehicles have started to gain public acceptance. This is due to desires for reduced environmental impacts and local energy dependence. Forecasts of EV sales worldwide are expected to exceed 10 million by 2020 [1]. Integrating electric vehicles (EVs) into the power grid without any negative impacts is important for their successful adoption in large numbers. While EVs have many positive benefits, such as reduced local emissions and petroleum independence, their charging can have adverse effects on the grid. While problems on the bulk power system are possible for large numbers of EVs [2],[3] impacts on the distribution system are expected to be significant. These impacts include line overloads, voltage sags, increased losses, sharp peak demands, and loss of equipment life [4]–[12]. However, it has been shown that through controlled charging, the negative impacts of EV charging can be significantly reduced and the number of EVs able to be integrated increases significantly [10],[13]–[17].

Several ways have been proposed in order to control EV charging to prevent negative

impacts on the distribution system. These methods can be broken into centralized charging control, decentralized charging control and autonomous charging control.

1.2.1 Centralized Charging Control

Most methods have focused on centralized charge scheduling and control. In [13], [14] the focus was to optimize the charging EVs with the objective of minimizing distribution system losses based on system forecasted load profile and EV availability. This had the effect of lowering the distribution system peak load and improving the voltage profile and load factor. It was shown in [15] that charging to minimize losses also helps mitigate severe transformer loading and extends transformer life over uncontrolled charging. The authors of [16] focused on integrating EVs by minimizing the distribution system load variance and found that it was also an effective method of flattening the feeder load profile. In [17] it was proven that minimizing feeder losses, minimizing feeder load variance, and maximizing feeder load factor are equivalent and that maximizing the feeder load factor is the simplest to compute. This work also utilized feeder load forecasts. In [18] a minimum cost formulation is developed for charging EVs that seeks to use dynamic real-time pricing to schedule EVs to when the price, and thus the load, is lower. Optimal price and losses based charging methods were compared in [19]. It was found that a price optimal formulation can sometimes cause distribution system overloads in the night hours due to low system prices but loss optimization would always flatten the load profile as much as possible.

Not all of the centralized charging control methods involve optimization. One work proposes a centralized charging control that allows the EVs to find, via a distributed

communication network either the closest charging station, and then only be allowed to charge if there are no network constraints, or the charging station that will allow for the quickest charge [20]. Another method communicates with the smart meters and appliances of the homes and shifts EV charging to off peak hours if the required demand is too high [21]. In another scheme, utilities allocate a fixed amount of energy for each distribution system based on the predicted supply. The energy allocation is communicated to the Substation Control Center where EVs will submit charging requests. The requests are either accepted or rejected based on the utility set limits [22]. Another work by the same authors proposed allowing certain customers to pay a premium for faster charging at the expense of the other EVs on the network [23].

A special case of centralized charge control is Vehicle-to-Grid (V2G), the provision of energy and ancillary services to the grid from an electric vehicle [20]–[26]. Several studies have shown that a significant facilitator of V2G is aggregators which combine the capacities of many EVs to bid into the appropriate electricity markets [26]–[28]. In [26] the aggregator concept framework is explained as to what services the aggregator would provide and how it would interface with the customers. In [27] the importance of aggregators was demonstrated by showing that the availability factor of the EVs to perform ancillary services cannot reach the same level of current generators without aggregators. In [28] it was shown how aggregators could simplify the dispatch of EVs to perform V2G while keeping all of the EVs at the necessary state of charge.

Recently there has been a flurry of activity surrounding more detailed applications of V2G and aggregated interface. It has been shown that EVs can be dispatched to follow system regulation signals [29],[30]. Simulations have shown that the EVs acting as smart

storage can provide fast and accurate responses for frequency regulation and spinning reserves to aid in the integration of wind and solar power [31]–[34]. These studies, however, did not consider market conditions when determining the amount of regulation services to be provided and there was no optimization of the V2G assets. Market conditions and asset optimization are essential to effectively use V2G. Another important study looked at the potential to provide V2G regulation and spinning reserves based on EV availability [34]. This study looked at the available EVs to perform V2G both from monthly averages and using Monte Carlo simulations. This study also did not perform any optimization of the V2G assets.

Several studies have looked at optimization of V2G assets from the aggregator perspective. In [35], an optimal charging sequence for EVs selling only regulation is formulated. This formulation assumes that periods of charging are decoupled from periods of performing regulation, that is, the POP is always zero when performing regulation. It also does not deal with any uncertainty. In [35], smart charging optimization without V2G and optimized V2G with only regulation is formulated. This formulation did not consider the change in battery SOC from dispatch of regulating power through symmetric bidding of regulation up and down. It also does not address uncertainty in prices or EV availability. The study in [36], allowed for full optimal V2G implementation, including asymmetric bidding and combined bidding of multiple V2G services. It looked at EV availability, price uncertainty, and dispatch uncertainty in only a deterministic manner, however, which may expose the aggregator and customers to undue risk. Another problem with [35]–[36] is that they deal with bidirectional power flow to the EVs. Bidirectional V2G may not be widely adopted due to battery

degradation issues, battery warranty issues, and customer concerns. In [37], an optimal bidding formulation for EVs performing regulation up and down with only unidirectional power flow was developed. The simulations were performed on a simulated market with constant prices of regulation services over the study year. None of the V2G studies, however, address examine charging impacts on the distribution system and they require significant communications bandwidth to dispatch the EVs so frequently. Additionally, the optimization requires significant computational power by the centralized controller.

1.2.2 Decentralized Charging Control

Some other methods have focused on decentralized control and optimization of EV charging. Decentralized control has the advantages of reduced communications infrastructure required and reduced computational burden. In [38] the coordination of EVs was performed using non-cooperative games to minimize generation cost. A distributed algorithm utilizing the forecasted grid power demand, number of vehicles, and state of battery state of charge (SOC) was proposed in [39] to level the load at night. Another algorithm that was developed is based on EVs setting their own charge profile based on price forecasts [40]. A utility can then adjust the price signals sent to the EVs as necessary to achieve the desired total load profile. Another decentralized method focuses on managing all of the charging within a parking lot while the parking lot is given its own maximum charge rate[41]. In [42], a multi-agent system was proposed to optimize the charging of EVs on the distribution system. All of these methods and other similar decentralized charging methods rely on communications from the utility of some sort. In [43] authors have developed a decentralized EV charging algorithm through solution of an optimal control problem. That problem is based upon all available information

(forecasted total power demand, estimated number of EVs and their plug-off time, SOC) and EV's charging power determined by a centralized controller.

1.2.3 Autonomous Charging Control

A few communication-free EV charging strategies have been developed to allow autonomous charging control. In [44] a rule based algorithm is developed that analyzes the distribution system and then imposes the necessary constraints in the cars programming. These constraints limit the maximum current that the EV can charge at during different times of the day and are static values. In [45], it was assumed that each charging station is equipped with a fuzzy controller. The controller inputs are the nodal voltage, i.e. the voltage at the charging point and the EV battery SOC. Based on these inputs, the controller decides on the actual power draw of the battery. Despite its novelty, the fuzzy controller tuning requires extensive effort. Comparable performance can be obtained using simpler control structures. Lopes et al. [46] introduced a voltage-feedback, frequency-feedback control structure for bi-directional V2G within a micro grid. The results showed the effectiveness of this structure in preventing voltage and frequency violations. However, the issue of fairness among EVs connected to different nodes in the system was not addressed. Additionally, a micro grid is a unique system where the voltage more closely related to the power balance than in the larger distribution system. SOC dependency of charging rate was not considered, either.

A recent work in [47] proposed an autonomous distributed V2G control strategy combined with smart charging control. This control scheme utilized the fact that RES power fluctuations directly results in the frequency fluctuations. Hence the authors made

use of storage capability of EV battery for providing distributed spinning reserve during the periods of imbalances due to RES along with charging EVs for the next trips. It presented a droop control based in frequency deviation. The frequency is measured locally at the EV charging outlet, hence eliminating the need for system wide information exchange. Although [47] dealt with an excellent detailed modeling and signal routing for EV charger, it analyzes an ideal situation by lumping 20000 EVs without taking into account the details of distribution system. Moreover, it also lacks the analysis of EV charging impact on grid voltage and load profile. In another recent publication [48], authors have proposed an autonomous control strategy based on local voltage and current measurements. The control scheme is simulated on a low voltage residential network with only three EVs connected on different buses. The network operated in both grid connected and islanded mode and hence making it a bi-directional problem. The smaller size of the system makes it infeasible to discuss and analyze impacts of EV charging on the overall load profile of the distribution system. It also lacks discussion about fairness in charging among the three EVs. Richardson et al. [49] proposed and compared local and centralized charging strategies for EVs. It is basically an optimization problem; the optimization is performed by the charger / charging station. With reference to local charging strategy, it contributes towards communication free charging, however it lacks the idea of fair charging, moreover the optimization done by every charger involves extra calculation burden.

The concept of communication-free charging introduced in [50] presents a basic, simple, and fair charging strategy based on local nodal voltages. It proposed an on/off control strategy that eliminates voltage violations, prevents line overloads, and flattens the load

profile. Fairness is ensured because the controllers for the EVs at downstream nodes have lower voltage set points than those at upstream nodes. This work utilizes four different types of charging scenarios namely opportunistic charging, basic proportional charging based on flat voltage reference, SOC-independent charging & SOC-dependent charging. This effective autonomous control scheme proved to coordinate among the EVs connected to the distribution nodes so that voltage violations are avoided. The scheme resulted in a flattened EV charging profile and consequently a smoother voltage profile during times of EV charging.

1.3 Outcome of Literature Review

It is evident from the literature that for the case of centralized charging, the strategy requires significant communication installations for dispatching the EVs along with a powerful and efficient computational system that will do the necessary optimization for EV scheduling. The literature for decentralized charging approach revealed that this strategy requires some sort of communication from the utility or Distribution System Operator (DSO) though it is less as compare to centralized one. In comparison to these two strategies, research in autonomous EV charging is still in infancy stages. Although researchers have started working towards developing localized charging strategies for EVs, there is still room for significant improvement. A lot of issues need to be addressed in order to convince its real time usage from perspective of both distribution companies and EV owners.

1.4 Thesis Objectives and Contributions

The work in [50] serves as a benchmark for this thesis. This thesis is a detailed extension of that work. The authors of this paper have put forward a communication free voltage feedback control with different charging models based on opportunistic, basic, SOC-independent and SOC-dependent charging. They have tested these charging models for an eighteen bus distribution system in absolute ideal conditions. To extend this work, following objectives have been selected which will serve as a contribution of this thesis.

1. To design a more practical voltage based EV charging strategy. The new design covers the following aspects:
 - a. A detailed modeling of the distribution system to cover wiring details of each home connected to each phase of a node.
 - b. Randomizing plug in time for EVs in the system.
 - c. Addressing the EV charging for a system that implements Time – of – Use (TOU) tariff structure.
 - d. Incorporating an end-of-charge time preference given to the EV owner.
2. To assess the performance of the control strategy during various contingencies and alteration in system parameters or configuration.
3. To study the coordination of the proposed control strategy with conventional voltage control devices. These devices include voltage regulator (VR) and shunt capacitors.
All above objectives will be achieved through simulation over MATLAB / SIMULINK
4. To make use of Real Time Digital Simulator (RTDS) for validating the proposed charging strategy.

5. To study different options for incentivizing EV owners so that they sign up into the proposed EV charging control program.

1.5 Thesis Outline

Chapter 1 is the introduction to the thesis.

Chapter 2 gives an overview of Electric Vehicles (EVs) in terms of facts & figures along with a brief description of how EV impacts the distribution systems.

Chapter 3 presents the detailed description of voltage feedback control strategy. It begins with describing basics of an EV charger followed by the description of the fundamentals of the proposed charging model. It then illustrates some critical terms associated with the control scheme including voltage droop characteristics, charging “Fairness”, procedure for selection voltage reference for the controllers, making the EV charging a function of its battery state of charge and EV owner preference of end of charge time / EV plug off time.

Chapter 4 presents the description of the studied test system and related assumptions. It also provides classification of various charging methods including Opportunistic, Basic, and Fair-SOC-dependent charging.

Chapter 5 analyzes EV charging management as per system description in chapter 5. It provides a comparison among different charging methods in terms of charging fairness, voltage profile and aggregated load profile. This chapter is basically divided into two sections. The first section is based on the assumption that plug-in and plug-off time is

same for all EVs while second section takes into account variable plug-in time and hence considering TOU tariff structure.

Chapter 6 presents different simulation analysis for assessing the controller performance. It includes voltage sag test, increase/decrease in EV penetration level, a reduction in the distribution system i.e. removal of downstream laterals.

Chapter 7 extends the EV charging management, described in chapter 6, to coordinate with conventional voltage control devices in an electrical distribution system. This chapter discusses and analyzes coordination with voltage regulators and shunt capacitors.

Chapter 8 presents the implementation of EV charging strategy on RTDS. The case from chapter 6 (Section-I) has been utilized with some modifications to test over RTDS platform.

Chapter 9 describes a scheme for incentivizing the EV owners so that they would participate in the EV charging control program.

Chapter 10 presents conclusion and recommendations for future work.

CHAPTER 2

OVERVIEW OF ELECTRIC VEHICLES

Electric vehicles are the latest form of vehicles that uses electric motors for the traction purpose. These vehicles are penetrating into the modern day society at a steady but good pace. The acceptance shown by society is based on the fact that these vehicles contribute to the greener environment along with an expected major contribution towards the core world issue of future scarcity of fossil fuels. It is quite evident that today's transport sector heavily relies on fossil fuels and hence becomes a major contributor of greenhouse emissions. Out of various transport vehicles, commuter / passenger cars consumes more than half of the total transportation energy [51]. Hence, the countries where quality clean environment is a major concern, governments aimed to attain best environmental and energy efficiency standards; the concentration of these vehicles is certain.

The electric vehicles can be referred to as controllable loads. This controllable property of electric vehicle makes it a powerful tool for smart grid operations. The presence of electric vehicles in today's smart grid environment has put forwarded a challenge in front of researchers and engineers to devise smart and efficient interaction schemes and logics for integrating these future bulk loads into the electric distribution network. The following sections present some terminologies along with facts and figures concerning electric vehicles.

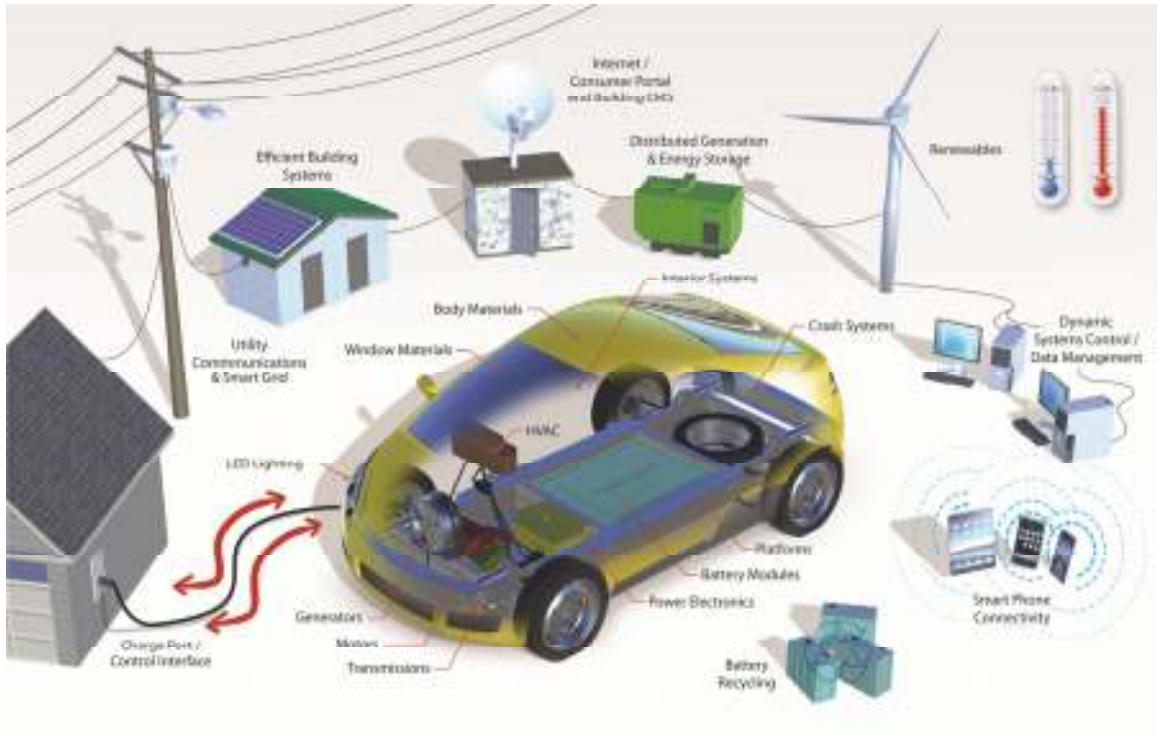


Figure 2-1 A plug in hybrid electric vehicle in Smart grid environment [52]

2.1 Types of Electric Vehicles

The electric vehicle system may include battery pack, propulsion electric motor, dynamo, mechanical transmission system and power control system. As per the arrangements of the said components, electric vehicles can be classified into four different categories named as:

- a. *Hybrid Electric Vehicle (HEV)* – It utilizes a small electric battery to support Internal Combustion Engine (ICE) and increase the fuel efficiency by about 25 percent as compared to conventional vehicles.
- b. *Plug-in Hybrid Electric Vehicle (PHEV)* – It is principally similar to HEV. The basic difference is that it contains a larger electric battery which can be charged by plugging into a socket and hence it utilizes electricity as a fuel.

- c. *Extended Range Electric Vehicle (EREV)* – It utilizes the ICE to drive dynamo which charges the electric motor. And the movement of vehicle is solely dependent upon electric motors rather than ICE as it is the case with HEV and PHEV.
- d. *Battery Electric Vehicle (BEV)* – It is also known as 100% electric vehicle, as it does not contain any internal combustion rather its entire traction system is based on electric motors. And hence they need to be plugged into the electric power grid to get charge.

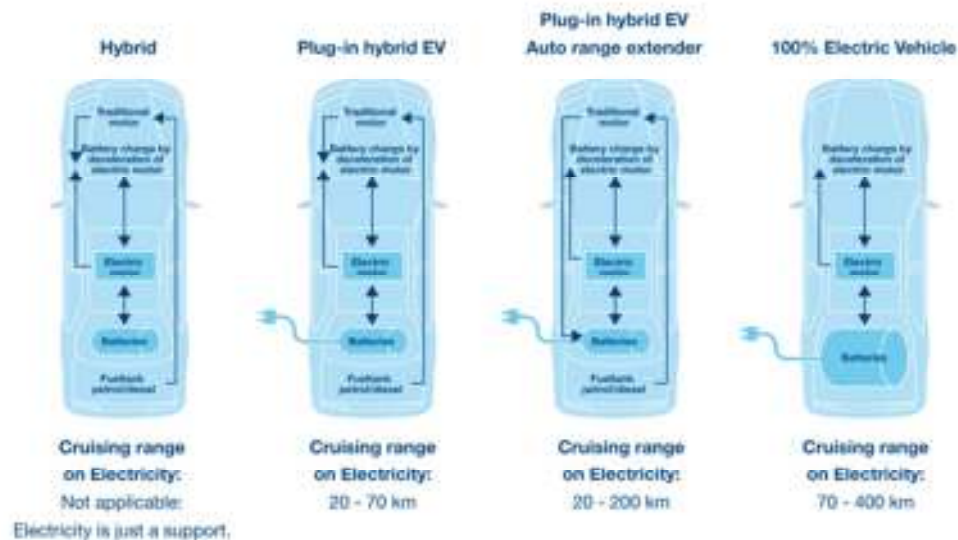


Figure 2-2 Different types of Electric Vehicles – A Comparison

2.2 Important Facts and Figures

The US market is considered to be as a bench mark for studying the trends and impacts of EVs. Hence, the sales of electric vehicles in US markets can be utilized to understand the inclination of consumers toward EVs and particularly plug in EVs. With reference to [53], the cumulative sales of EVs in USA is constantly increasing and currently, up to September'2013, the electric drive market share is 3.9% of total vehicle sales. Figure 2-3 shows cumulative sales of plug in EVs in USA from 2011 till date.

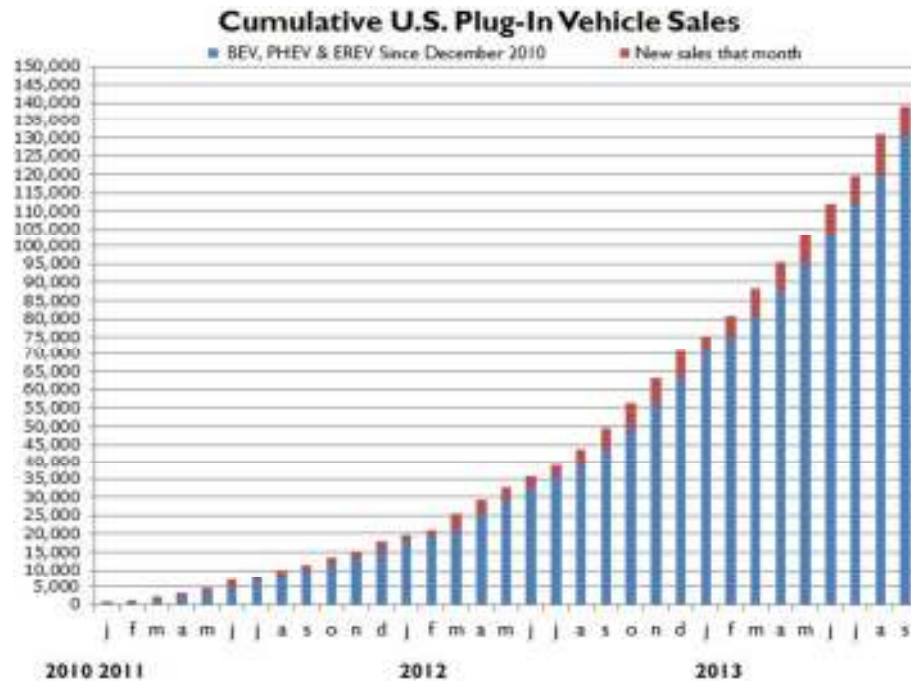


Figure 2-3 Cumulative U.S. Plug-In Vehicles Sales (2011 – till date) [53]

Clean Energy Ministerial (CEM), Electric Vehicles Initiative (EVI) program and International Energy Agency (IEA) are names of international repute who are working towards agenda of penetrating electric vehicles into the society for achieving benefits, mentioned earlier.

Figure 2-4 and Figure 2-5 are from a report [54] published by these three organizations. These figures show worldwide sales of the PHEV and BEV and hence provide a trend of worldwide plug-in EVs.

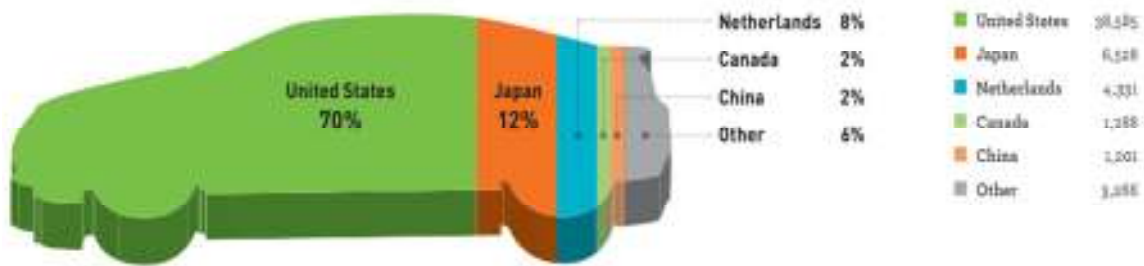


Figure 2-4 Country wise Sales of World PHEV in 2012

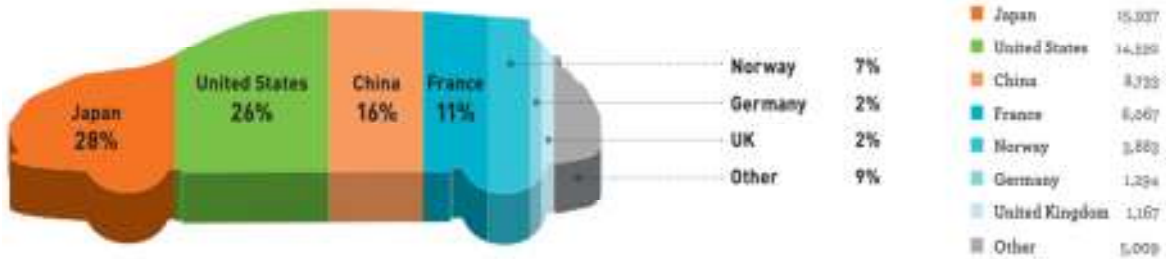


Figure 2-5 Country wise Sales of World BEV in 2012

2.3 Technological Impacts of Electric Vehicles

The above mentioned facts and figures depicts that very soon the power distribution systems will have a plenty of power demand caused by the battery charging of electric vehicles. And hence EVs will become a significant part of power distribution system. The continuous increase and emphasis on EV deployment is undoubtedly due to its vast advantages. But along with that it has certain disadvantages or in other with the increase in EV penetration the power system will have to face certain unavoidable problems. A brief description of potential benefits and problems, caused by EVs, are as follows:

2.3.1 Potential Benefits

1. EVs have low operating costs as compare to the conventional vehicles with only Internal Combustion Engine (ICE).
2. They participate in reducing the greenhouse emissions.
3. The Vehicle-to-Grid (V2G) services, provided through EVs, generate new business opportunities.

2.3.2 Problems

1. Electric vehicles contribute towards the increase in active power loads of a distribution grid; hence the overall system suffers from line overloads and poorer voltage profiles.
2. As a consequence of problem #1, they participate in increasing the grid losses.
3. Uncontrollable charging of EVs lead to sharp peak demands.

CHAPTER 3

VOLTAGE FEEDBACK CONTROL STRATEGY

An electric vehicle charger converts the AC power from the grid into a constant DC current to charge the batteries. From the grid the EV, therefore, is often seen as a constant current source [55]. When connected to the grid through an SAE J1772 charging station, a pilot signal is supplied to the EV from the station that tells what the maximum AC current draw is from that connection point. The EV charges at that current unless the battery management system reduces the maximum current draw to improve battery life near the end of the charging cycle, or if the EV charger cannot handle that high current level. The charging current can be varied either by varying the pilot signal at the charging station or at the EV itself. The proposed voltage-based controller adjusts this EV charging current, and therefore the charging load, based on the AC voltage observed at the point of connection.

The objectives of EV battery charging control are mainly to maintain the distribution system nodal voltages within acceptable limits and to flatten the feeder load profile. These will ensure that the feeder losses are reduced and overloads are avoided [17]. At a given distribution transformer, node k along a specific phase, the load is the composition of the other household loads and the EV loads. Since the voltage profile of the system is a function of its loading levels, the voltage profile can be significantly enhanced by controlling the load. In this work, the only controllable loads considered are the EVs.

In the proposed charge control structure, the feedback signal that is used as an input for

the controller is the voltage at the point of charging (POC). The controller output is the regulated charging rate, or the charger current draw (ID_i). Since unidirectional power flow is assumed, the charging current minimum limit is zero and its maximum limit is taken from the EV charger specifications or the maximum rating of the charging station, whichever is lower? For each EV, based on the POC voltage and, possibly, the EV battery state of charge, the controller decides on the regulated charging current of that EV.

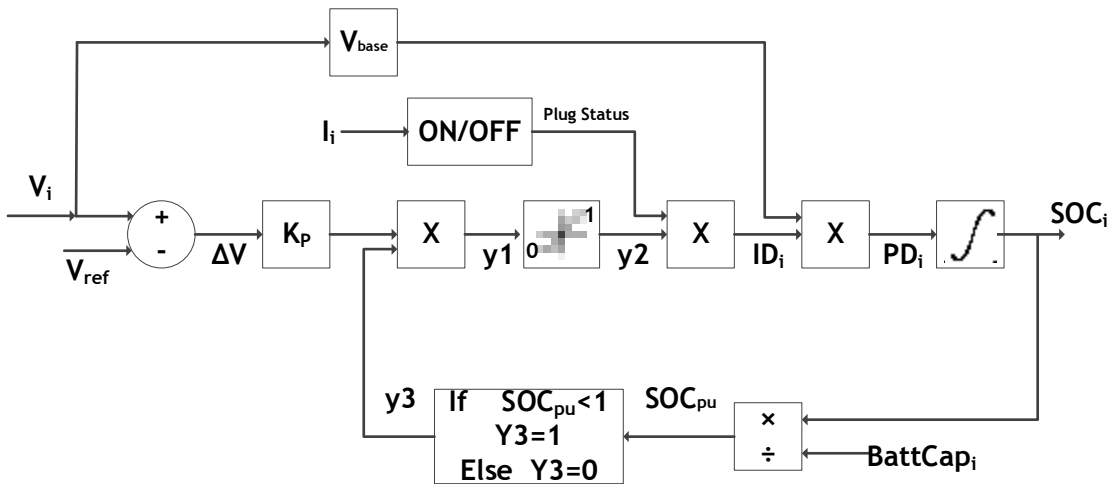


Figure 3-1 Block diagram for basic proportional control

Figure 3-1 shows a block diagram for the voltage feedback control scheme. Notice that there is one controller per EV. In order for the charging current, ID_i , to be nonzero, the following three conditions must be satisfied:

- a- The EV must be plugged in.
- b- The voltage at the charging point is within permissible limits.
- c- The battery state of charge must be still below the maximum battery capacity.

In its simplest form, the proposed controller is a proportional controller [56]. The output

of the proportional controller is continuous value equivalent to the product of ' ΔV ' and selected proportional gain ' K_p ' and can be either positive or negative. The output of proportional controller is then multiplied with a Boolean variable ' y_3 '. ' y_3 ' remains unity until the current SOC of battery is less than total battery capacity otherwise it is equal to zero. The resultant signal ' y_1 ' is passed through a saturation block to give per unit charging current draw as ' y_2 '. The value of ' y_2 ' is maintained between 0 and 1 i.e. no charging and full charging, respectively. The plug status is again a Boolean variable that serves two purposes; one to ensure the charging when car is plugged in by setting itself to unity and zero otherwise and second converting the per unit signal of ' y_2 ' to the actual current draw ' ID_i '. The actual current draw ' ID_i ' is then multiplied with base voltage to give actual power draw ' PD_i ' which is then fed into the continuous time integrator to calculate current battery SOC of the EV. In its simplest mathematical form, the control strategy can be stated as:

$$ID_i = K_{p,i} * (V_i - V_{ref,i}) \quad (1)$$

where ' $K_{p,i}$ ' is the proportional control gain for the i^{th} EV, ' $V_{ref,i}$ ' is the reference voltage level for the i^{th} EV in per unit, and V_i is the actual real-time voltage in per unit at the charging point. Because the system loading is measured in power and not current, it is helpful to refer to the EV power draw, ' PD_i ', which is merely the current draw ' ID_i ', multiplied by the node voltage as shown in Figure 3-1. Therefore, for the rest of this work, only ' PD_i ' will be referenced even though it is ' ID_i ' that is actually directly modulated.

The control strategy as given in (1) can be thought of effectively as a voltage droop

characteristic for each EV. That is, if the voltage at a given node is close to its minimum tolerance, all EVs connected to that POC reduce their charging rate so as to avoid voltage violations. The contribution of each EV is dependent on its own droop characteristics, i.e. its $K_{p,i}$ gain. The EVs with the lower gains will charge at lower rates than the EVs with the higher gains.

In this sense, this voltage droop characteristic is similar to the frequency droop characteristic used in automatic generation control to maintain generation-load balance at all times. Frequency control, however, is fundamentally different from voltage control; the former is a global issue for a given power system, while the latter is a local issue at the node level. Another distinct characteristic of voltage control is that the local nodal voltages are not independent of each other. In the case of radial distribution systems, the voltage at a downstream primary node is always less than or equal to the voltage at the primary nodes upstream to it, assuming the absence of voltage support mechanisms such as distributed shunt capacitors. In addition, lowering the load at the downstream node improves the voltage not only at that node but also at all upstream nodes.

3.1 Voltage Droop Characteristics – Proportional Control

Suppose that the minimum voltage level at a given POC is 0.95 pu. It is required to construct a voltage droop curve for the i^{th} EV that meets the following requirements, as long as $SOC_i < BattCap_i$:

- If $V_i \leq V_{ref,i}$, $PD_i = 0$,
- If $V_i > V_{ref,i}$, $PD_i > 0$.

- The relationship between V_i and PD_i is linear.

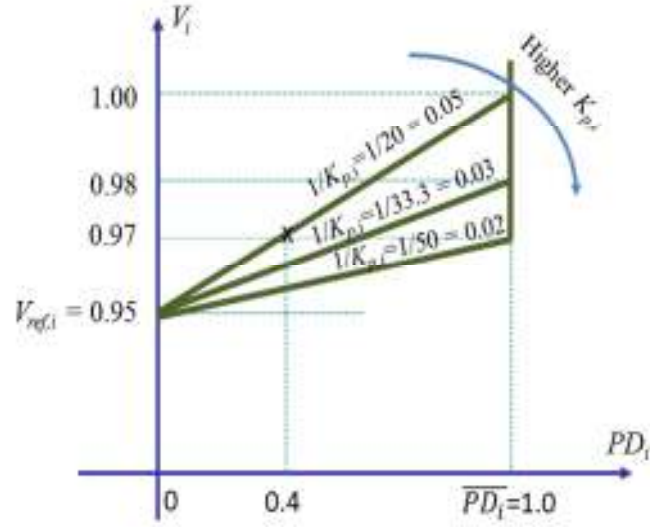


Figure 3-2 Charging rate vs. voltage relationship

Figure 3-2 shows a group of curves that meet the above mentioned requirements. These curves relate PD_i to V_i as follows:

$$PD_i = \begin{cases} 0 & \text{if } V_i \leq V_{ref,i} \\ K_{p,i}(V_i - V_{ref,i}) & \text{if } V_{ref,i} \leq V_i \leq V'_i \\ 1 & \text{if } V_i \geq V'_i \end{cases}$$

(2)

$K_{p,i}$ represents the inverse of the slope of the voltage droop curve. It can be thought of as the sensitivity of PD_i to the change in voltage from its lower constraint. For example, consider two EVs A and B with two proportional gains $K_{p,A} = 20$ and $K_{p,B} = 50$. The two EVs are connected to the same POC, whose minimum allowable voltage level is $V_{ref,i} = 0.95$ pu. The droop characteristics of these two EVs are the top and bottom

curves shown in Figure 3-2, respectively. If the POC voltage is at or below 0.95 pu, none of the EVs will be charging. However, if the POC voltage is 0.97 pu, EV A will be charging at PD_A of 40% while EV B will be charging at 100%. Note that this still does not guarantee voltage violation due to EV charging, because even if all PD connected to that POC are set to zero, chances are other EVs at either downstream or upstream nodes are still charging (lack of controllability at the nodal level). Hence, coordinated tuning of K_{pi} and $V_{ref,i}$ is essential. This coordination is done offline, so real-time operation does not require any coordination or communication among the different EVs.

3.2 Charging “Fairness”

A very important aspect of an EV charging strategy is “fairness”. That is, the contribution of each EV to mitigate voltage violations should be decided upon in a manner that does not consistently charge an EV significantly slower or faster than another based on their locations in the network. This fairness can be thought of in two directions: horizontal fairness and vertical fairness. Horizontal fairness corresponds to the fact that all EVs charging at more or less the same POC voltage should be charging at more or less the same rate PD_i . Since $V_{ref,i}$ for all these EVs are approximately the same, horizontal fairness can be achieved by simply setting $K_{p,i}$ of these EVs to be identical. Vertical fairness is related to the level of contribution of EVs connected to POCs at different voltage levels. It is desirable that all EVs connected to the same feeder to have almost equal charging opportunities. That is, it won’t be appropriate or acceptable that EVs connected to downstream, i.e. lower voltage, POCs suffer from much lower regulated charging rates than those connected to upstream, i.e. higher voltage, POCs. Vertical fairness can be assured in one of two ways:

- 1- Adjusting $K_{p,i}$ such that EVs connected to downstream POCs have higher $K_{p,i}$ than those of EVs connected to upstream POCs.
- 2- Adjusting $V_{ref,i}$ such that EVs connected to downstream POCs have lower $V_{ref,i}$ than those of EVs connected to upstream POCs.

In this work, the second option is selected and the $K_{p,i}$ gains of all EVs in the system are set to be identical.

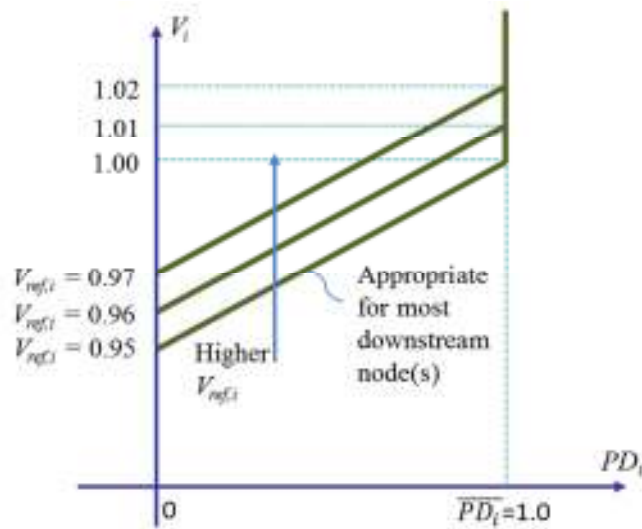


Figure 3-3 Shifting droop characteristics by increasing $V_{ref,i}$

Figure 3-3 shows a set of voltage droop characteristics for different values of $V_{ref,i}$ and one common value of $K_{p,i} = 20$. For a common $K_{p,i}$, a higher $V_{ref,i}$ is reflected as an up-shift into the droop curve. Therefore, it is appropriate for downstream nodes to have lower droop characteristics (i.e. lower $V_{ref,i}$) than those of upstream nodes.

3.3 Voltage Point Selection

The basis for selecting the voltage set points is that EVs connected across the distribution

system contribute almost equally, irrespective of their charging point location, in order to avoid any network violations. If all voltage set points are set identically, the EVs connected to downstream POCs (or those connected to the primary nodes through long secondary wiring) will generally be at disadvantage compared with those connected to upstream POCs (or have short secondary wiring). Therefore, as a general rule of thumb, the more downstream the POC is, the lower the voltage set point should be. The following are two methods for selecting these voltage set points to achieve that goal:

1. Iterative Method on Voltage Set Points:

For a typical daily load profile, distribution power flow is run and voltages are observed. Based on the observed voltage levels, a set of voltage set points for the EVs is selected. Then, if PD_i values a certain EV is unreasonably high (low), the corresponding $V_{ref,i}$ is raised (lowered). $V_{ref,i}$ values are adjusted till PD_i 's of all EVs across the system are at comparable levels.

2. Moving Average Method:

At each EV point of charging i , the value of the daily minimum voltage $V_{min,d,i}$ is tracked. This typically is associated with the daily peak period. These minimum voltage values are averaged out for the past several days. This average value is then used as a voltage set point, or a voltage reference, $V_{ref,i}$, for the i^{th} EV. This reference voltage needs to be constrained by the minimum permissible voltage level. That is,

$$V_{ref,i} = \max\left(\frac{1}{D} \sum_{d=1}^D V_{min,d,i}, 0.952\right)$$

where D is the number of days. A value of 0.002 pu is added to the minimum permissible voltage level as a safety margin. The advantage of this method over the

first method is that it is simple and systematic.

3.4 Charging as a Function of State of Charge

An additional property that can be added to the control scheme is the dependence of the charging rate on the EV battery SOC. This can be included by multiplying the controller gains by $(1 - SOC_{pu,i})$, where $SOC_{pu,i} = SOC_i/BattCap_i$. This term will bias the effective controller gains more towards the least charged EVs and less towards the most charged EVs.

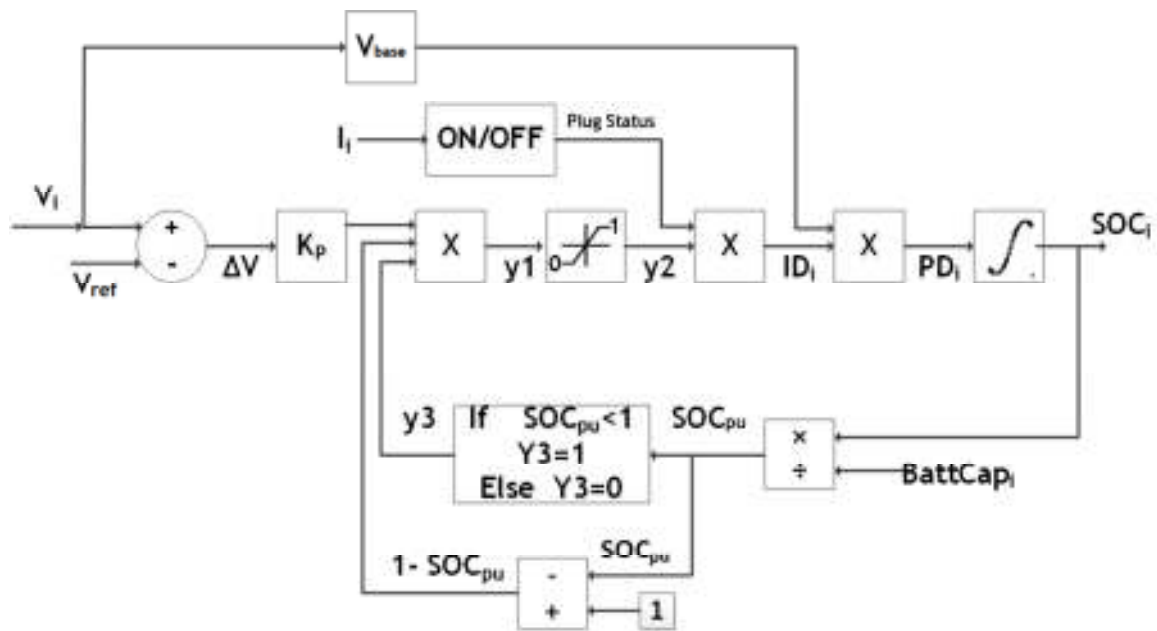


Figure 3-4 Block diagram for SOC-dependent proportional control

The reader should be reminded that it is assumed that all EVs in the system share the same values for the set of proportional gains $K_{p,i}$. Therefore, the EVs connected to downstream POCs will generally be at disadvantage. For P control, therefore, the voltage droop characteristics are similar to those shown in Figure 3-3; parallel lines shifted vertically according to their vertical intercepts $V_{ref,i}$. Multiplying the controller

proportional gain of the i^{th} EV by $(1 - SOC_{pu,i})$ effectively changes the slope of the droop characteristic of that EV without changing the vertical intercept. Therefore, for EVs with the same reference voltage, the ones with the higher state of charge will charge at a lower rate than those with the lower state of charge. This is illustrated in Figure 3-5.

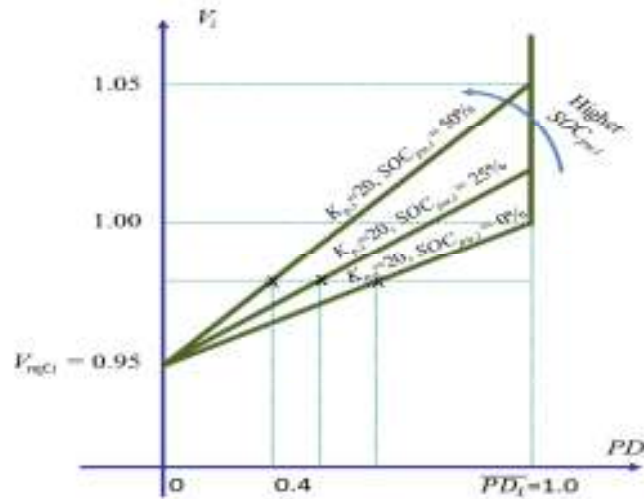


Figure 3-5 Droop characteristics as a function of battery SOC

3.5 Preferred End-of-Charge Time (ECT)

The control scheme can be further modified in order to include any possible preference of the ECT for the EV owner. This is done by limiting the EV power draw to a value that is dependent on the remaining uncharged battery capacity. Thus, the minimum power draw for each EV is defined as the average value required over the remaining charging interval. That is, for an EV with a current state of charge of $SOC(t)$ and a total battery capacity of $BattCap_i$, the power draw, given by (2), is modified to

$$PD_i = \begin{cases} 0 & \text{if } V_i \leq V_{ref,i} \\ PD_i^* & \text{if } V_{ref,i} \leq V_i \leq V_i' \\ 1 & \text{if } V_i \geq V_i' \end{cases} \quad (3)$$

where

$$PD_i^* = \max\{K_{p,i}(V_i - V_{ref,i}),$$
(4)

$$(BattCap_i - SOC(t))/(d - t)\}$$
(5)

d is the preferred total charge time (in hours). Note that this additional term cannot guarantee that the EV will charge fully before the ECT. This is because this PD_i^* term in (3) applies only when the POC voltage is higher than $V_{ref,i}$. Otherwise, PD_i will be set to zero. However, careful selection of the gain value maximizes the likelihood of achieving this desirable feature.

CHAPTER 4

DESCRIPTION OF TEST SYSTEM

4.1 Radial Distribution System

The distribution test system used for simulating the EV impacts from charging is shown in Figure 4-1

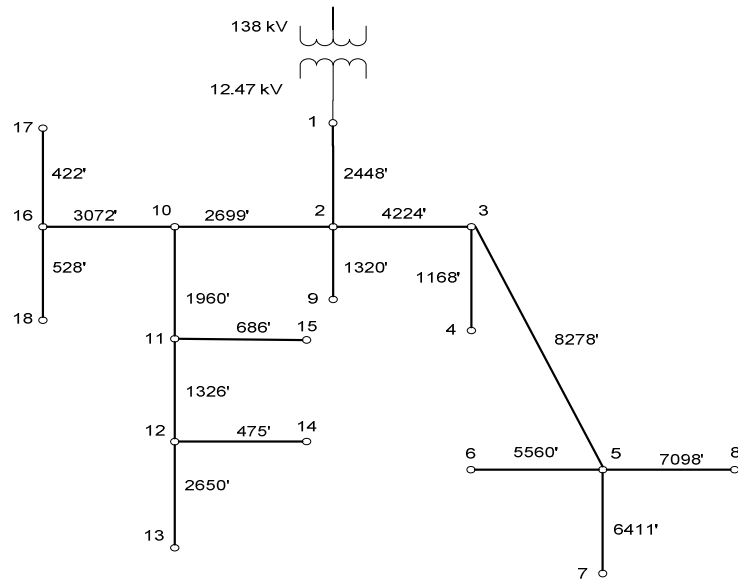


Figure 4-1 The distribution feeder test system. Load buses are 2-18.

This is an unbalanced three phase system with 17 load buses on each phase. This system was originally introduced in [57], and was one of the systems used to study EV charging impacts in [17]. It has also been used in micro grid studies [58], [59].

The primary distribution system operates at a nominal 12.47 kV line-to-line voltage. The conductors are organized in a symmetric geometry with a geometric mean spacing of

4.69 ft. Every load bus has 20 houses connected to each secondary phase. It is assumed that all houses on a given node are connected in parallel to the transformer and thus have the same nodal voltage. The positive and zero sequence impedances are $Z_1=0.3201 + j0.1612$ and $Z_0 = 0.4525 + j0.5231$ ($\Omega / 1000\text{km}$). The self and mutual impedances are evaluated then evaluated to form an impedance matrix for performing the load flow analysis. The parameters of the distribution system are found in Table 4-1.

Table 4-1 Distribution System Parameters

Phase Conductor:	ACSR 2
Neutral Conductor:	ACSR 4
Max Amps:	180
Houses	510

The load profile for each house is based on Residential High Winter Ratio (ResHiWR) load profiles on July 20, 2010 found in the ERCOT system with five minute resolution [60]. To the base load profile, normally distributed random noise is added to model variations in individual usage. All twenty houses on each secondary line are then aggregated to form equivalent node loads. Figure 4-2 shows an aggregated load profile for the Non-EV loads for day-15, this load profile has been utilized throughout the thesis simulation works.

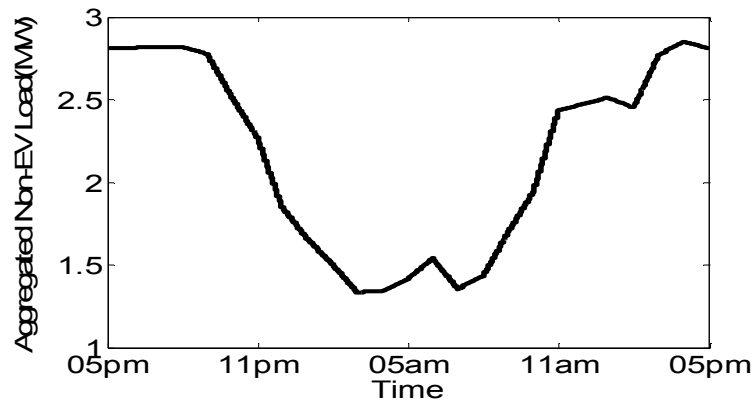


Figure 4-2 Aggregated load profile for Day-15 [60]

A distinguished feature of radial distribution systems is that there always exists a unique path from any given node back to the source. This key feature is actually the basis of the backward / forward sweep algorithm. This method is also named as Ladder Iterative technique. This power flow algorithm works by updating voltages and currents (or power flows) along these unique paths [61].

The secondary distribution system is modeled based on the field site configuration of Utility E in [62], which has several splice boxes as well as houses connected directly to the distribution transformer through triplex lines as shown in Figure 5-2. The parameters of the secondary distribution network are given in Table 5-2. A small additional resistance is also added to model the EV charging cable. This secondary system has been modeled only on the most upstream node (Node#2) and most downstream node (Node#6).

Table 4-2 Secondary Network Parameters

Parameter	Value
EV Charger Penetration %	50%
Distribution Service Transformer	150 kVA, %Z = 1.8
Secondary Conductor (transformer to splice box)	350 Al, 4/0 Al Neutral
Service Conductor (to the houses)	#2 Al
No. of customers	20

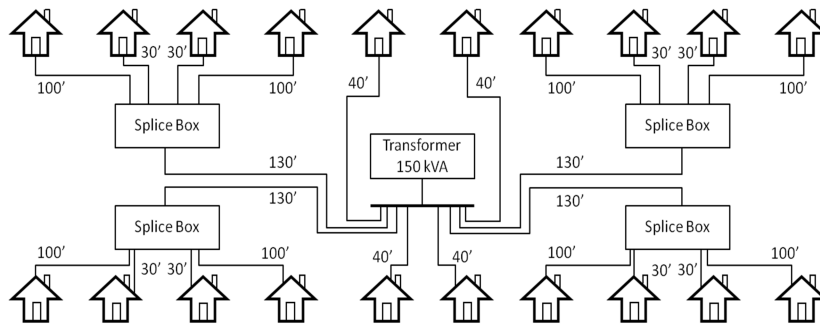


Figure 4-3 Secondary distribution network topology

4.2 Assumptions and Specifications for Electric Vehicles

An average of one EV per two houses in the system, i.e. a 50% penetration level, is assumed. Each EV is randomly assigned to a house on the secondary network. This level is chosen because it has been shown to cause significant problems with EV charging [13], [17]. Each EV has a maximum charge rate of 6.6 kW and needs to charge 24 kWh to reach full capacity. This corresponds to a 2013 Nissan Leaf [63]. Average initial state of charge of each EV is assumed to be about 40% of the battery's full capacity.

4.3 Assumptions for EV Plug-in / Plug-off Time

It is assumed that the system under study is under a time-of-use (TOU) tariff structure. A lower tariff is applied from 7 pm to 7 am. Therefore, it is expected that the majority of EV owners plug in their EVs at or after 7 pm. To take this into account and the fact that EV plug-in time is expected to be random, the EV plug-in time is assumed to follow a Gaussian distribution centered at 8 pm and with a standard deviation of one hour. The distribution of plug-in times is shown in Figure 4-4. In addition, it is assumed that 10% of the EV owners have preferred ECTs, which range between 3 and 6 hours. These have also been assigned randomly.

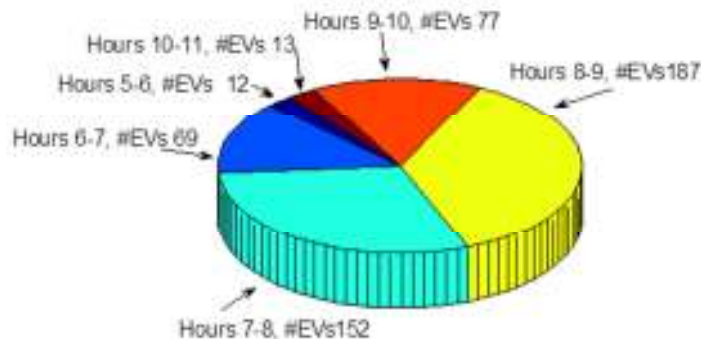


Figure 4-4 Distribution of EVs with respect to plug-in times

4.4 Types of Charging Schemes

In order to simulate and analyze the effectiveness the proposed EV charging control for the described test system, three types of charging schemes have been utilized. These schemes are described briefly as follows.

4.4.1 Opportunistic Charging

Opportunistic charging can also be termed as dumb charging. In this type of charging there is no control over the charging rate of the EV battery. The EVs are assumed to be charged at the maximum allowable rate of their chargers as soon as they are plugged in.

4.4.2 Basic Proportional Control Charging

In this type of charging a fixed value of reference voltage is assigned to all the proportional EV controllers, installed at different nodes. The fundamental idea behind this charging scheme is to maintain the overall voltage profile of the system above the lower range and a value little bit higher than the lower range is set as a flat voltage reference. In this work the flat voltage reference will be 0.955 per unit which 0.5% greater than lower permissible voltage of 0.95 per unit.

4.4.3 Fair, SOC-Dependent Proportional Control Charging

The idea behind this type of charging is to achieve fairness among EVs at various nodes of the distribution system. Fairness implies that EVs at upstream nodes with good voltage profile and EVs at downstream nodes with low voltage profile are charged at comparable rates and finished charging time is also as close as possible. To achieve fairness along with avoiding voltage violations, two aspects have been modified. The first aspect is to have different voltage reference values for different nodes, according to their positions in

the distribution system. The method described in section 4.3 is used for computing voltage references. The second aspect is to make the proportional EV control a function of battery SOC. The addition of this signal expects to achieve a flatter voltage and load profile which would serve as a great advantage of this technique.

CHAPTER 5

SIMULATION RESULTS FOR EV CHARGING MANEGEMENT

This chapter will present the simulation results for two broader cases. The first case will assume that all the EVs are plugged in at the same time i.e. at 5 pm. The second case will assume different plug-in times for all EVs in between 5 pm and 11pm.

5.1 Same Plug-In Time for all EVs

As a preliminary case for testing the proposed charging strategies; this section considers same plug in time for all EVs along with only primary modeling of the distribution system i.e. considering the ideal case that all the homes / EVs are plugged in at the same nodal point and thus having same nodal voltage. This effectively ignores the all the wiring from the transformers' secondaries to the houses, i.e. secondaries with zero impedances.

The simulations are performed for the entire system under study, however the results shown are for the most upstream node (Node # 2) and one of the most downstream node (Node # 6).

5.1.1 Opportunistic Charging

In opportunistic charging, the EVs are assumed to be charging at maximum charging rate as soon as they are plugged in, i.e. at 5 pm. The results of opportunistic charging at several nodes are shown in Figure 5-1 to Figure 5-6. A significant jump is observed at all nodes in the total load at the first few hours of charging. In addition, a voltage dip,

considerably below the permissible limit of 0.95 pu, due to the sudden and un-controlled increase in loading is noticed at a number of nodes. In general, downstream node-6 suffer from much lower voltage levels than upstream node-2.

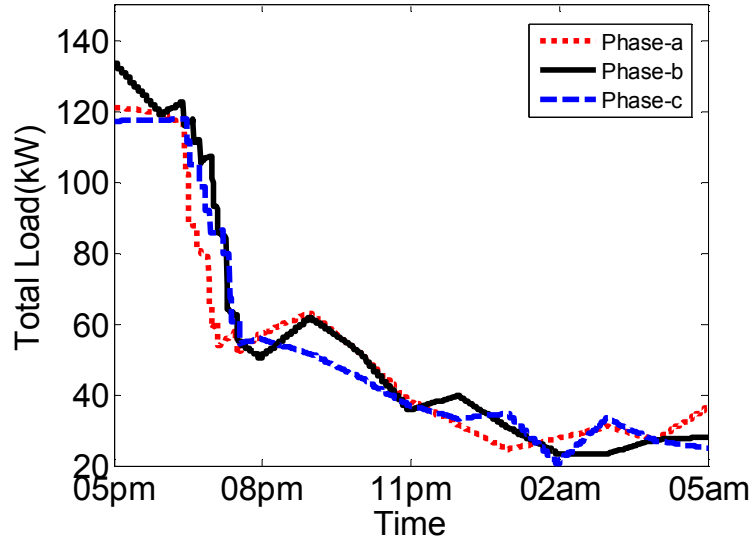


Figure 5-1 Total load at node 2, using opportunistic charging

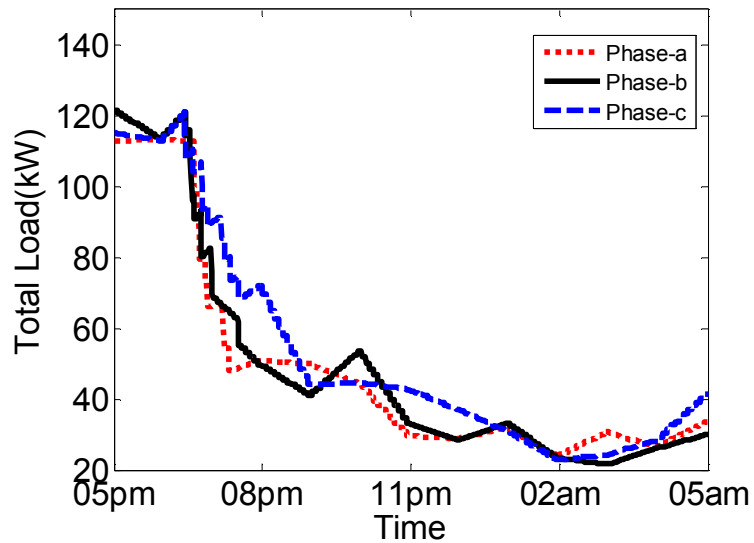


Figure 5-2 Total load at node 6, using opportunistic charging

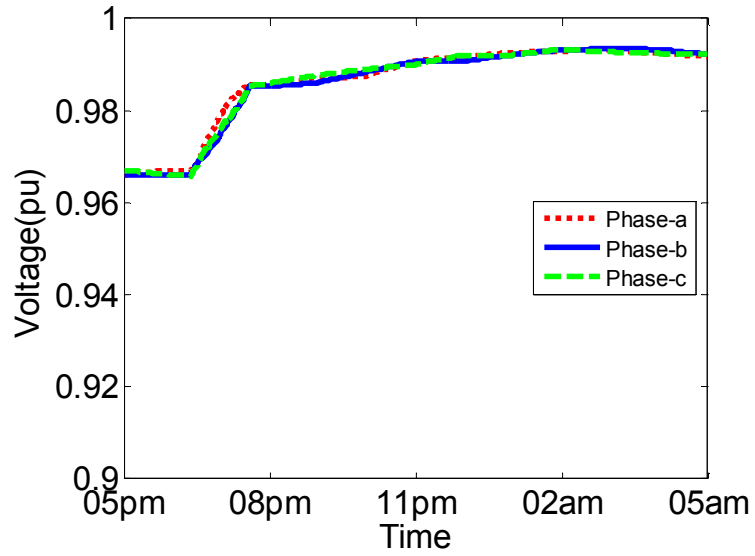


Figure 5-3 Voltage profile at node 2, using opportunistic charging

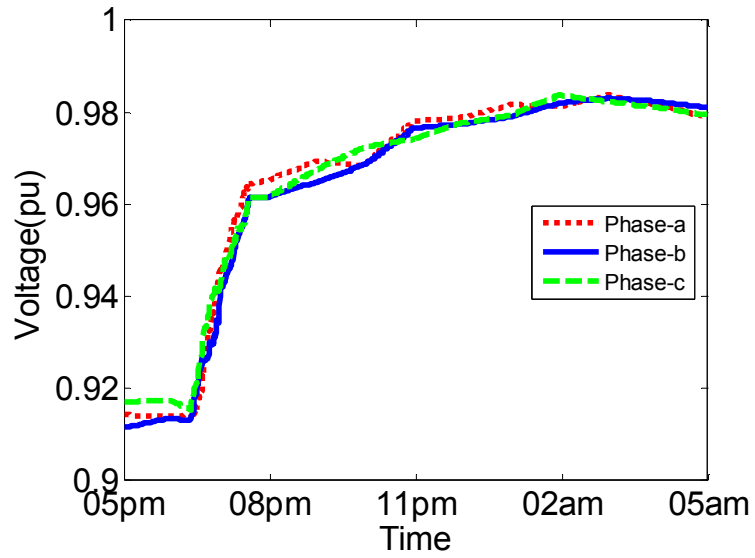


Figure 5-4 Voltage profile at node 6, using opportunistic charging

The average SOC_s at both the nodes and in the overall system is independent of the voltage levels at the nodes and hence SOC_s are found to have similar trends, as shown in Figure 5-5 and Figure 5-6.

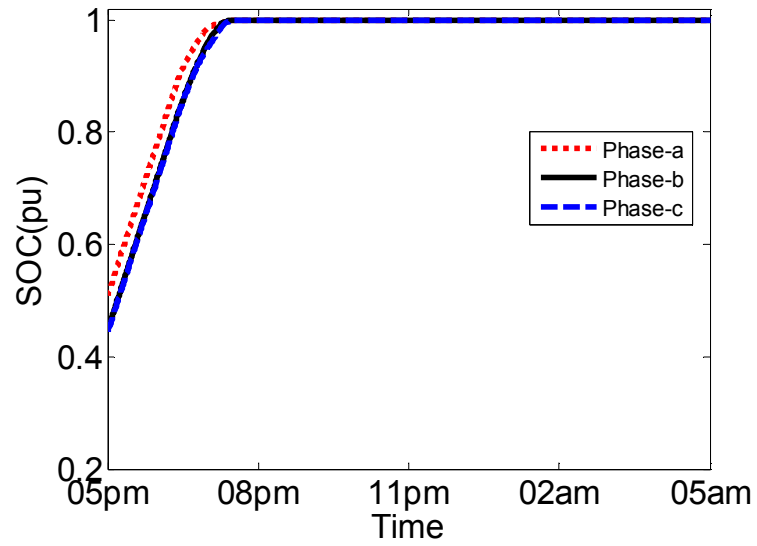


Figure 5-5 Average battery SOC at node 2, using opportunistic charging

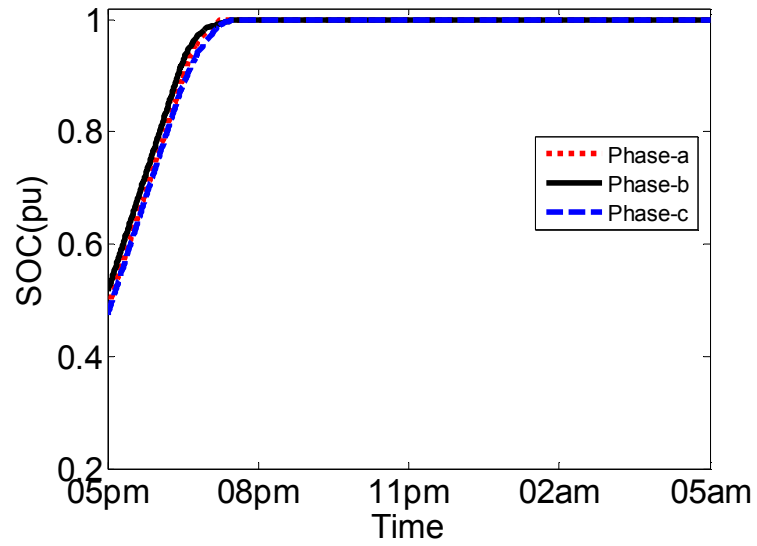


Figure 5-6 Average battery SOC at node 6, using opportunistic charging

5.1.2 Basic Proportional Control Charging and Flat V-reference

In this case, the voltage set points of all nodes in the system are set at a flat voltage reference of 0.955 pu. After several trials, the proportional gain is set to 20 for all EVs. At this value of gain, all EVs are charged fully before the end of the charging period, i.e.

before 5 a.m. Figure 5-7 to Figure 5-12 show the impact of using the proposed basic proportional control scheme on the nodal performances at nodes 2 and 6. The results clearly show the effectiveness of this simple, distributed control scheme on enhancing the voltage profiles, especially at the downstream nodes.

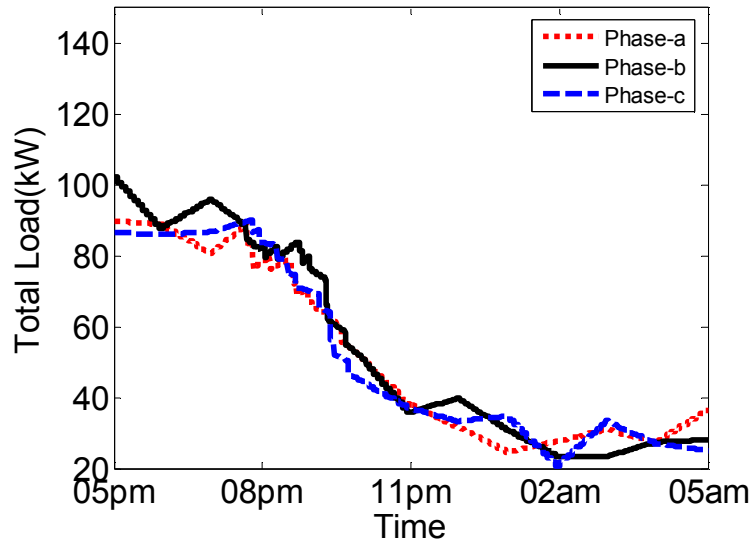


Figure 5-7 Total load at node 2, using basic proportional control & flat voltage set point

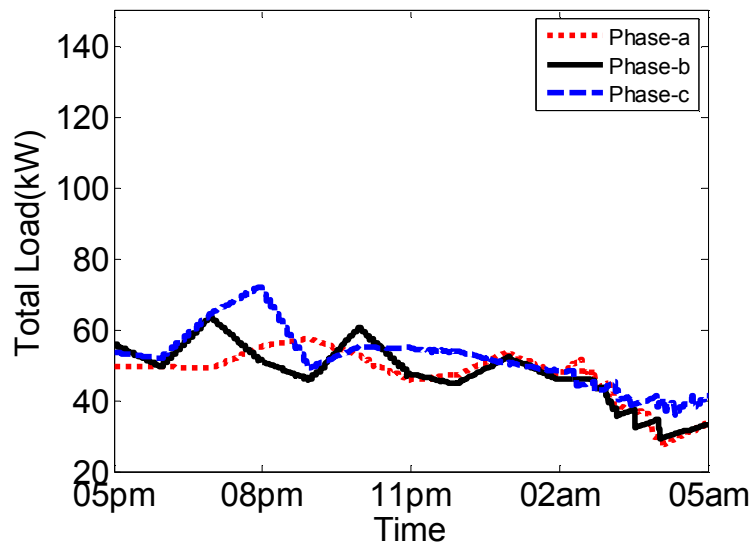


Figure 5-8 Total load at node 6, using basic proportional control & flat voltage set point

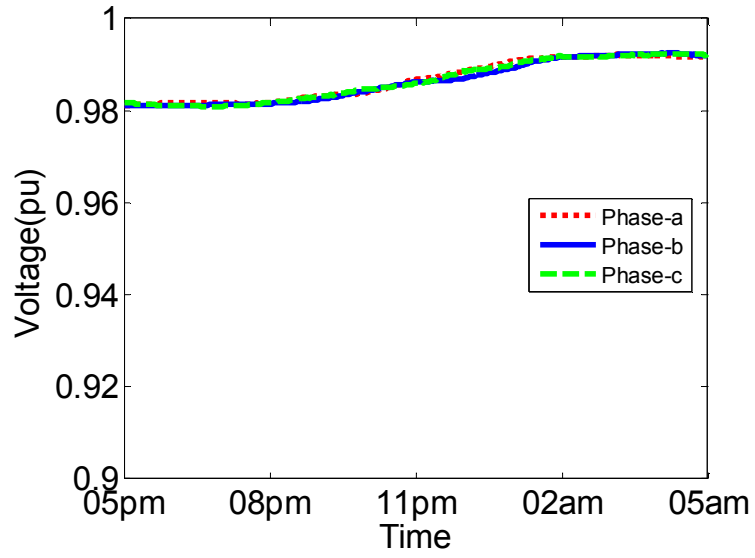


Figure 5-9 Voltage profile at node 2, using basic proportional control & flat voltage set points

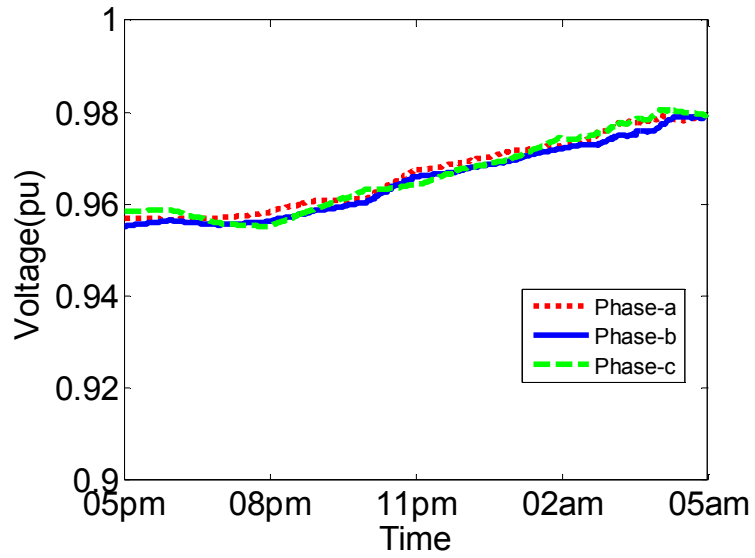


Figure 5-10 Voltage profile at node 6, using basic proportional control & flat voltage set points

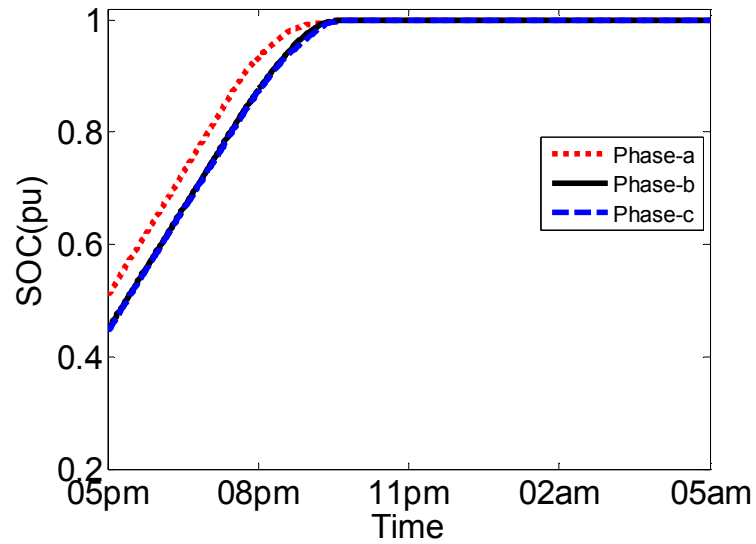


Figure 5-11 Average battery SOC at node 2, using basic proportional control & flat voltage set points

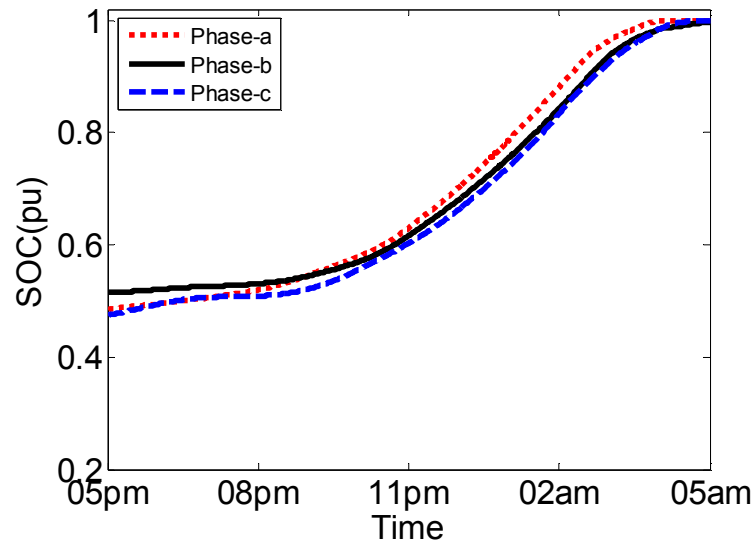


Figure 5-12 Average battery SOC at node 6, using basic proportional control & flat voltage set points

5.1.3 Fair, SOC-Dependent Charging

In order to improve the charging fairness, upstream node voltage reference values should be set at higher levels than downstream node. The voltage references for SOC-

dependency case are shown in Table 5-1, calculated as per the algorithm described in Section 4.3. The differences in charging time among EVs connected to the same node as well as among EVs connected at different nodes can be further reduced by making the proportional gain a function of the battery SOC. The effective proportional gain linearly decreases as $SOC_{pu,i}$ increases. Therefore, K_p has to be set at a higher value than that of the basic proportional control with flat V reference case.

Table 5-1 Voltage Set Points for Fair Charging for Phases A, B and C

Node	Set Point	Node	Set Point
1	---	10	0.975, 0.975, 0.975
2	0.984, 0.984, 0.984	11	0.971, 0.971, 0.971
3	0.974, 0.974, 0.974	12	0.970, 0.969, 0.969
4	0.974, 0.974, 0.973	13	0.969, 0.968, 0.968
5	0.961, 0.961, 0.961	14	0.970, 0.969, 0.969
6	0.959, 0.959, 0.959	15	0.971, 0.971, 0.971
7	0.959, 0.958, 0.958	16	0.971, 0.971, 0.971
8	0.958, 0.958, 0.957	17	0.971, 0.971, 0.971
9	0.984, 0.983, 0.984	18	0.971, 0.971, 0.971

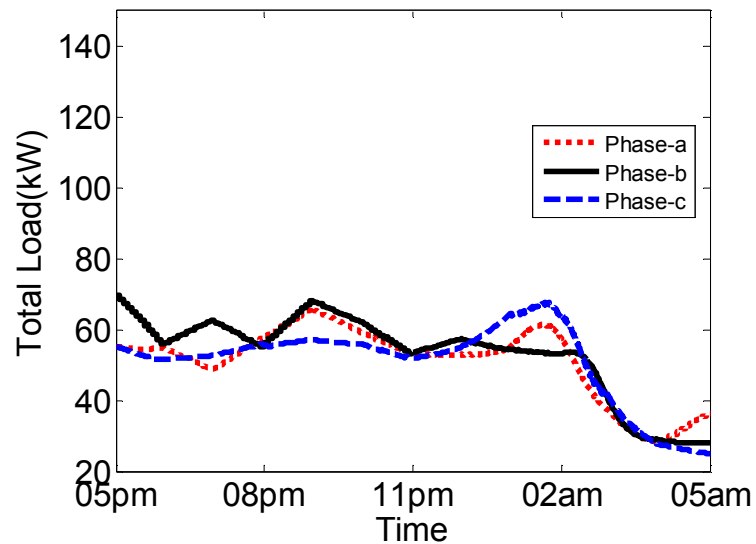


Figure 5-13 Total load at node 2 using fair, SOC-dependent proportional control

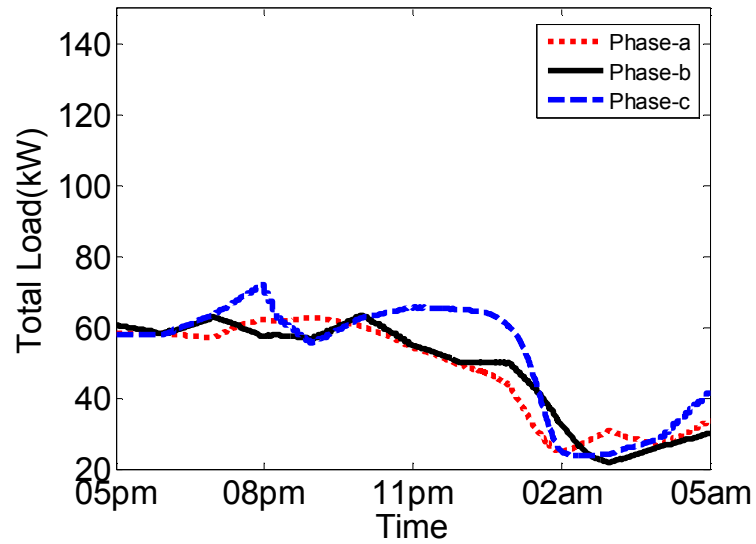


Figure 5-14 Total load at node 6 using fair, SOC-dependent proportional control

Figure 5-13 to Figure 5-18 show the nodal loads, nodal voltage profiles and nodal average SOC at nodes 2 and 6, due to the use of an SOC-dependent proportional gain with $K_p = 1000$. The results show that SOC-dependent proportional charging not only improves fairness among EVs across the distribution system, but also results in flatter voltage profiles and flatter total system load profile.

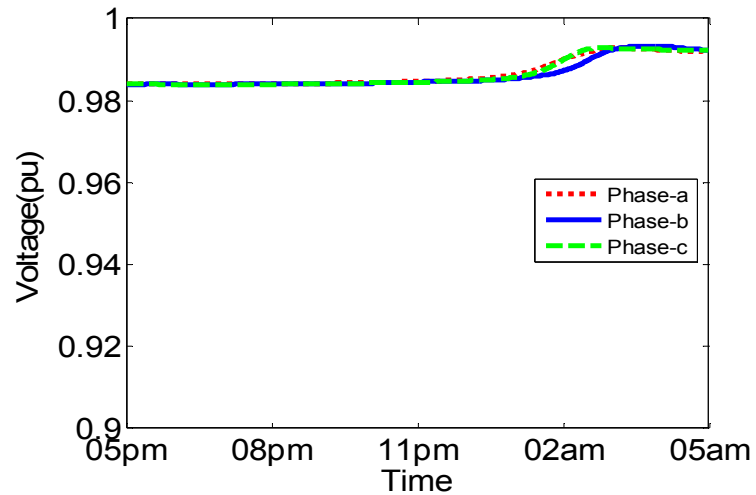


Figure 5-15 Voltage profile at node 2, using fair, SOC-dependent proportional control

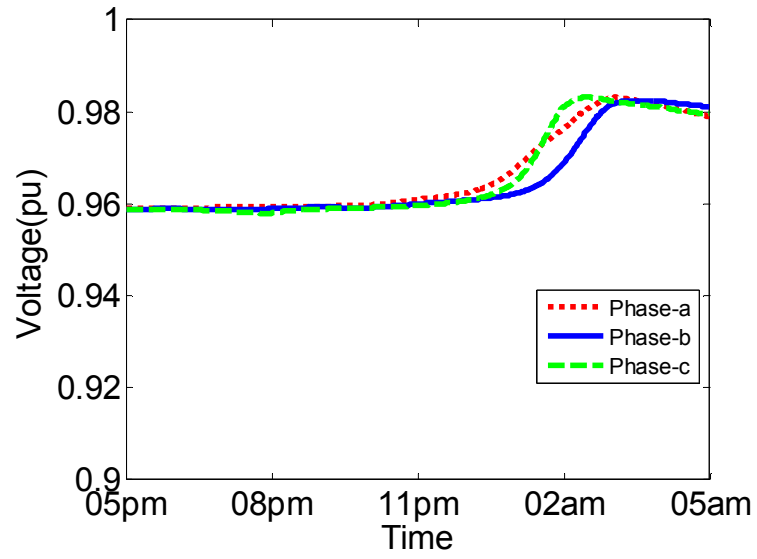


Figure 5-16 Voltage profile at node 6, using fair, SOC-dependent proportional control

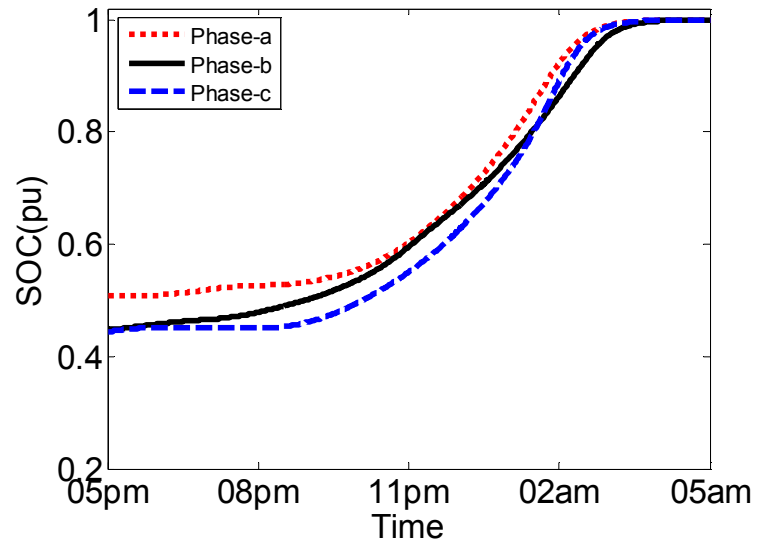


Figure 5-17 Average battery SOC at node 2, using fair, SOC-dependent proportional control

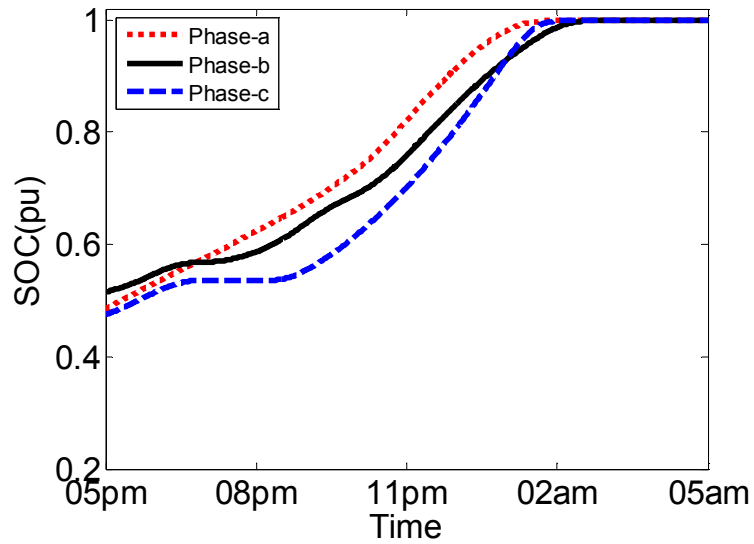


Figure 5-18 Average battery SOC at node 6, using fair, SOC-dependent proportional control

Table 5-2 summarizes the comparison in performance among the two different voltage feedback control cases: using flat reference voltages ($K_p = 20$) and using SOC-dependent fair charging ($K_p = 1000$). The results in Table 6-2 indicate the superiority of SOC-dependent charging in terms of closing the gap between the earliest and the latest times to full charge. Note that only the results corresponding to nodes 2 and 6 are shown. This is because they are the most extreme nodes in terms of the required time to full charge.

Table 5-2 Comparison in terms of average time to full charge

Control Scheme	Average time at Node 2 (hr)			Average time at Node 6 (hr)			Difference between earliest and latest (hr)
	Phase a	Phase b	Phase c	Phase a	Phase b	Phase c	
Flat V_{ref}	4.8	4.8	4.7	11.8	12	11.2	7.3
SOC-dependent	9.8	10.0	9.7	8.6	9.0	8.1	1.9

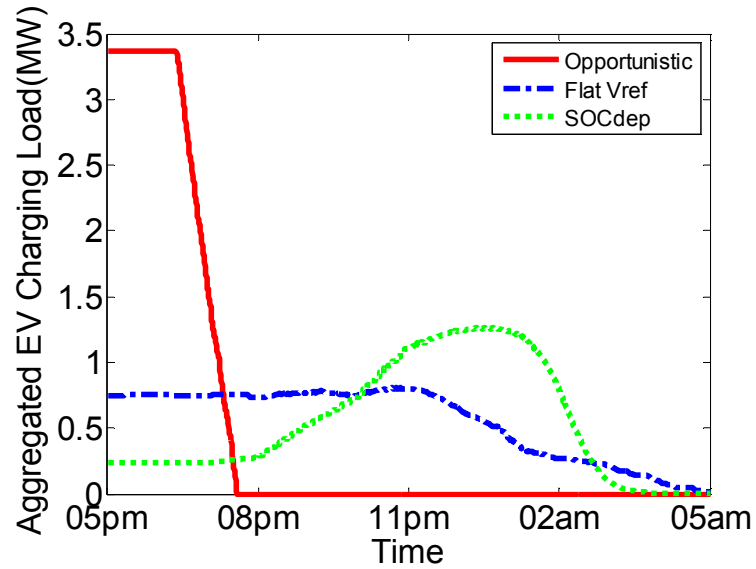


Figure 5-19 Aggregate EV charging load for the distribution system

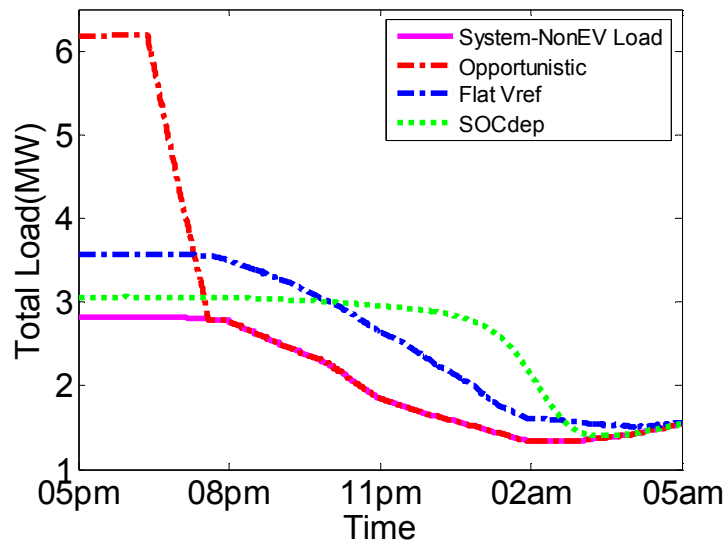


Figure 5-20 Total load (EV + non-EV) for the distribution system

Figure 5-19 and Figure 5-20 show a comparison in terms of the aggregate EV load and the total (EV and non-EV) load of the distribution system. The results demonstrate the effectiveness of the proposed control schemes in flattening the distribution system load profile.

5.2 Variable Plug-in Time for all EVs

The results in this section are for the case of variable plug-in time for EVs as described in section 4.3. Moreover, to add a more practical sense, all the following simulation results are based on the detailed distribution system modeling i.e. considering secondary network topology for node-2 and 6 as described in Section-4.1 (Figure 4-3).

5.2.1 Opportunistic Charging

The results of opportunistic charging are shown in Figure 5-21 to Figure 5-25. A significant jump is observed in the total load within the first several hours of charging. In addition, a voltage dip, considerably below the permissible limit of 0.95 pu, due to the sudden and un-controlled increase in loading is noticed at a number of primary nodes and secondary POCs.

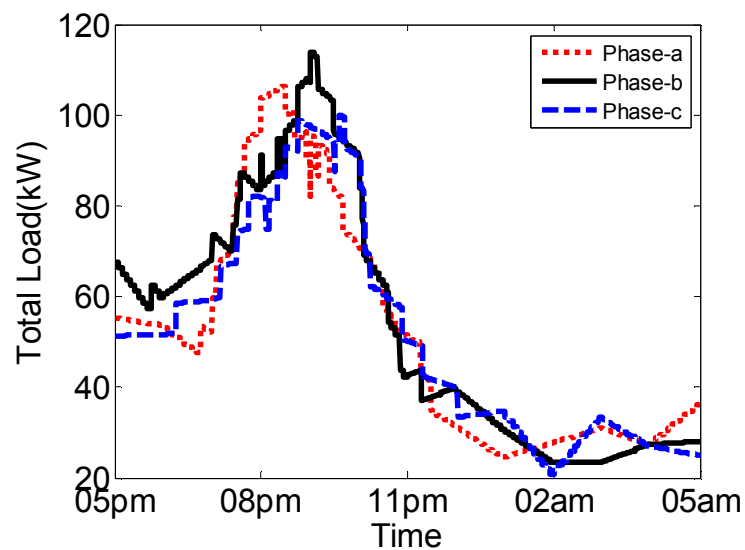


Figure 5-21 Total load at primary node 2 using opportunistic charging

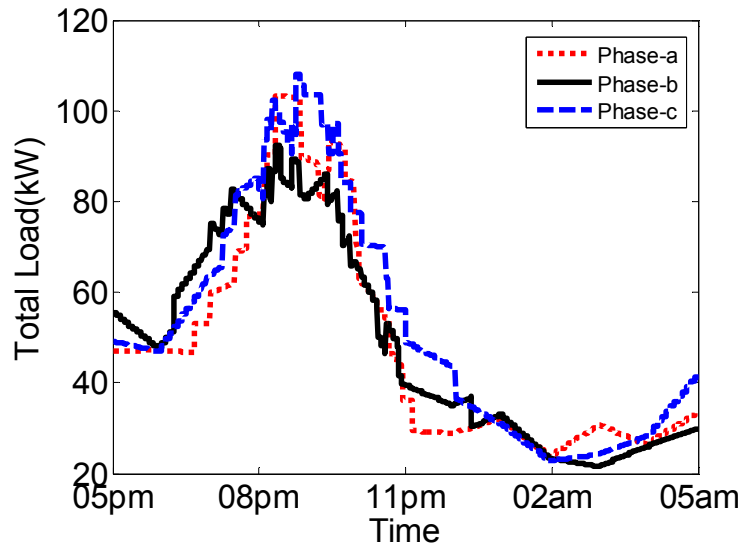


Figure 5-22 Total load at primary node 6 using opportunistic charging

Note that, in general, downstream primary nodes suffer from lower voltage levels than upstream primary nodes. Therefore, two extreme cases are the POC with the shortest secondary wire length connected to primary node 2 (labeled as POC A), and the POC with the longest secondary wire length connected to primary node 6 (labeled as POC B), are considered. And in order to make the comparison more appropriate, it has been ensured that EVs at both POCs have same initial SOC's and plug-in time. POC A is expected to have a very high POC voltage as compare to POC B.

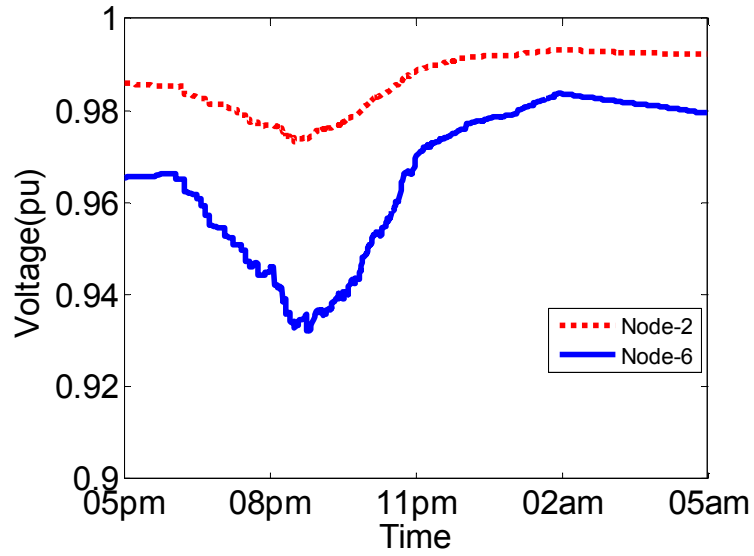


Figure 5-23 Voltage profile at Node-2 & 6 (phase-c), using opportunistic charging
 In the results that follow, more emphasis is going to be given to these two extreme cases.
 Note that the trend for SOC's are exactly similar for EVs at both POCs which is expected
 due to charging being opportunistic or dumb.

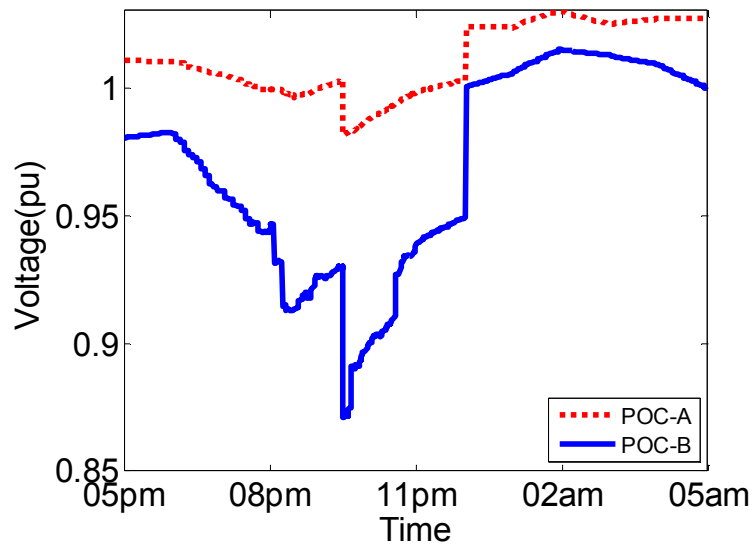


Figure 5-24 Voltage profiles for POC-A & POC-B, using opportunistic charging

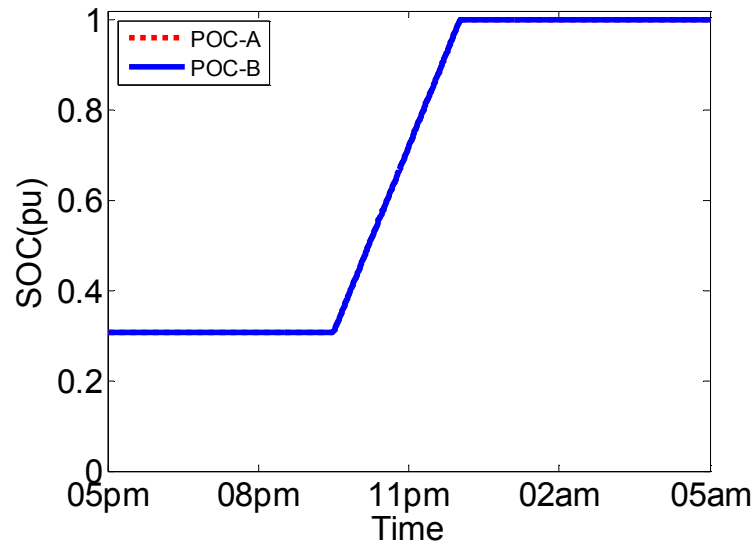


Figure 5-25 Battery SOC's for POC-A & POC-B, using opportunistic charging

5.2.2 Basic Proportional Control Charging and Flat V-reference

In this case, the voltage set points of all EVs in the system are set at a flat voltage reference of 0.955 pu. After several trials, the proportional gain is set to 50 for all EVs. At this value of gain, all EVs are charged fully before the end of the charging period, i.e. before 5 a.m.

Figure 5-26 to Figure 5-30 show the impact of using the proposed basic proportional control scheme on the performances at nodes 2 and 6. The results clearly show the effectiveness of this simple, distributed control scheme on enhancing the voltage profiles, both at the primary node level and at the secondary POC level.

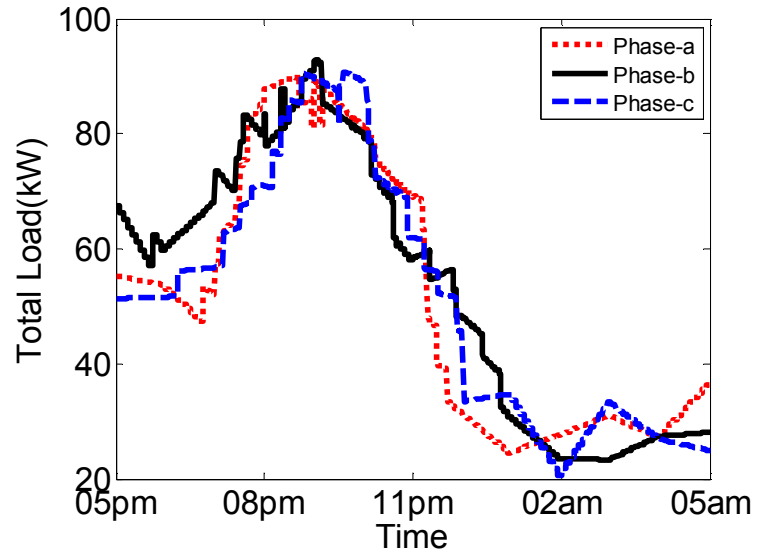


Figure 5-26 Total load at primary node 2 using basic proportional charging

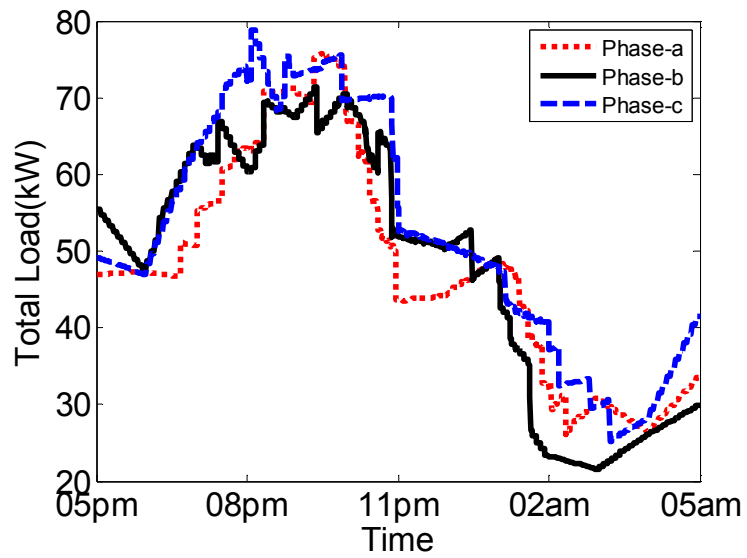


Figure 5-27 Total load at primary node 6 using basic proportional

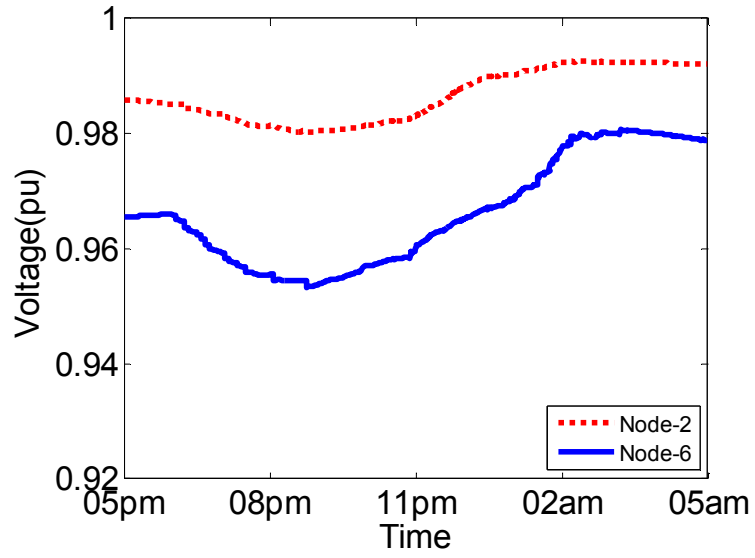


Figure 5-28 Voltage profile at Node-2 & 6 (phase-c), using flat V-reference

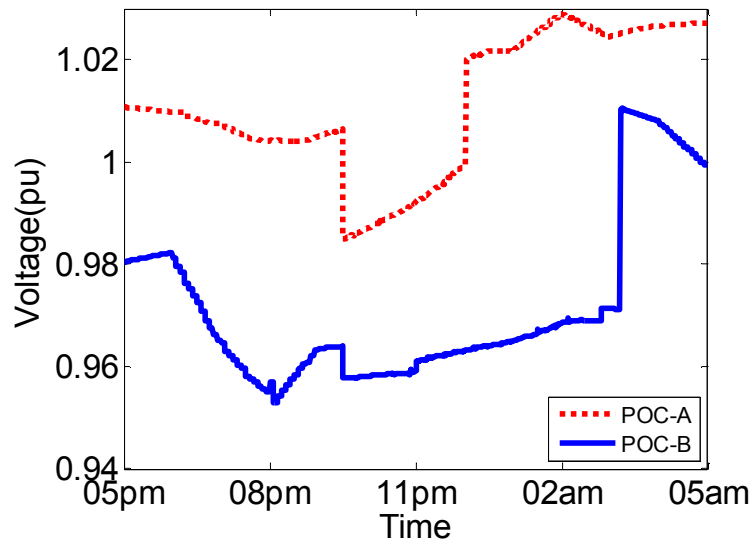


Figure 5-29 Voltage profiles for POC-A & POC-B, using flat V-reference

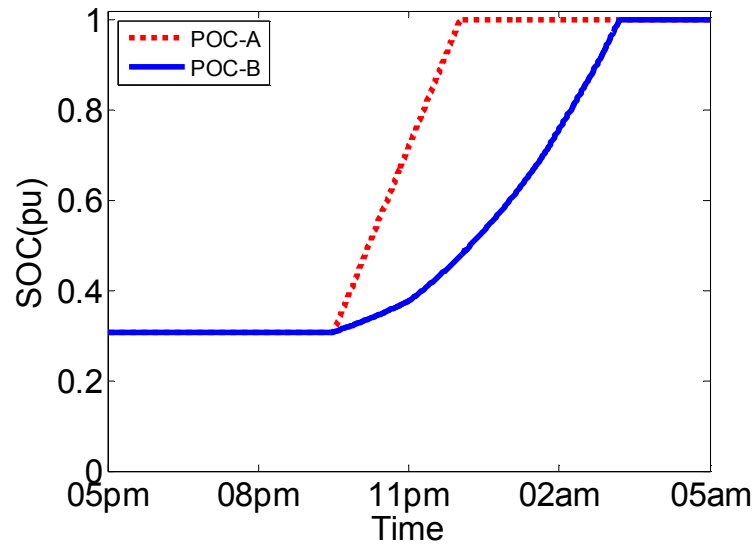


Figure 5-30 Battery SOC's for POC-A & POC-B, using Flat V-reference

5.2.3 Fair, SOC-Dependent Charging

Figure 5-31 and Figure 5-37 show the nodal loads, nodal voltage profiles, POC A's and B's voltage profiles and their SOC's, aggregated EV charging load, and total distribution system load due to the use of a more fair SOC-dependent control scheme at different K_p values. Comparing the SOC resulting from using the moving average voltage references to the SOC resulting from using a flat reference voltage clearly shows significant improvement in the level of fairness. In other words, the difference among the EVs in terms of how fast each of them fully charges, is significantly reduced. The results in this section are based on detailed model at node-2 and 6, so now every EV controller has its individual voltage reference. Table 5-3 represents the voltage reference values for some of the EVs at nodes 2 and 6.

Table 5-3 Voltage Set Points for Fair Charging for Sample EVs at Node-2 and 6

Node	Sample POC Voltage References
2	0.985, 1.017, 0.998, 1.019, 1.000
6	0.955, 0.988, 0.969, 0.991, 0.956

In addition to improving fairness among EVs across the distribution system, this control scheme results in flatter total system load profile and flatter voltage profiles during the period of intense charging. This can be explained by the fact that this control scheme allows for the use of a much higher controller gain that decreases gradually as SOC_{pu} gets higher. Note that although the focal point of this research is the distribution system, these load profiles indicate that this new scheme will also benefit the bulk power system by shaving the evening peak load through delaying some of the EV charging load to night and early morning hours.

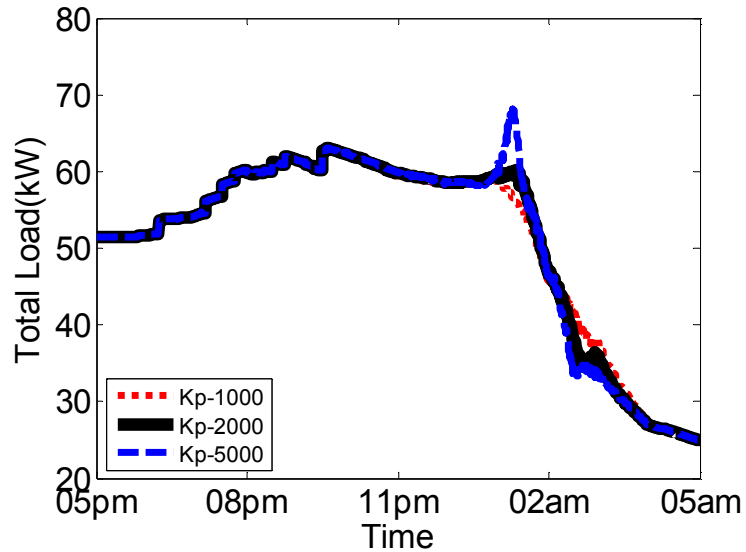


Figure 5-31 Total load at primary node 2-c using fair, SOC-dependent control

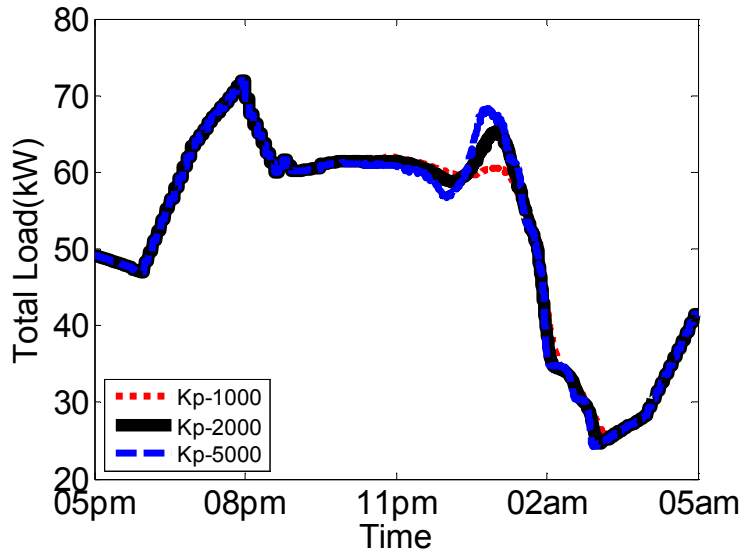


Figure 5-32 Total load at primary node 6-c using fair, SOC-dependent control

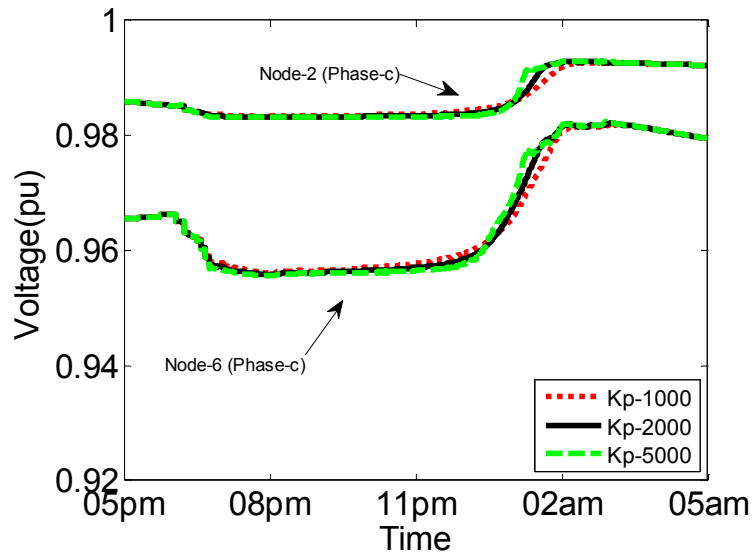


Figure 5-33 Voltage profiles at nodes 2-c and 6-c using fair, SOC-dependent control

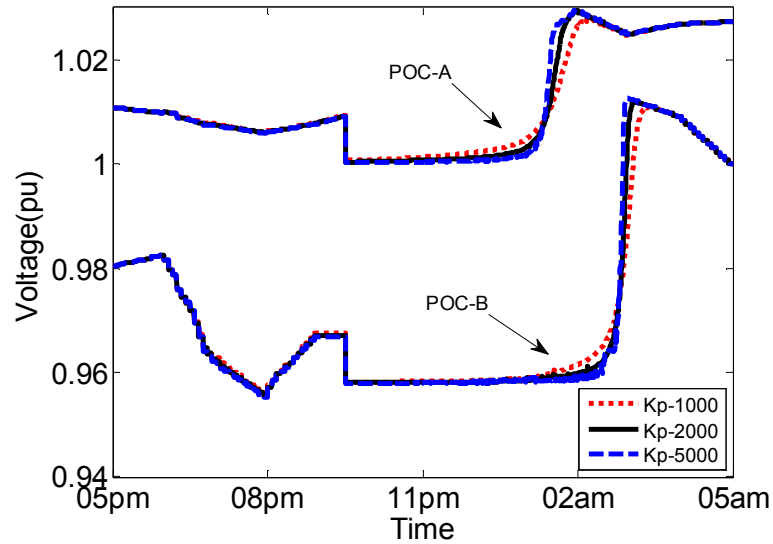


Figure 5-34 Voltage profiles for POCs A and B EVs using fair, SOC-dependent control

As can be seen from Figure 5-31 to Figure 5-37, a higher proportional gain results in faster EV charging, even flatter system aggregate load profile, and flatter voltage profiles during the period of intense charging. This stems from the fact that in proportional control a higher gain results in lower steady-state error, i.e. lower deviation from V_{ref} . On the other hand, the higher the gain, the faster the rise in voltage is toward the end of intense charging period. This is because a higher gain makes the EVs finish charging at closer time periods, which results in more abrupt transition from the period of intense charging to the period of no charging. In fact, one of the advantages of SOC-dependency is that it tends to slow down this abrupt transition. This is because as battery SOC gets higher, the effective controller gains get lower, hence the actual power drawn by each EV gets reduced. In addition, the fact that EV plug-in time is naturally random actually helps mitigate, to some extent, this transition issue. Still, the controller gain K_p should not be selected to be excessively high in order to avoid unwanted sudden overshoots in load

profiles (see Figure 5-32, for example) or even oscillatory responses. In the system under study, it is observed that at $K_p=6000$, simulations did not converge, an indication of stability issues.

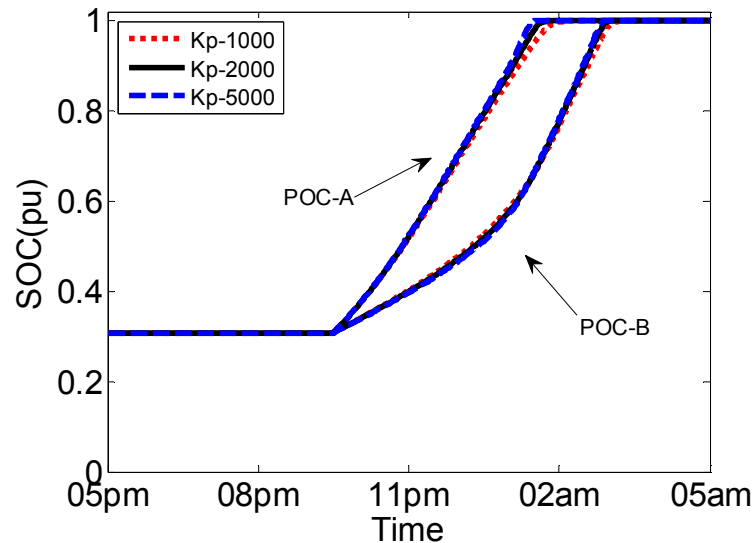


Figure 5-35 Battery SOC for POCs A's & B's EVs using fair, SOC-dependent control

Taking all these considerations into account, a value of $K_p=2000$ is recommended for this system. At this gain value, EV charging is reasonably fast and the voltage profiles are reasonably flat. The transition from period of intense charging to the period of no charging is acceptably smooth. In addition, a sufficient gain margin is maintained to avoid instability.

Note that although multiple tests are required to ensure proper controller tuning here, one important advantage of the proposed control scheme is that it consists of only a single parameter to be tuned. This significantly simplifies this tuning process.

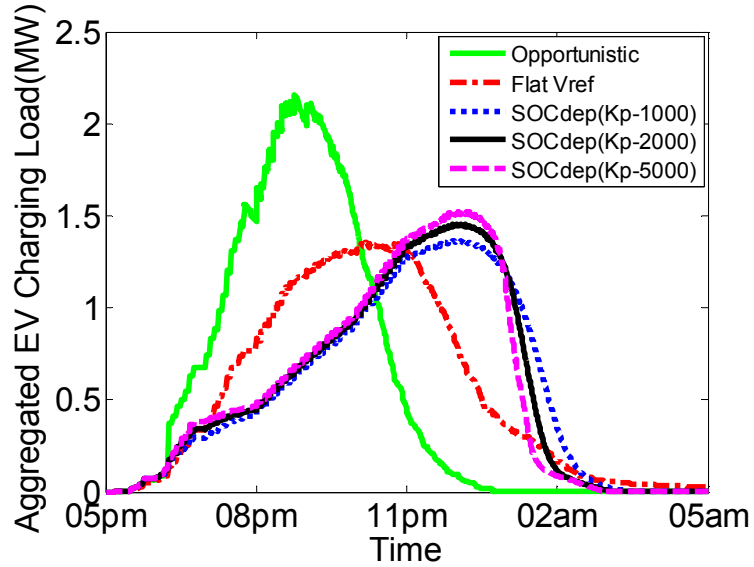


Figure 5-36 Aggregate EV charging load for the distribution system

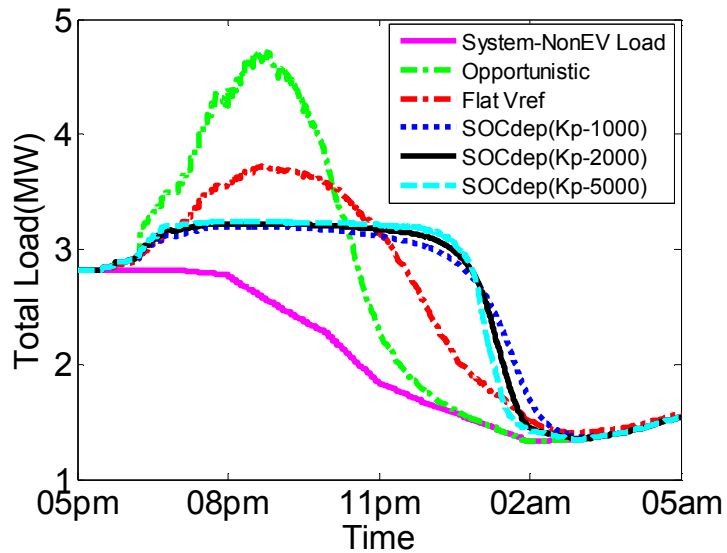


Figure 5-37 Total load (EV + non-EV) for the distribution system

Table 5-4 summarizes the comparison in performance among the two voltage feedback control schemes. These results indicate the effectiveness of SOC-dependent charging in closing the gap between POCs A's and B's times to full charge. Note that only the results corresponding to POC A and POC B are shown. However, the EVs at the other POCs follow a similar trend.

Table 5-4 Comparison in terms of time to full charge – Basic vs. SOC-dependent Schemes

Gain	Node-02	Node-06	Difference (hrs)
	POC A	POC B	
Flat V_{ref}	2.5	5.7	3.2
1000	5.4	6.0	0.8
2000	4.6	5.6	1.0
5000	4.2	5.4	1.2

CHAPTER 6

PERFORMANCE ANALYSIS OF PROPOSED CONTROL

In this section, the performance of the proposed fair, SOC-dependent EV charge control scheme is further studied. All the subsequent tests are carried out for the case of Fair and SOC-dependent charging with $K_p=2000$.

6.1 EV Penetration Level Test

The robustness of the proposed control scheme with respect to varying levels of EV penetration are assessed. Table 6-1 shows a comparison in terms of the time needed to fully charge the EVs at nodes 2 and 6. The average and latest charging times at phase c of the two nodes as well as the charging times for EVs connected to POCs A and B are shown for EV penetration levels of 40%, 50% (base case), and 60%. The results demonstrate reasonable tolerance of this control scheme to different levels of EV penetrations.

Table 6-1 Comparison in terms of time to full charge (in Hours) – SOC-dependent scheme at Different EV Penetration Levels

Penetration Level (%)	Node-02			Node-06		
	POC A	Mean Phase c	Latest	POC B	Mean Phase c	Latest
40	4.2	5.8	7.7	5.0	5.1	7.3
50	4.6	6.5	8.2	5.6	5.7	7.7
60	4.8	7.1	9.6	6.0	6.5	9.7

6.2 System Reconfiguration Test

The robustness of the proposed control scheme with respect to probable system reconfiguration is also studied. This is carried out by removing one representative peripheral node at a time from the distribution system to simulate switching that node onto an adjacent feeder during a reconfiguration event. Table 6-2 shows the corresponding charging times. These results confirm the robustness of the proposed scheme to moderate system reconfigurations.

Table 6-2 Comparison in terms of time to full charge (in Hours) – SOC-dependent scheme after Disconnecting a Peripheral Node

Node Removed	Node-02			Node-06		
	POC A	Mean Phase c	Latest	POC B	Mean Phase c	Latest
# 04	4.4	6.2	7.9	5.3	5.3	7.4
# 08	4.3	6.2	7.9	5.0	4.8	6.9
# 13	4.3	6.2	7.9	5.5	5.6	7.6
# 15	4.3	6.1	7.9	5.5	5.5	7.6
# 17	4.3	6.2	7.9	5.6	5.5	7.6

6.3 End of Charge Time Preference Test

An assessment of the performance of the charge control scheme due to an increase in the numbers of EV owners with preferred ECT is carried out as well. Figure 6-1 and Figure 6-2 show the test results for different percentages, 0% (base case), 10%, 30%, and 50%, of owners simultaneously having preferred ECT. For each EV with a preferred ECT, a random integer number between 3 and 6 hours is assigned. The results show that this control scheme can accommodate a moderate percentage of EV owners with preferred ECT. However, if that percentage is high, the control scheme cannot prevent voltage

violations. Nevertheless, the control scheme effectively manages to maintain a mild level of voltage violation even at a percentage that is as high as 50%. Note that all EVs with preferred ECTs are charged fully before the specified ECTs. These tests show that once the parameters are tuned, moderate changes in the network do not require retuning. This reduces the computational burden of implementing such a scheme.

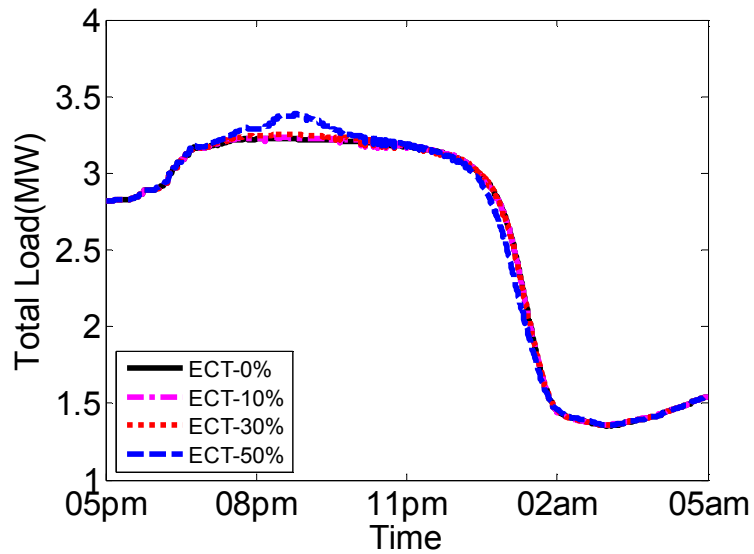


Figure 6-1 Total load for distribution system at different percentages of ECT preference

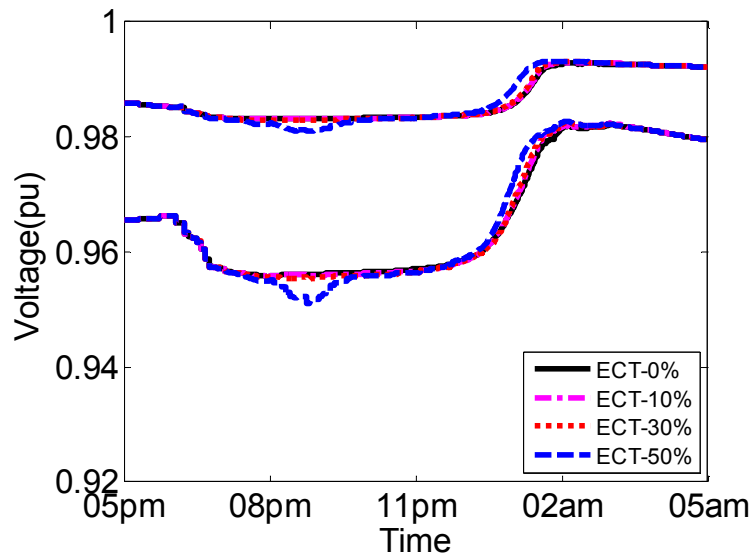


Figure 6-2 Voltage profiles at nodes 2 & 6 at different percentages of EV owners with preferred ECT

6.4 Voltage Sag Test

Finally, a voltage sag test is performed to ensure a stable response of the system with the proposed control scheme. When the voltage sag event is simulated, the voltage at node 1 (the most upstream node) is assumed to drop suddenly from 1.0 pu to 0.7 pu for a duration of 30 seconds. Due to the sag, it is also assumed that some non-EV loads are interrupted. This is simulated by a reduction in non-EV loads at all nodes by 25% for 90 seconds. The test results are shown in Figure 6-3 to Figure 6-4. Note that immediately after the voltage sag, the EV loads jump to very high levels. This is due to the voltage increase caused by the drop in the non-EV loads. This situation settles after a few minutes and the EV loads go back to normal levels.

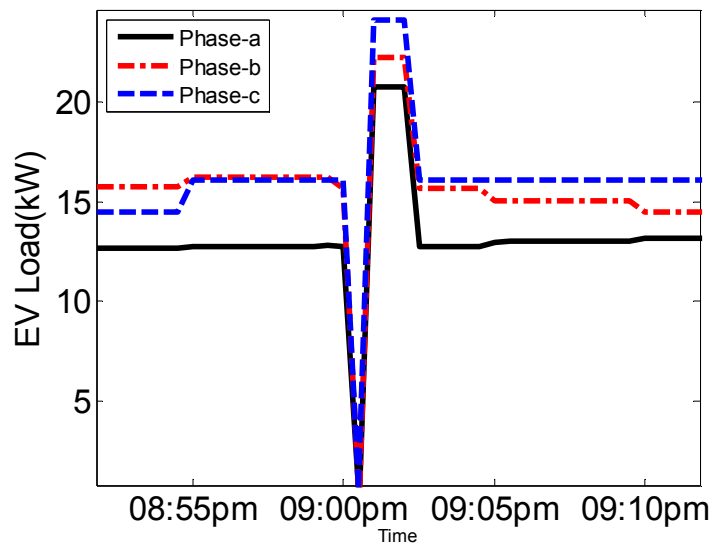


Figure 6-3 Total EV load at node 6 during the voltage sag test

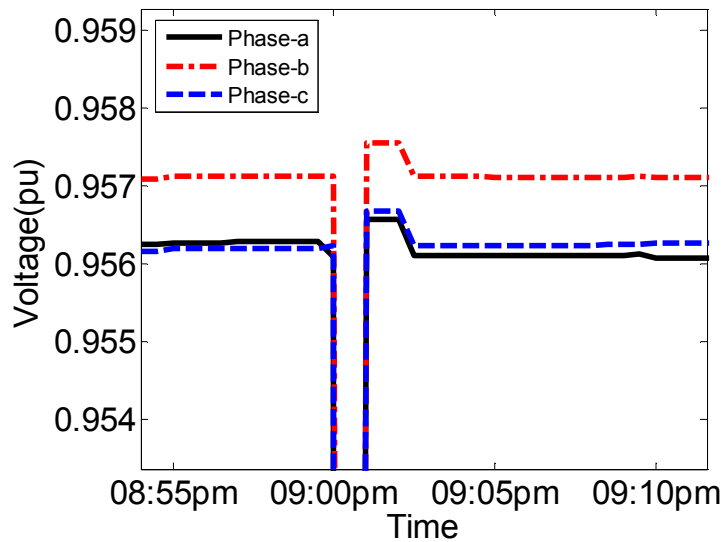


Figure 6-4 Voltages at node 6 during the voltage sag test.

6.5 Moving Average Test

It is noteworthy that using the moving average of the daily minimum voltages for the previous several days has the tendency of dragging V_{ref} at the POCs with low voltages further down over time. In order to prevent that from happening, V_{ref} at all POCs must be constrained. In this case study, V_{ref} is limited to be above 0.952. This effectively solves the voltage dragging issue not only at the low-voltage POCs but also at the higher voltage ones. For verification, a test is carried out for about two months. For this computationally-intensive test, the secondary network is assumed to be lossless in order to reduce the computation time. The voltage references for selected POCs have been recorded and plotted. Figure 6-5 and Figure 6-6 shows V_{ref} profiles for POCs at nodes 2 and 6 over this time horizon. These figures demonstrate the effectiveness of constraining V_{ref} at all POCs in solving this voltage dragging problem.

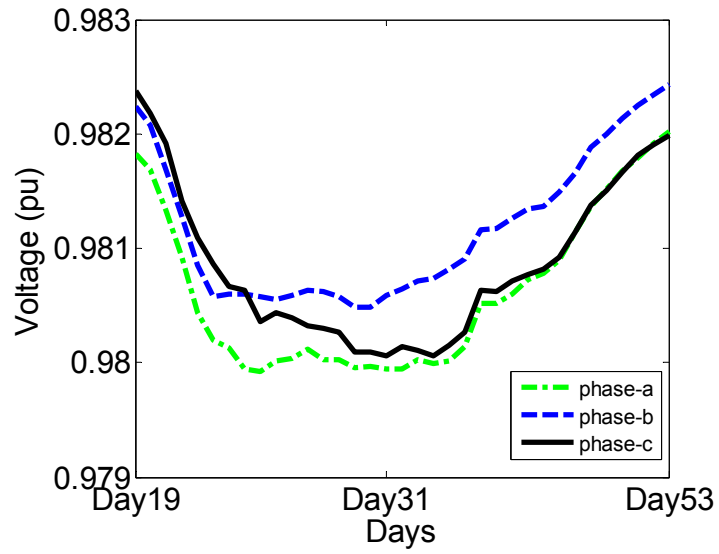


Figure 6-5 Vref profiles using moving averages constrained by 0.952, Node-2

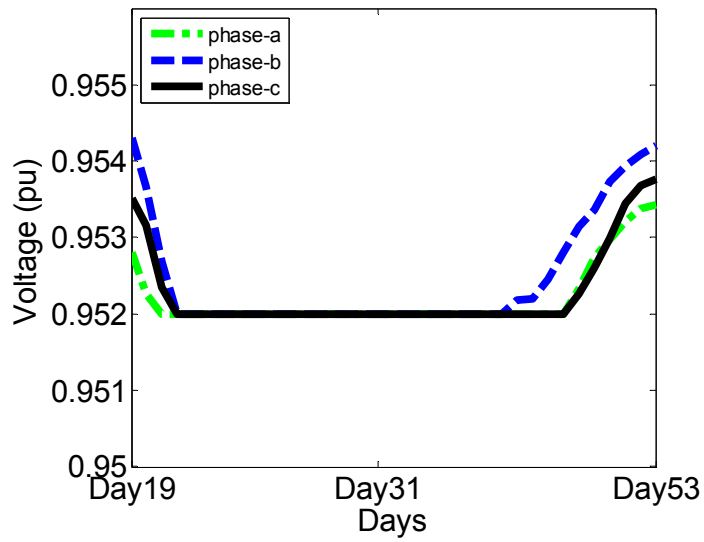


Figure 6-6 Vref profiles using moving averages constrained by 0.952, Node-6

CHAPTER 7

COORDINATION WITH VOLTAGE CONTROL DEVICES

Voltage control devices are commonly used to regulate the voltage of a distribution system within permissible limits all the time. The desired value of voltages can be obtained either by directly controlling the voltage or reactive power injection, which effectively improves voltage profile. The devices which are utilized for voltage control are on load tap changers (OLTC), switched shunt capacitors and step voltage regulator. This work will focus on the latter two voltage control devices. These devices work on the assumption that there is uni-directional power flow in the system and voltage decreases from the source towards the remote end or downstream feeder.

These devices are almost essential participants in a conventional distribution system. Therefore, it is quite logical to study the impacts of these devices over the proposed fair charging strategy because in real implementation the proposed EV charging strategy is expected to have a challenge of working efficiently in the presence of voltage control devices. Thus this chapter presents the analysis of coordinated operation of voltage control devices with the proposed charging strategy to understand and assess the effectiveness of the proposed charging strategy in the presence of voltage control devices.

7.1 Voltage Control with Voltage Regulator

A voltage regulator is a tap-changing auto-transformer with the ability to continuously monitor its output voltage and automatically adjusts itself by changing taps until the

desired voltage is obtained. A voltage regulator could be single phase or three phase with either 16 steps or 32 steps. The number of steps actually decide the per step voltage change; in case of 16 steps the per step voltage change is 0.00625 per unit while for 32 steps is 0.003125 per unit. This work has dealt with single phase 32-step regulators [61]

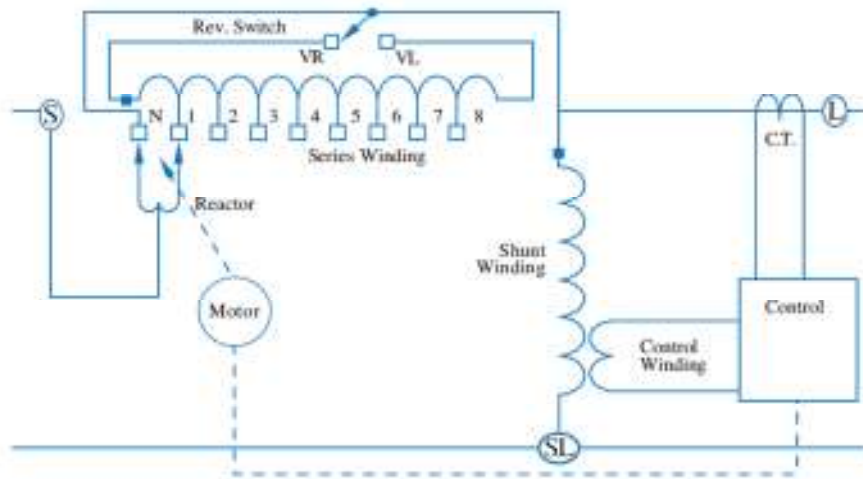


Figure 7-1 Basic circuit diagram for step voltage regulator [64]

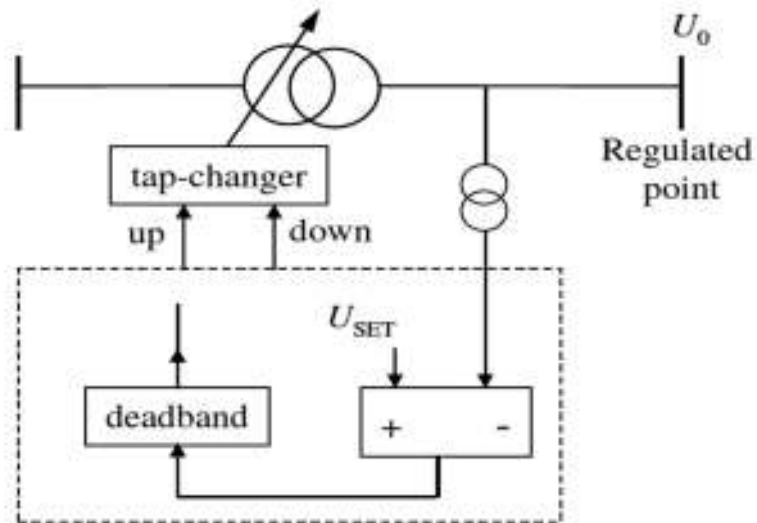


Figure 7-2 Controller for Step voltage regulator [65]

The voltage regulator basic arrangement is shown in Figure 7-1. The voltage regulator controller Figure 7-2 keeps the specified bus voltage U_0 constant within the range

$$U_{LB} < U_0 < U_{UB}$$

where,

$U_{LB} = U_{set} - U_{DB}$ is the lower boundary voltage

$U_{UB} = U_{set} + U_{DB}$ is the upper boundary voltage

U_{set} is the set point voltage

U_{DB} is the dead band (usually equals to per step voltage in per unit)

Normally, this simple arrangement of voltage regulator is installed just at the point where voltage needs to be maintained within specified limits. However, if there is a cable or conductor connection between the voltage regulator and the point where voltage needs to be maintained, then another arrangement is used which contains a line drop compensation function. For simplicity and without loss of generality, the former case is assumed in this work.

7.1.1 Simulation Results

The voltage regulator is applied on the most upstream node (Node#2) and the two downstream nodes (Node#5 & 6) one at a time. The voltage regulator controller settings are based on three factors; these factors are set as follows:

Voltage Set point:

It is the set point which the utility desired to maintain at the node. For this study it is selected as 0.99 per unit.

Step Voltage:

It is the amount of change in voltage caused by one step. This study is focused on 32 steps regulator, so the step voltage is 0.003125 per unit.

Bandwidth:

The amount of variance allowed in voltage before regulator changes tap. This is selected as 0.003125 per unit.

The application of voltage regulator has caused the voltage references for the EV charge controller to change considerably. Now the voltages for the last fourteen days are calculated by activating the voltage regulator controller. This calculation has to be performed for every scenario. For this work we have three scenarios, one is to have a voltage regulator at node # 2, second at node # 5 and third at node # 6. The results of these cases are as follows and compared with the base case (Figure 7-3, Figure 7-4 and Figure 7-5). This is to analyze that how the inclusion of voltage regulator has impacted the charging fairness, voltage profile and EV power draw.

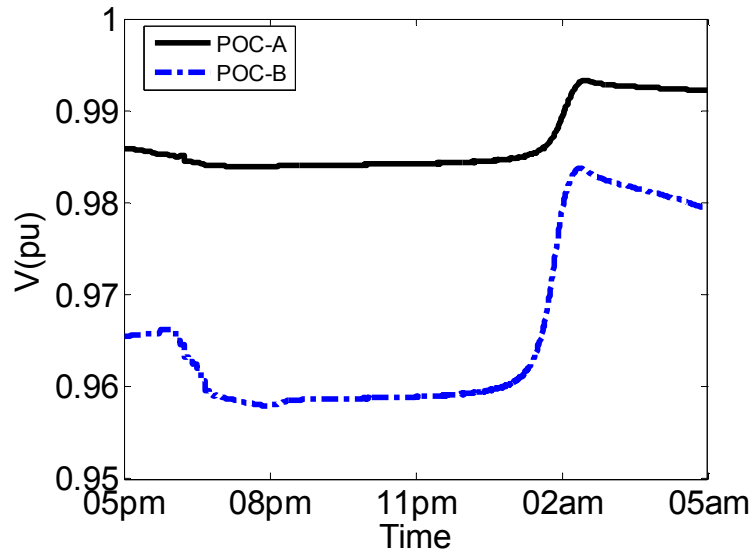


Figure 7-3 Voltages at POC-A and B without voltage control devices

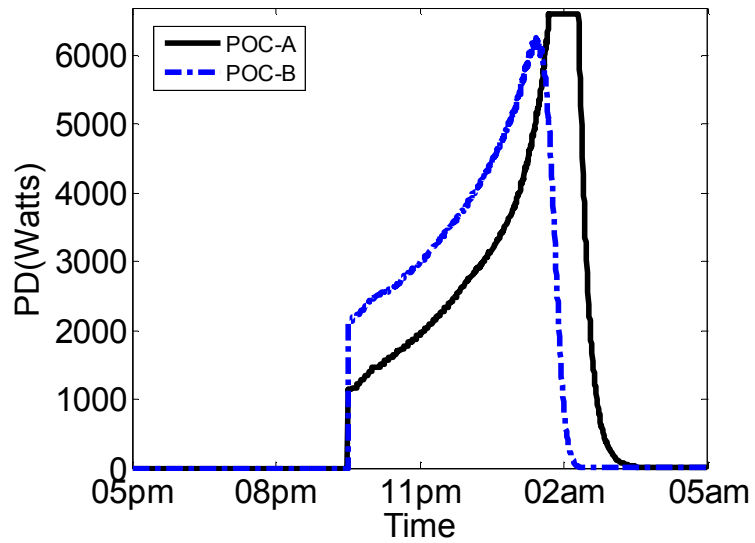


Figure 7-4 Power draw for EVs at POC-A & B without voltage control devices

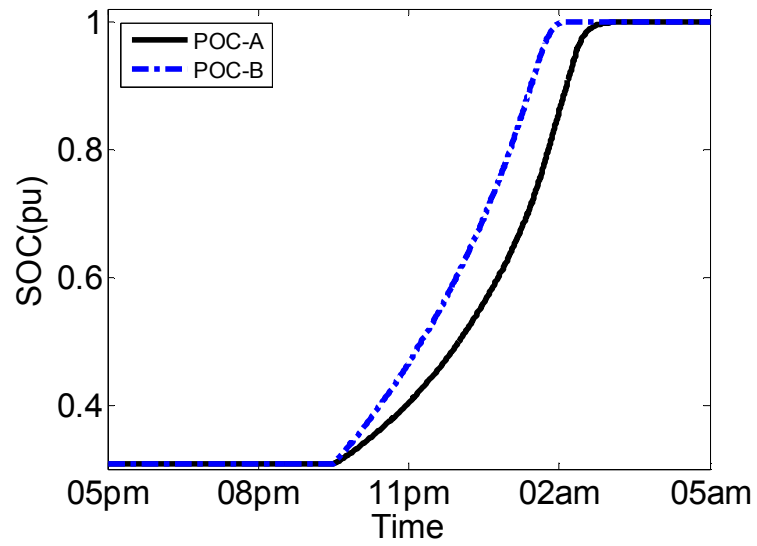


Figure 7-5 Battery SOC for POCs A's & B's without voltage control devices

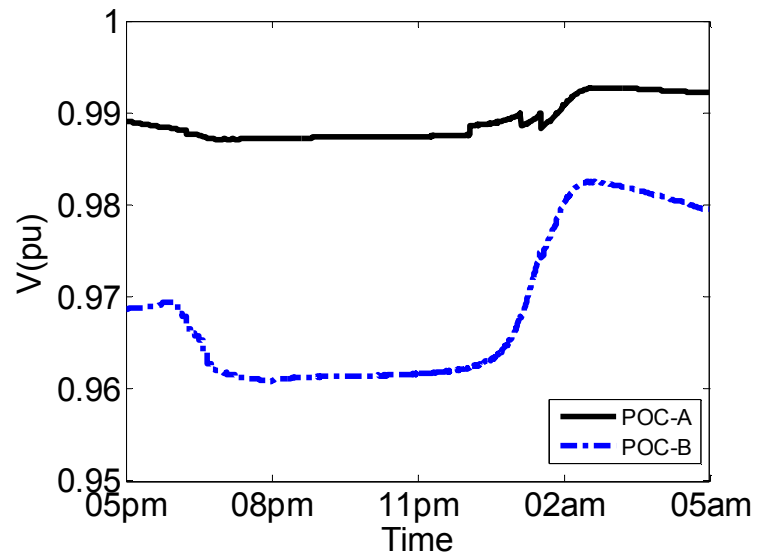


Figure 7-6 Voltages at POC-A and B, voltage regulator at Node-2

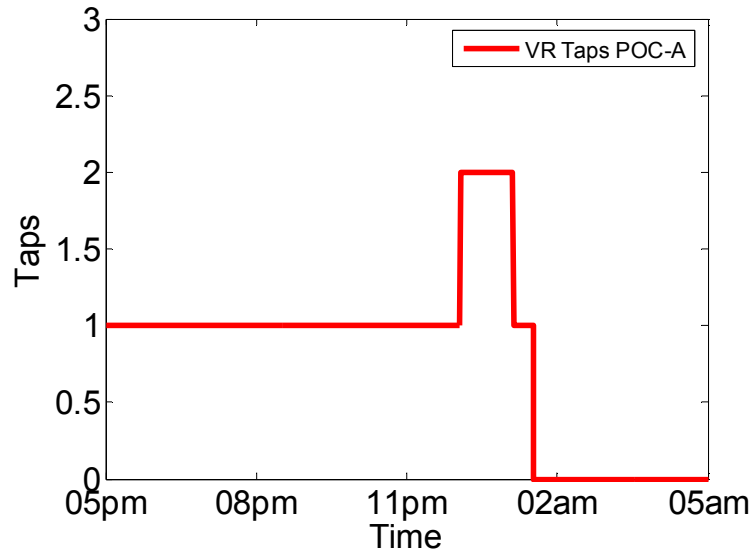


Figure 7-7 Taps for Voltage regulator at Node-2

Figure 7-6 shows the voltages at POC-A and POC-B, it is evident that installation of voltage regulator at node # 2 has increased the voltage on both node # 2 and 6 as compare to the base case (Figure 7-3). It is noteworthy that since the voltage at node # 2 was already near to the desired set point of 0.99 per unit, the change from the base case is not quite considerable. Hence, Figure 7-7 shows only a maximum two steps change in voltage regulator.

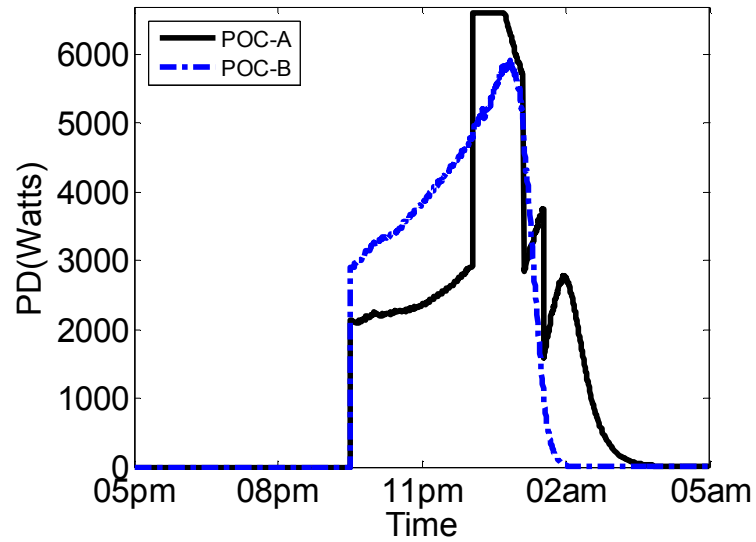


Figure 7-8 Power draw for EVs at POC-A & B, voltage regulator at Node-2

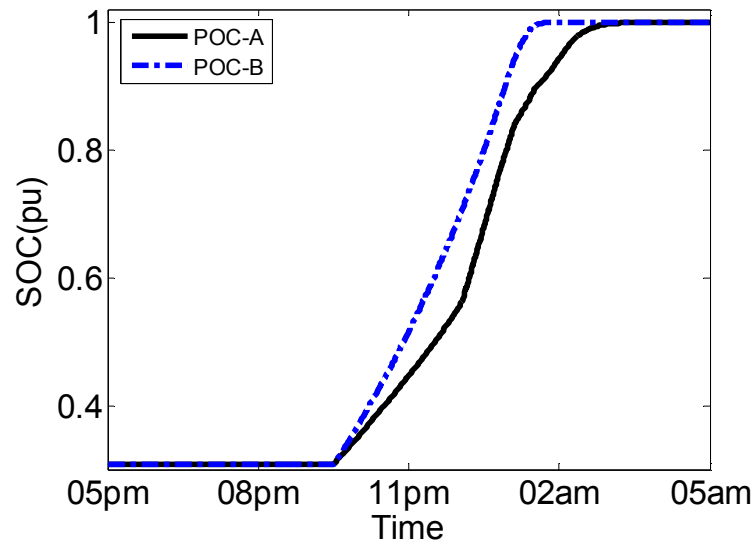


Figure 7-9 Battery SOC for POCs A's & B's, voltage regulator at Node-2

By comparing Figure 7-8 with base case, Figure 7-4, it can be seen that improvement in the voltage profile has caused an increased in power draw on both POC for the initial hours but as soon as the $1 - SOC_{i,pu}$ factor becomes considerable it controls the power draw to maintain the fairness between the EVs at both POCs. A jump can be observed in PD of POC-A, this is the point where regulator adjusts its steps. After the jump, the

voltage itself maintains its value within permissible range due to decrease in the load profile and then $1 - SOC_{i,pu}$ factor smoothens the PD, as expected. The difference between charging at POC-A and POC-B is increased but still the increase is not very significant and fairness level is maintained as required. When the voltage regulator is installed at Node # 5, it can be seen from Figure 7-14 that voltage at POC-B has increased considerably as the difference between actual voltage at POC-B and set point of 0.99 per unit was quite appreciable and hence the regulator has to increase larger steps to achieve desired voltage.

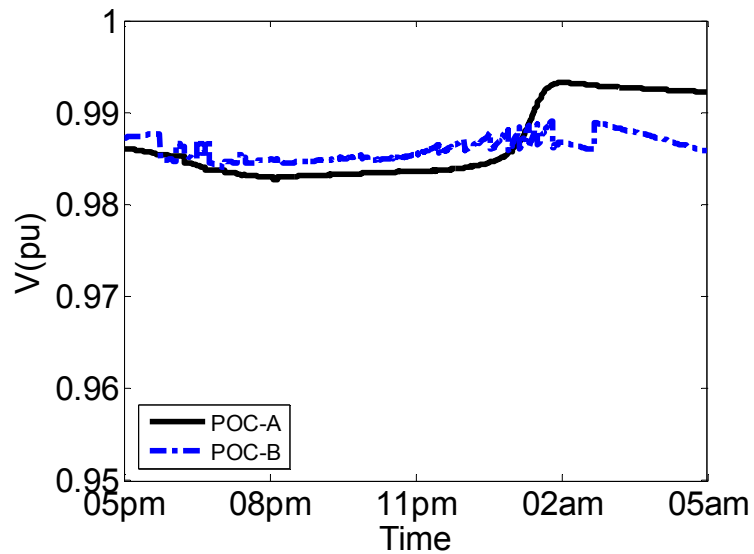


Figure 7-10 Voltages at POC-A and B, voltage regulator at Node-5

An important fact is revealed by the power draw curve Figure 8-12 that application of voltage regulator at a downstream node will have more impact towards the resulting power draw at the node where it is applied and consequently the initial increase in the power draw has caused a linear increase in SOC. After-wards, the $1 - SOC_{i,pu}$ factor plays its part. The POC-A seems to be almost not influenced by application of voltage regulator

at POC-B. The SOC curves in Figure 8-13 show fairness which is not much different from the base case (Figure 8-5).

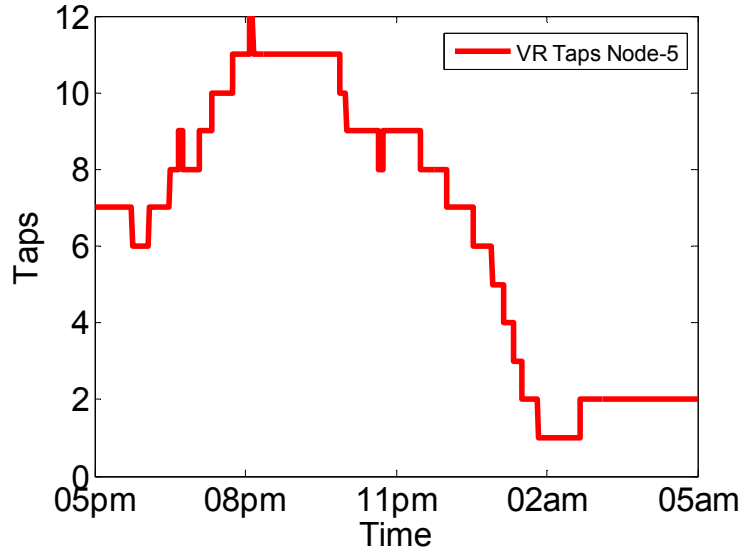


Figure 7-11 Taps for Voltage regulator at Node-5

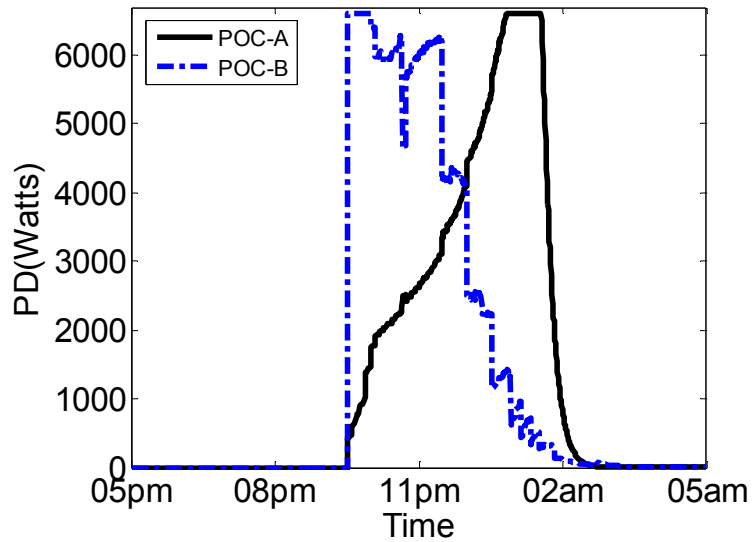


Figure 7-12 Power draw for EVs at POC-A & B, voltage regulator at Node-5

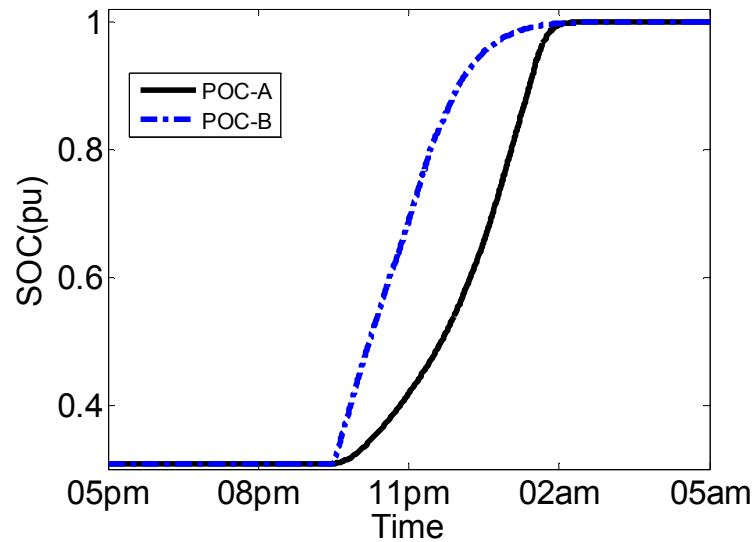


Figure 7-13 Battery SOC for POCs A's & B's, voltage regulator at Node-5

The application voltage regulator at node # 6 also brought forward trends and observations similar to the application of voltage regulator at node # 5, as shown in Figure 7-14 to Figure 7-17. It is worth mentioning here that with reference to the distribution system topology (Figure 4-1) that installation of voltage regulator is much realistic and economical than installing at node # 6. The reason is quite simple that the voltage regulator at node # 5 improves the voltage profile at node # 5, 6, 7 & 8; however installation of voltage regulator at node # 6 only improves its own voltages.

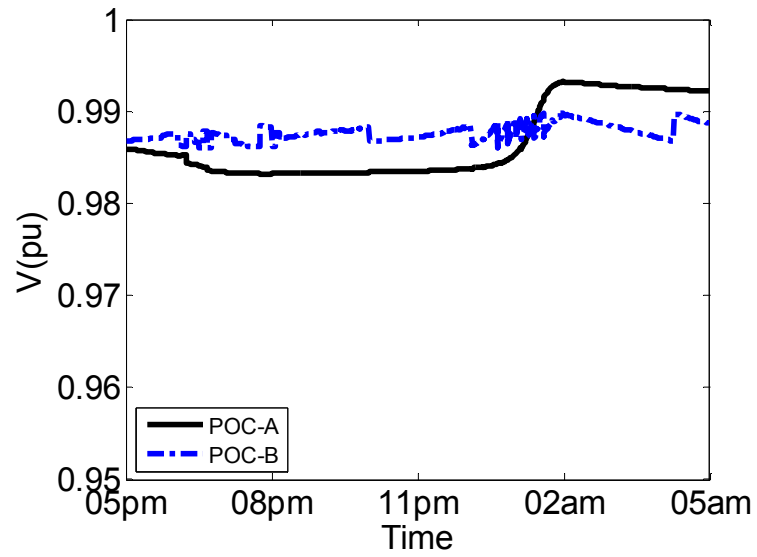


Figure 7-14 Voltages at POC-A and B, voltage regulator at Node-6

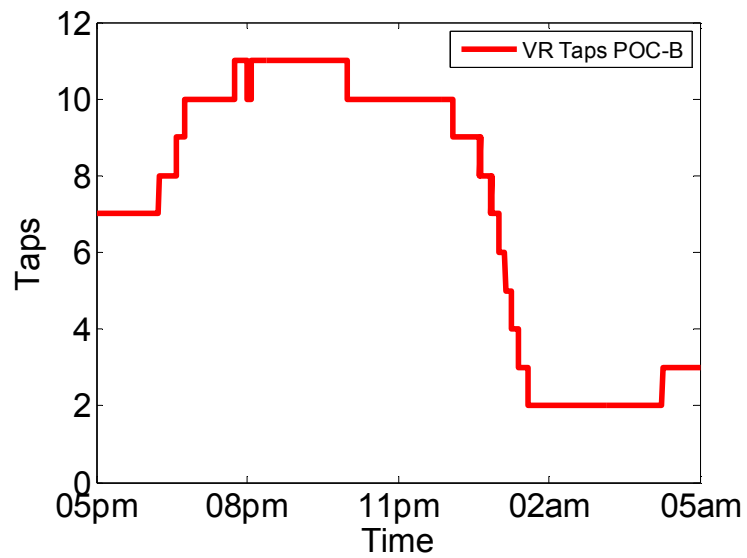


Figure 7-15 Taps for Voltage regulator at Node-6

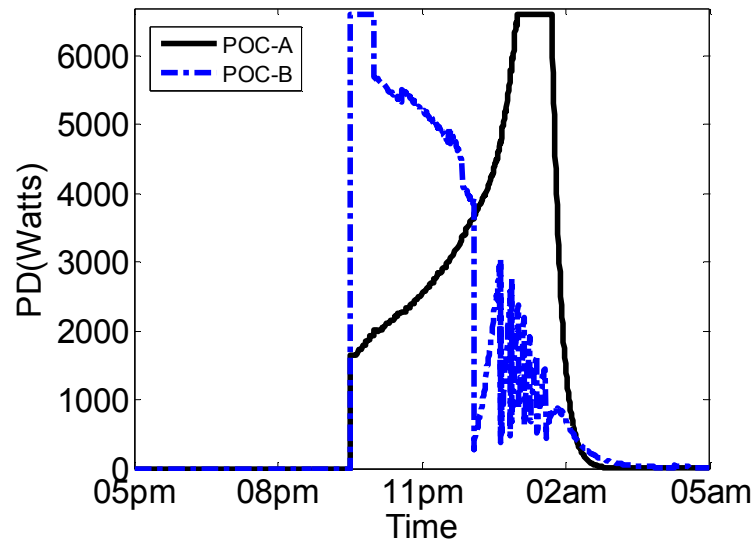


Figure 7-16 Power draw for EVs at POC-A & B, voltage regulator at Node-6

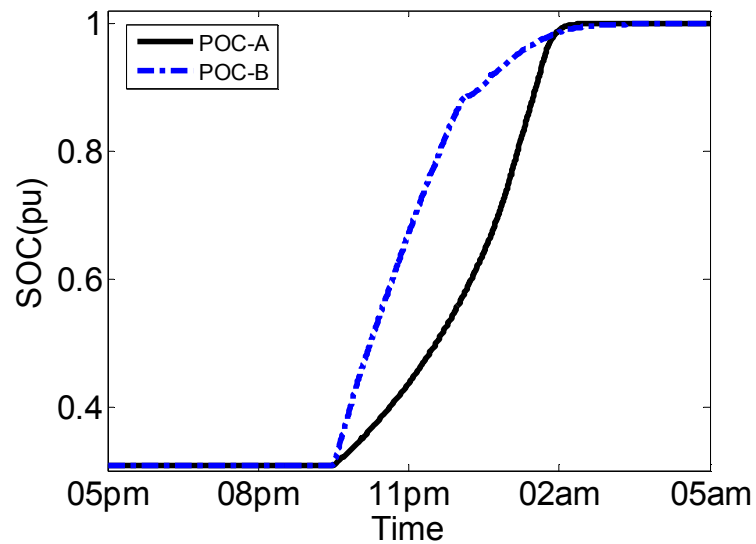


Figure 7-17 Battery SOC for POCs A's & B's, voltage regulator at Node-6

Figure 7-18 shows that installation of voltage regulator at nodes-2, 5 and 6 has increased the overall EV load up to almost 1 AM and then it dropped smoothly because of SOC

dependency. This shows and depicts the fact the installation of regulator in a radial distribution system, irrespective of its location (either at upstream and downstream) increases the power draw on all the nodes and hence resulted in an overall increase in EV charging load. Figure 7-19 shows that increase of EV charging load in early hours has caused an increase in the peak loading. These results show that the proposed charging strategy works fine in the presence of voltage regulator.

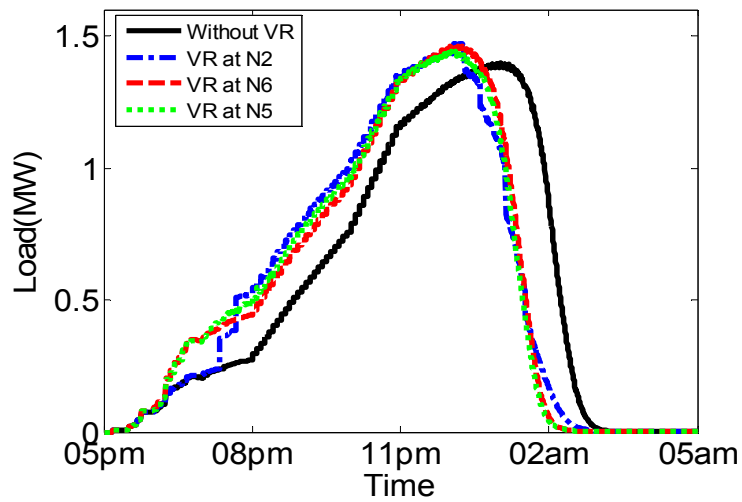


Figure 7-18 EV load comparison with and without voltage regulators

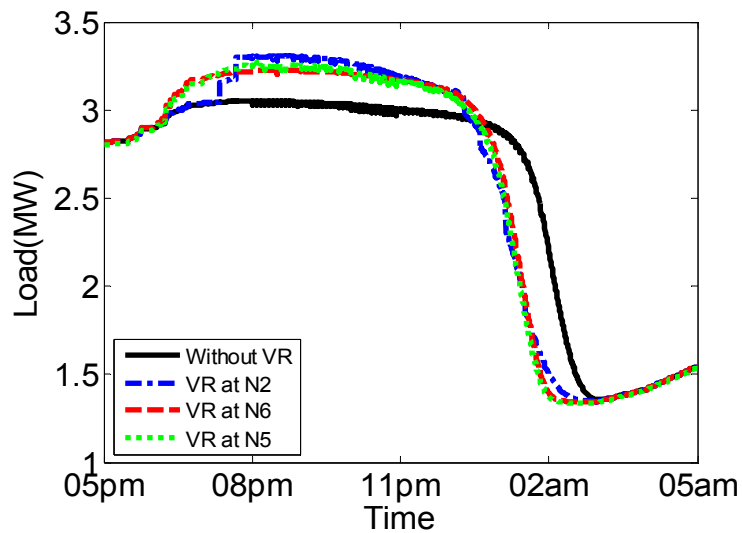


Figure 7-19 Total (EV+Non EV) load comparison with and without voltage regulator

7.2 Voltage Control with Shunt Capacitors

Shunt capacitors inject reactive power to the system according to [65]

$$Q_C = Q_{C, \text{rat}} * U_C^2$$

where

Q_C is the reactive power injected by the capacitor in Mvar

$Q_{C, \text{rat}}$ is the Mvar rating of the capacitor

U_C is the voltage in pu (relative to the capacitor voltage rating).

The reactive power injected by the capacitor will compensate the reactive power demand and thereby boost the voltage. Consider that a shunt capacitor injecting reactive power Q_C is connected to the load bus. The voltage drop on the feeder can then be approximated as [65]

$$U = (R_{LN} * P_L + X_{LN} * (Q_L - Q_C)) / U_2$$

which indicates that the capacitor reduces the voltage drop. Further, when the capacitor properly compensates the reactive power demand, the capacitor will decrease the feeder current. This will in turn decrease the feeder losses P_{Loss} .

In order to properly compensate the reactive power demand that changes from minimum to maximum, the shunt capacitor may need to be switched on at the load maximum and to be switched off at the load minimum. When the load varies during the day, the switched capacitors should be properly controlled. Different conventional controls can be used to control switched capacitors, such as time, voltage and reactive power [65]. Time controlled capacitors are especially applicable on feeders with typical daily load profiles in a long term where the time of the switching-on and off of the shunt capacitor can be predicted. The main disadvantage of this control is that the control has no flexibility to

respond to load fluctuation caused by weather, holidays, etc. Voltage controlled capacitors are most appropriate when the primary role of the capacitor is for voltage support and regulation. Reactive power controlled capacitors are effective when the capacitor is intended to minimize the reactive power flow. This work utilizes the voltage controlled shunt capacitors.

For the simulation of automatic voltage controlled shunt capacitor, an appropriate step voltage setting needs to be determined. For this purpose an initial study can be performed for a fixed value shunt capacitor by switching it in for the entire study period and then measuring the difference in voltage with reference to the case without shunt capacitor.

The voltage controlled shunt capacitors are switched in when the measured voltage is less than the desired value beyond the specified bandwidth / dead band. The resulting difference is then divided by the step voltage value to get the required number of steps of shunt capacitors to be switched in. In order to avoid an unnecessary increase in the voltage the result of division is floored to be on the safe side.

7.2.1 Simulation Results

The switched shunt capacitors have also been applied at Node-2 and Node-6, one at a time. The total available capacity is assumed to be 1 MVar for each of the nodes. For node-2 each capacitor step is assumed to be 0.1 MVar which causes a voltage change of about 0.0007 per unit; a separate simulation is carried out to investigate the voltage changes caused by the insertion of one step capacitance. For node-6 the each capacitor step is taken to be 0.01 MVar, the step is reduced because a step of 0.1 MVar causes a

change of 0.007 per unit voltage which is a very large value. The step size of 0.01 MVar causes a step change of 0.0007 per unit. The shunt capacitor controller settings are:

Voltage Set point

It is the set point which the utility desires to maintain at the node. Selected as 0.995 pu.

Step Capacitor (Step Voltage)

It is the amount of reactive power injected by one shunt capacitor. The resultant voltage change can be termed as step voltage. For both node-2 and 6, it is 0.0007 per unit.

Bandwidth

Bandwidth is the amount of variance allowed in voltage before the capacitor switches in.

It is set equal to step voltage.

The case of shunt capacitors also requires re-calculating the voltage references just like the case of voltage regulators.

Figure 7-20 shows a similar trend to that shown in Figure 7-6 (POC voltages for VR at node-2). Figure 7-21 shows that shunt capacitors are utilized to their full capacity to maintain the voltage and remaining job has been carried out by the EV charging control strategy and hence the resultant voltage profile tries to be at the desired value of 0.995 pu. Most capacitors switched off in the period of low loading as expected.

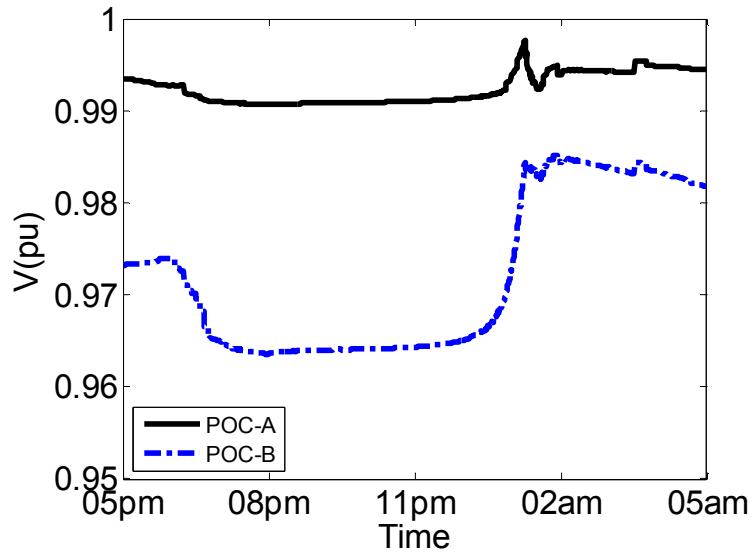


Figure 7-20 Voltages at POC-A and B, shunt capacitors at Node-2

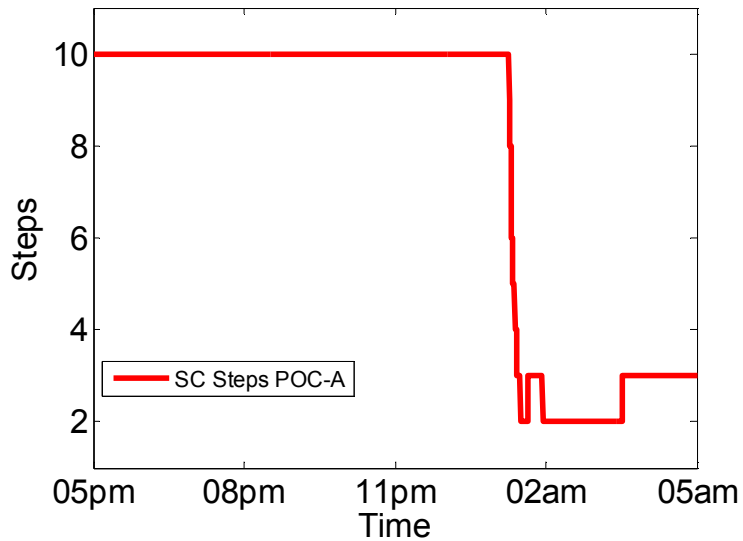


Figure 7-21 Shunt capacitor steps Node-2

Again Figure 7-22 and Figure 7-23 show similar trend as Figure 7-8 and Figure 7-9. The results show that installation of switched shunt capacitors at node-2 coordinated with EV charging strategy increased the power draw in the initial period of charging but overall fairness is undisturbed.

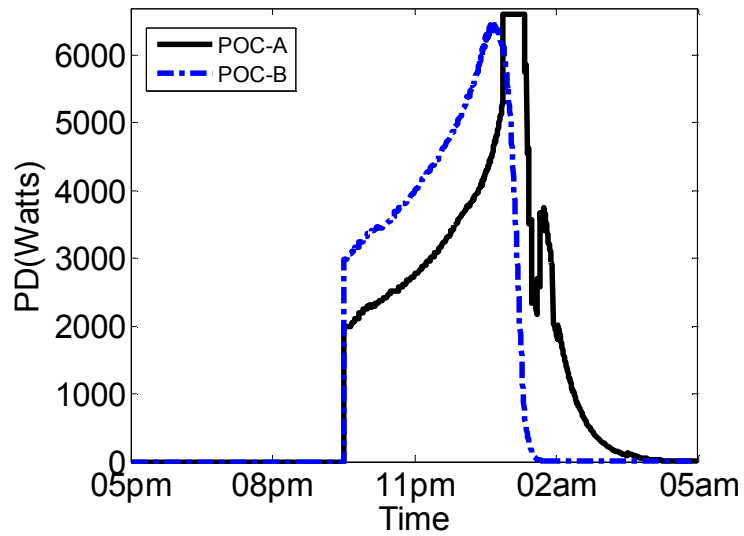


Figure 7-22 Power draw for EVs at POC-A & B, shunt capacitor at Node-2

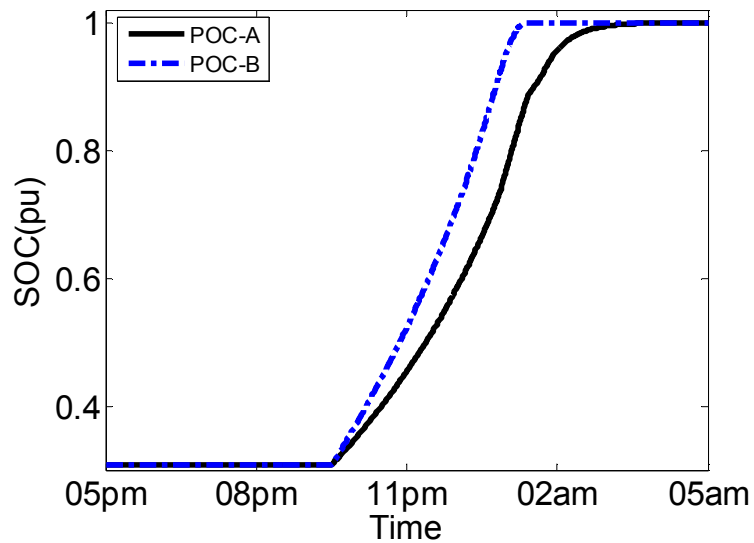


Figure 7-23 Battery SOC for POCs A's & B's, shunt capacitor at Node-2

An overall analysis of the Figure 7-24 to Figure 7-27 revealed that the trend similar to shunt capacitor installation at node-2. The shunt capacitors are utilized to their maximum in the period of intense EV charging and heavy Non-EV loading and then the capacitors

gradually switched off. The power draw curve, however shows that shunt capacitor installation at node-6 produced an appreciable change in PD at POC-B while POC-A has affected negligibly.

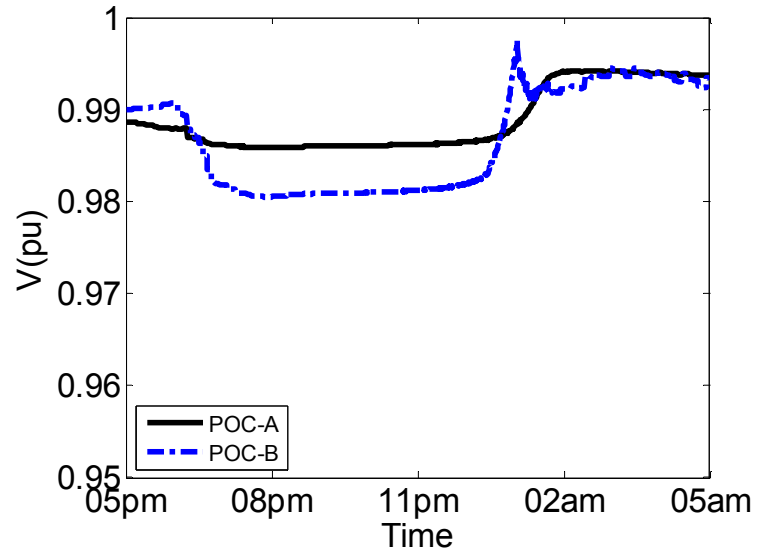


Figure 7-24 Voltages at POC-A and B, shunt capacitors at Node-6

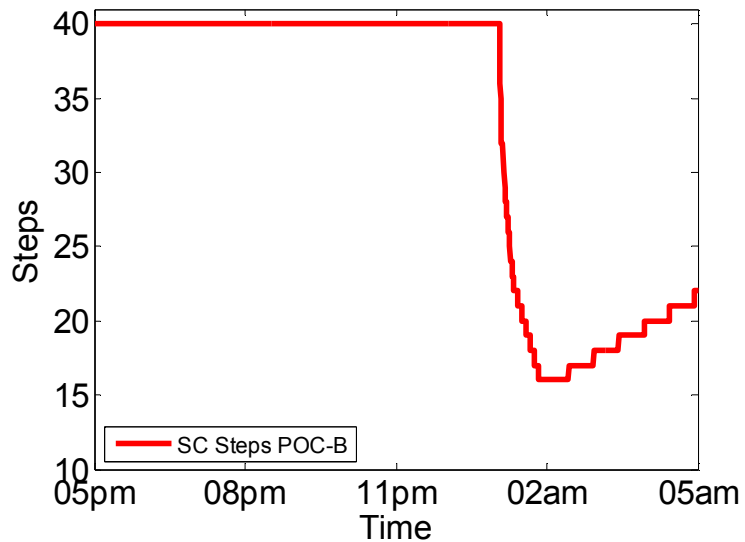


Figure 7-25 Shunt capacitor steps Node-6

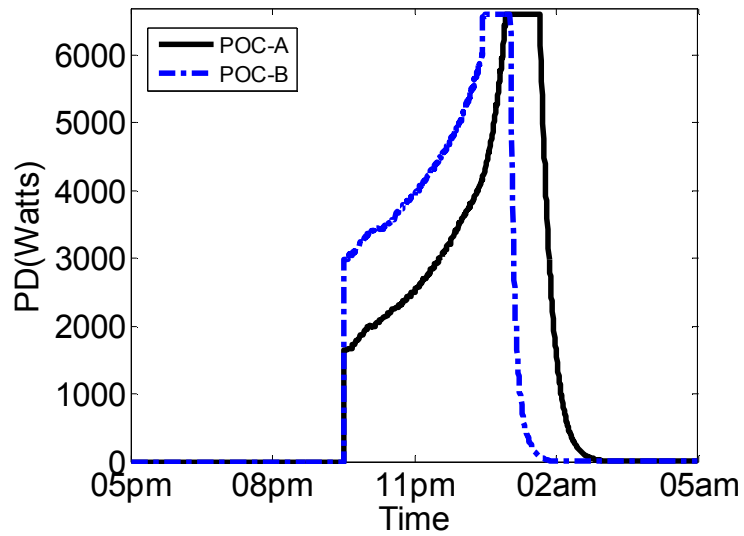


Figure 7-26 Power draw for EVs at POC-A & B, shunt capacitor at Node-6

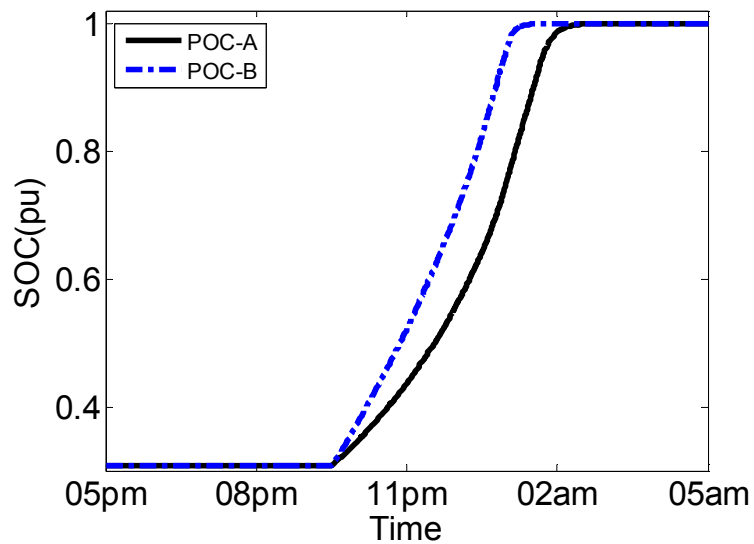


Figure 7-27 Battery SOC for POCs A's & B's, shunt capacitor at Node-6

Figure 7-28 and Figure 7-29 shows that installation of shunt capacitors at each of the nodes have increased the overall EV load up to almost 1 AM and then it dropped smoothly because of SOC dependency.

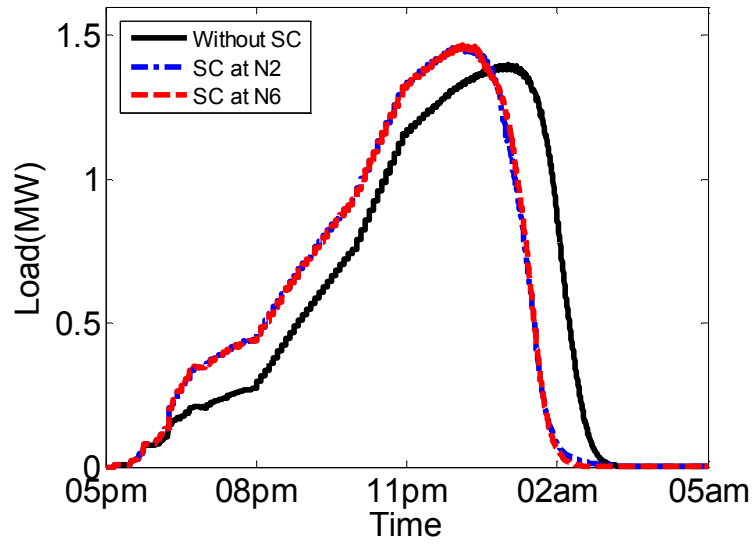


Figure 7-28 EV load comparison with and without shunt capacitors

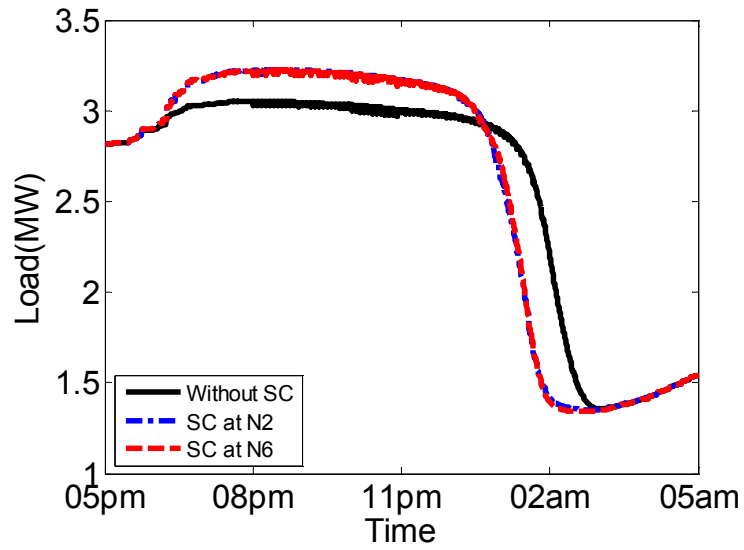


Figure 7-29 Total (EV+Non-EV) load comparison with and without shunt capacitors

Table 7-1 shows charging statistics at node-2 and node-6, both in the presence and absence of voltage control devices. The difference of charging time between POC-A & POC-B, for the base case, found to be 1 hour. In comparison to base case, voltage control devices disturbed the fairness, as mentioned earlier, but the maximum disturbance took place for the case of voltage regulator at node-2 which makes the difference between POC-A & B charging time equals to 1.5 hours which is still 50% less than the basic charging scheme. Hence, it can be inferred that voltage control devices can efficiently coordinate with the proposed charging strategy.

Table 7-1 Comparison in terms of time to full charge (in Hours) – SOC-dependent scheme with Voltage Control Devices

Case	Node-02			Node-06		
	POC A	Mean Phase c	Latest	POC B	Mean Phase c	Latest
No Voltage Control Device	5.6	6.9	9.5	4.6	5.8	8.1
Regulator at Node-2	5.9	7.1	8.9	4.3	5.4	7.3
Regulator at Node-5	4.8	6.1	8.6	5.3	5.9	7.2
Regulator at Node-6	5.0	6.1	8.6	6.5	6.4	8.5
Shunt Cap at Node-2	6.3	7.4	9.1	4.0	5.1	7.4
Shunt Cap at Node-6	5.1	6.3	8.7	4.1	5.1	7.2

CHAPTER 8

IMPLEMENTATION OF PROPOSED CHARGING

STRATEGY OVER RTDS PLATFORM

8.1 Real Time Digital Simulator (RTDS)

The RTDS solution algorithm represents power system in the basis of nodal analysis techniques. In order to calculate the instantaneous voltages at various nodes within the system, the inverse conductance matrix is multiplied by a column vector of current injections. The conductance matrix is generally a square, rather sparse matrix whose entries depend on the circuit components connected to the nodes. The ability to separate the conductance matrix into block diagonal pieces enables the simultaneous solution of the node voltages associated with each block. This so-called subsystem solution method is an important consideration in the parallel processing implemented in the RTDS. Each subsystem is simultaneously solved by different portions of the specialized hardware. The concept of mathematically isolated subsystems proved to be a significant consideration during the development of an interface to the analog simulator. [66]

The RTDS simulator is a powerful computer that accomplishes the task of real time simulation via parallel computation. Using trapezoidal integration and exploiting the delay in travelling waves on transmission lines, the system is capable of performing time domain simulation at real-time speed using time steps less than 50 micro seconds. Such

small time steps enable the RTDS to accurately and reliably simulate power system phenomena in the range of 0 to 3 kHz. [66]

8.2 RTDS Hardware

The RTDS hardware [67]–[69] is based on digital signal processor (DSP) and reduced instruction set computer (RISC) and utilizes advanced parallel processing techniques in order to achieve computational speeds required to maintain continuous real-time operation. The design is modular so that different power system sizes can be accommodated by adding units (racks) to the simulator. Each rack of hardware includes both communication and processor cards which are linked together through a common communication backplane. In case a network exceeds the capabilities of one rack it can be divided into different racks by splitting the network into subsystems and each rack then becomes responsible for the calculation of one subsystem. Racks are identical and each rack contains three distinct types of cards, namely tandem processor card (TPC), workstation interface card (WIC) and inter-rack communication card (IRC).

8.3 RTDS Software

There are several levels of software involved with the RTDS simulator. At the lower level are the component models that have been optimized for real time operation. The highest level of software is the graphical user interface (GUI) known as RSCAD which allows simulation circuits to be constructed, run, operated and results to be recorded and documented. [68], [69].

8.4 RTDS Applications

The RTDS technology combines the real-time operating properties of analogue simulators with the flexibility and accuracy of digital simulation programs. Due to this, the RTDS simulator has found widespread applications in power systems. It is currently applied to many areas of development, testing and studying of power system planning, feasibility studies, system operation and behavior, integrated protection and control, etc.

Furthermore, since the RTDS responds in real-time to events initiated through the user interface software (i.e. operator's console) it provides an excellent method for training operators and educating engineers in the principles of power system operation. In addition, because the RTDS is housed in one or more standard 19 inch cubicles, it can conveniently be taken to substation where equipment, such as protective relays, can be easily tested. [64 – 67]

8.5 System Modeling

The voltage feedback charging strategy proposed in this thesis is validated on RTDS platform to check for its applicability in real systems. Note that the available RTDS facility at KFUPM is unable to accommodate the entire detailed system and strategy models. Therefore, several simplifying assumptions had to be made. The case of same plug-in time for all EVs has been utilized.

In order to perform the simulation test runs, the original distribution system and controller structure has to go through following modifications:

1. The loads at all the nodes / buses should be modeled as unbalanced loads, however due to RTDS memory constraints only six nodes can have unbalanced loads. Node #

2, 5, 6, 7, 8 & 10 are modeled with unbalanced single phase loads as shown in Figure 8-1. The reason for selecting these nodes is that Node # 2 & 10 represent the most upstream nodes of all while Node # 5, 6, 7 & 8 represent the most downstream nodes of all. The loads at remaining nodes are modeled as shown in Figure 8-2.

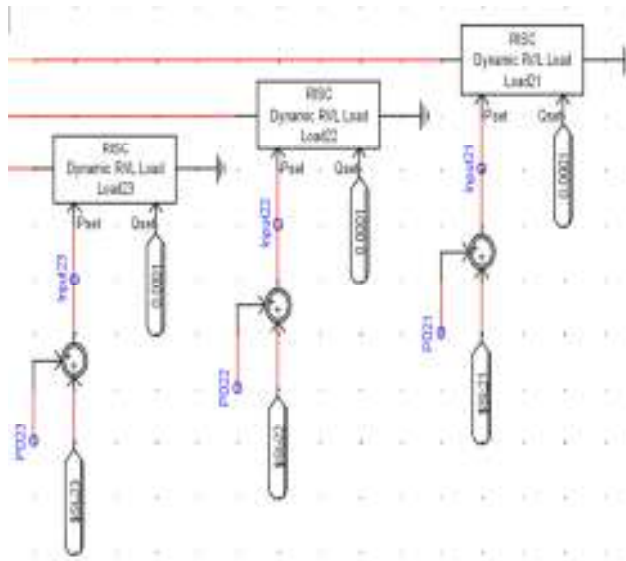


Figure 8-1 Unbalanced loads

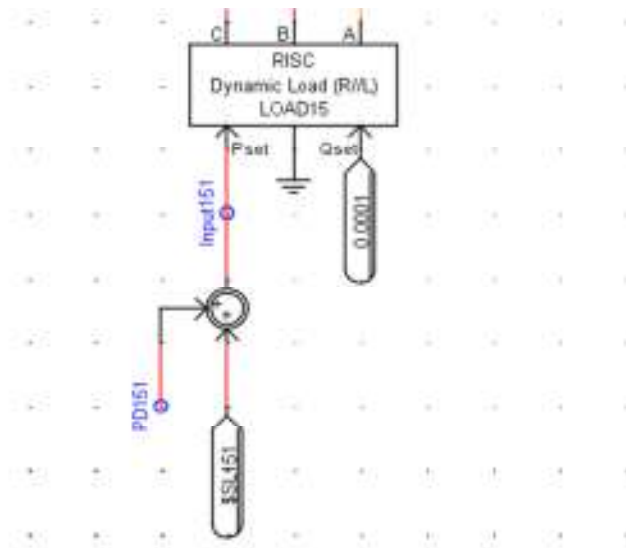


Figure 8-2 Balanced Loads

2. It was not possible in RTDS to include the proportional controller for each EV. Hence, for nodes with unbalanced loads, the ten EVs on each phase are lumped together i.e. their initial SOC's are added up and a single controller is modeled which gives the total power draw for all those EVs at that phase.
3. For nodes with balanced loads, SOC's are added together up for every ten EVs and then the resultant three lumped SOC's are averaged out. Finally a single controller is implemented which takes the average measured voltage of the three phases and correspondingly calculates power draw for ten EVs which are actually for thirty EVs due to balanced loadings.
4. In order to suppress any possible undesirable oscillations in the controller response, a rate limiter is applied to the EV power draw signal of the charge controller. The maximum rate limit is fixed at 100% of EV power draw because in RTDS every simulation run gives a transient response at the initial instant which is a very low value and then it gradually builds up to attain the actual value. This change was found to be from 0 to 100% of PD and hence RLmax fixed as 100%. Now in absence of lower limit or a very high value of lower limit of -100% causes abrupt fluctuations in power draw signal which affected the voltage profile and sometimes the voltage falls below to the setpoint. Hence, various values are tried between 1% to 100%. By trial and error 50% was found to be the maximum value at which considerable reduction in fluctuations took place. While minimum value was found to be 5% that causes much improved performance and overall flatter power draw signal for specified hour. Values are also tested below 5% but they did not show much improvement.

EVs at all nodes. Following the same algorithm, the calculated voltage references are given in Table 8-1.

Table 8-1 Voltage Set Points for Fair Charging for Phases A, B, and C - RTDS

Node	Set Point	Node	Set Point
1	---	10	0.9878,0.9881,0.9879
2	0.9912,0.9915,0.9913	11	0.9868,0.9870,0.9869
3	0.9832,0.9838,0.9834	12	0.9864,0.9866,0.9865
4	0.9830,0.9837,0.9833	13	0.9861,0.9863,0.9862
5	0.9691,0.9704,0.9697	14	0.9863,0.9866,0.9864
6	0.9668,0.9680,0.9674	15	0.9867,0.9870,0.9868
7	0.9662,0.9678,0.9672	16	0.9869,0.9871,0.9870
8	0.9659,0.9675,0.9664	17	0.9868,0.9870,0.9869
9	0.9911,0.9913,0.9912	18	0.9868,0.9870,0.9869

The simulation results obtained in this chapter clearly validate the results presented for case # 1 (Chapter-5, same plug-in time). The results shown below have shown absolutely the same trend as evident from Simulink based simulations. All the RTDS simulations are performed on hourly data from ERCOT data base.

8.6.1 Opportunistic Charging

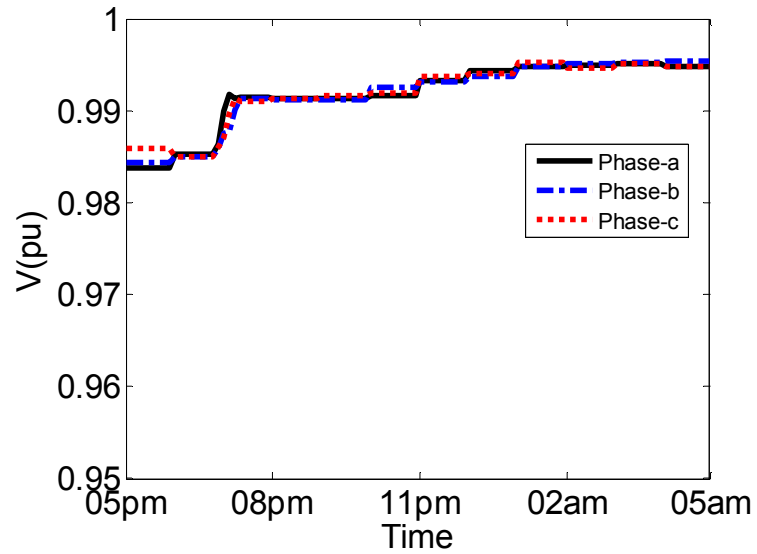


Figure 8-5 Voltage profile at node 2, using opportunistic charging

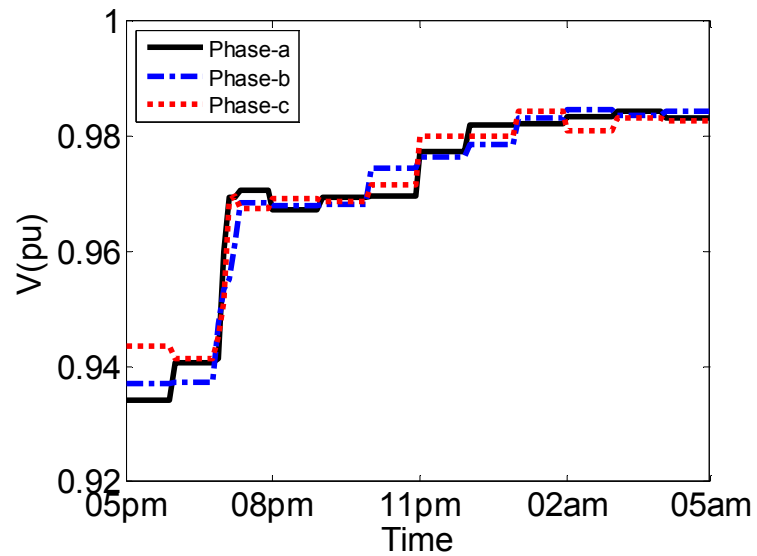


Figure 8-6 Voltage profile at node 6, using opportunistic charging

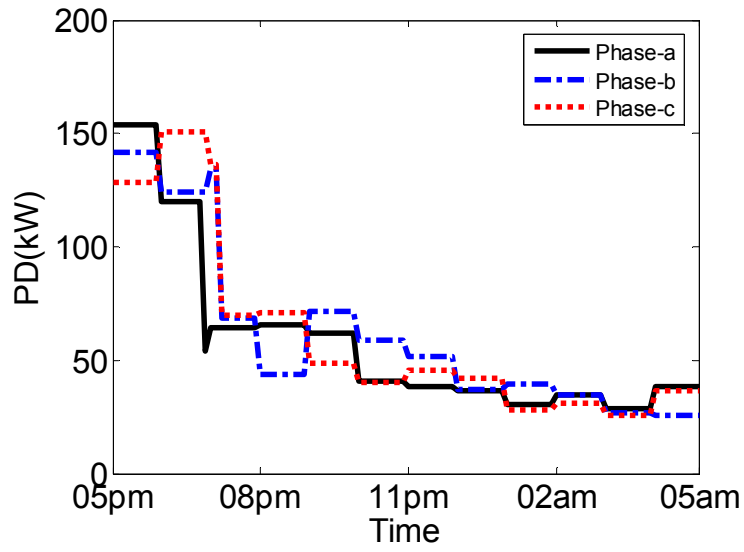


Figure 8-7 Total load at node 2, using opportunistic charging

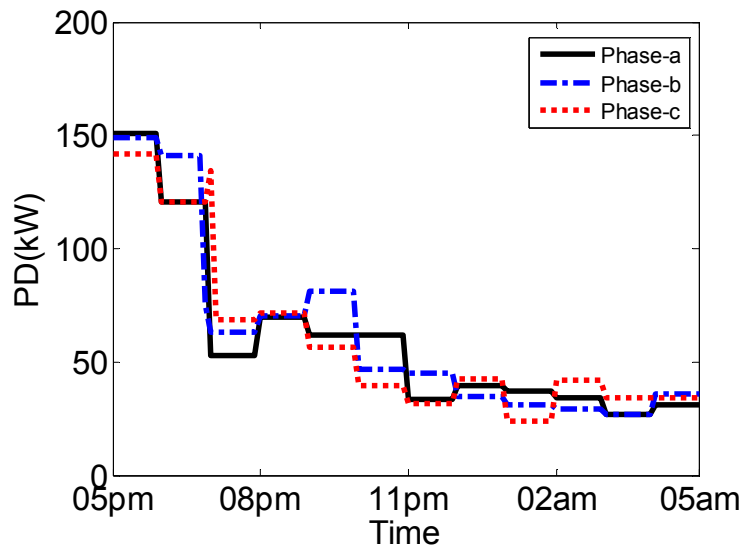


Figure 8-8 Total load at node 2, using opportunistic charging

8.6.2 Basic Proportional Charging

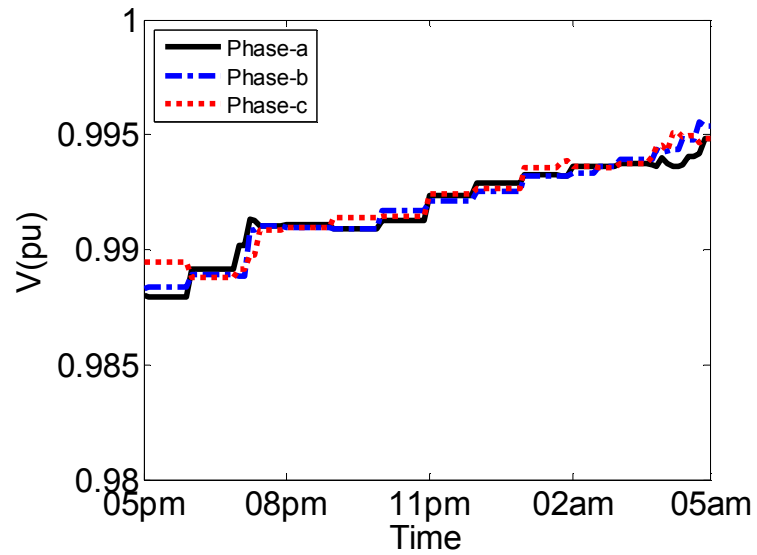


Figure 8-9 Voltage profile at node 2, using basic proportional control with flat voltage set points

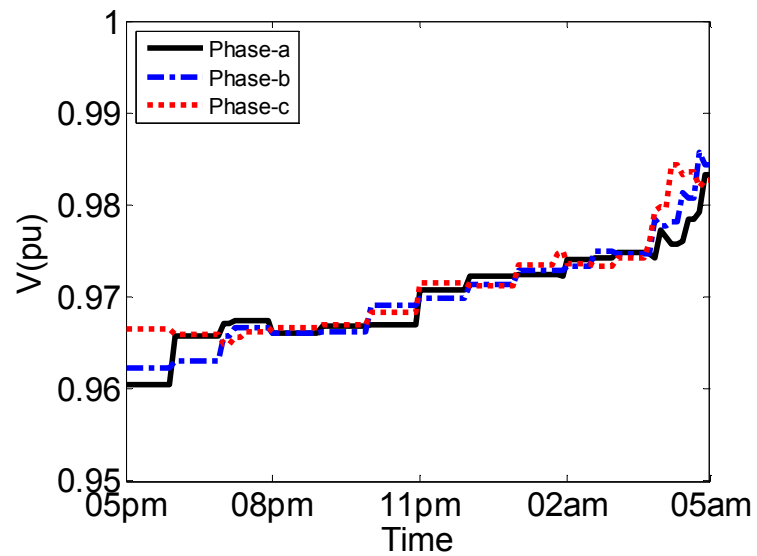


Figure 8-10 Voltage profile at node 6, using basic proportional control with flat voltage set points

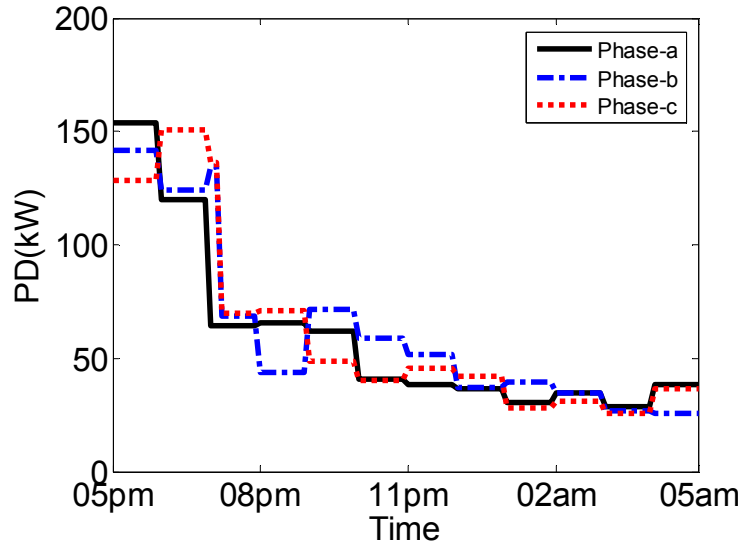


Figure 8-11 Total load at node 2, using basic proportional control with flat voltage set points

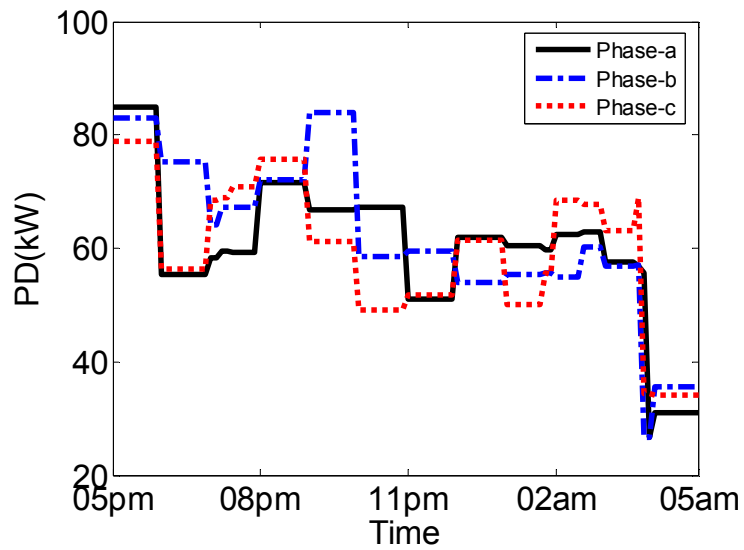


Figure 8-12 Total load at node 6, using basic proportional control with flat voltage set points

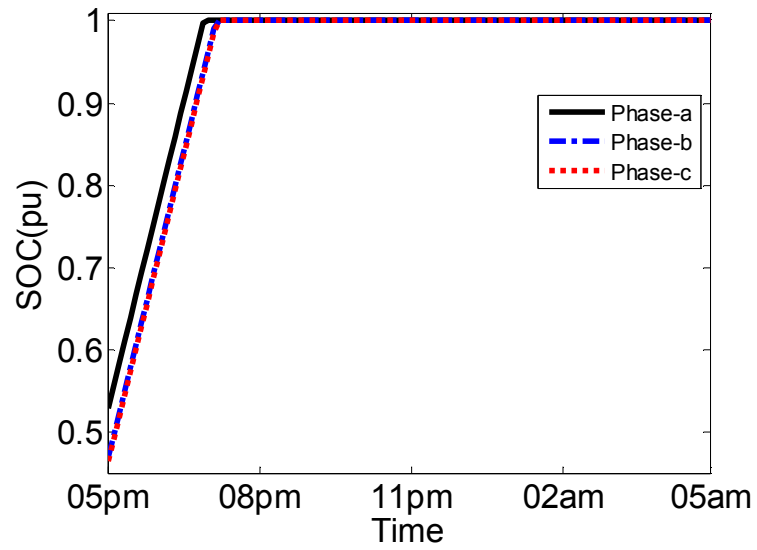


Figure 8-13 Average battery SOC at node 2, using basic proportional control with flat voltage ref

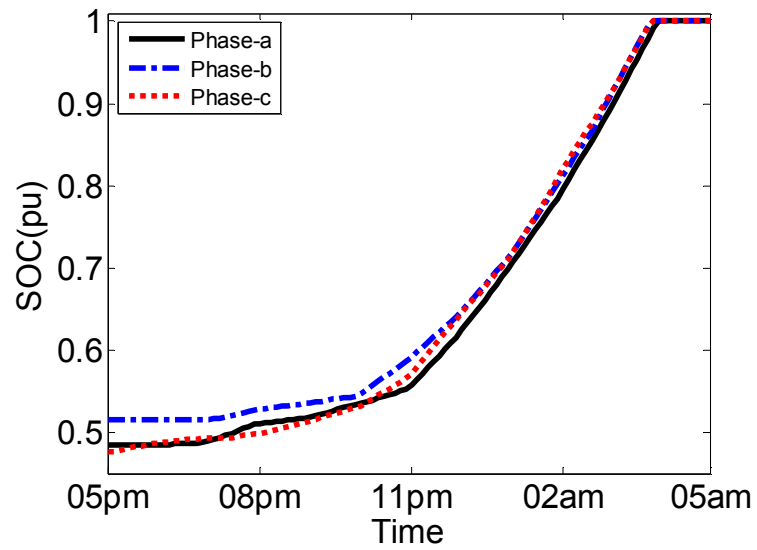


Figure 8-14 Average battery SOC at node 6, using basic proportional control with flat voltage ref

8.6.3 More Fair, SOC-dependent Charging

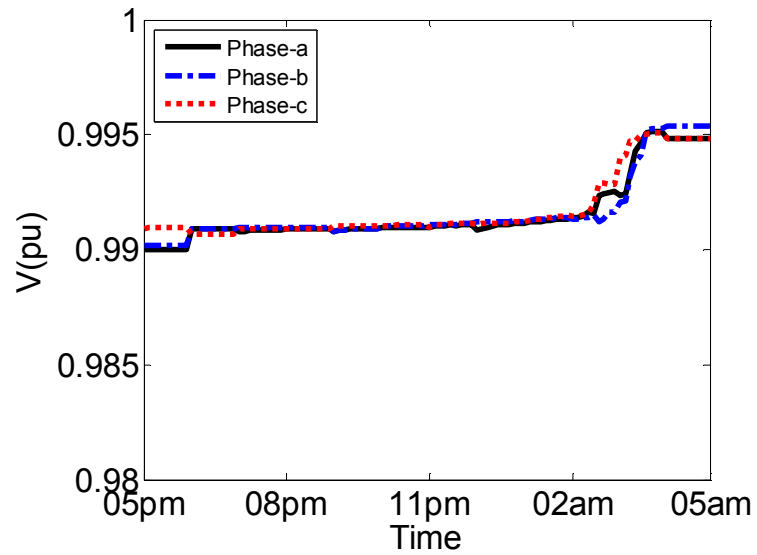


Figure 8-15 Voltage profile at node 2, using fair, SOC-dependent proportional control

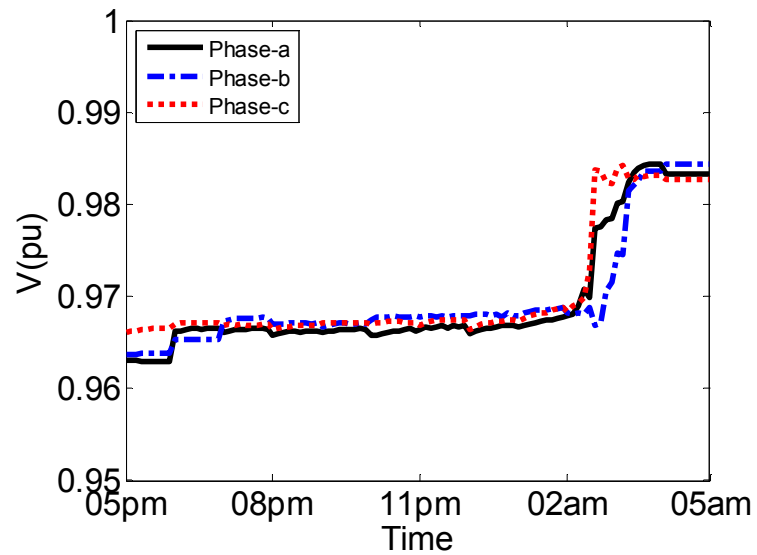


Figure 8-16 Voltage profile at node 6, using fair, SOC-dependent proportional control

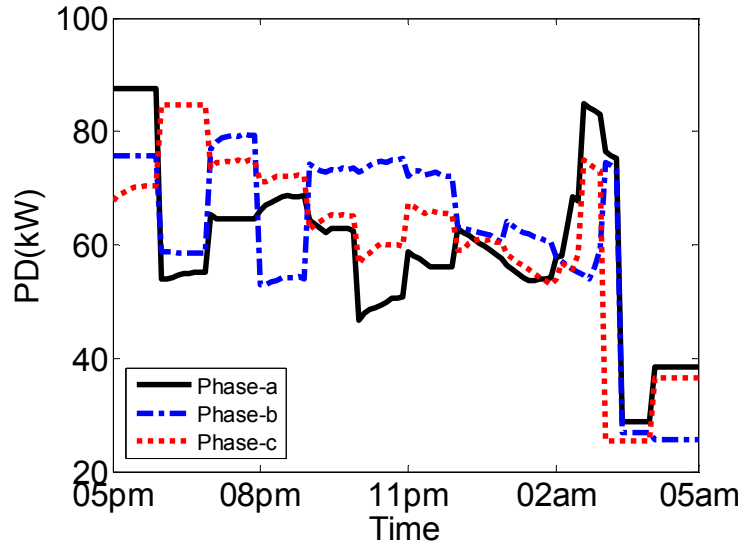


Figure 8-17 Total load at node 2 using fair, SOC-dependent proportional control

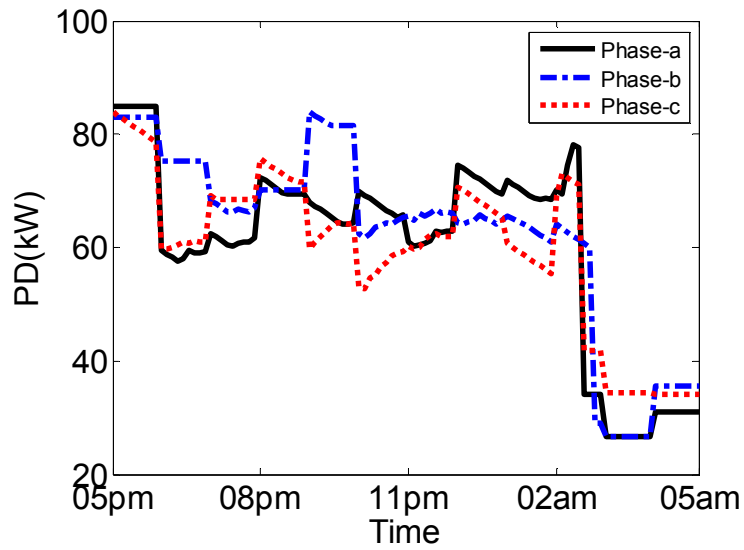


Figure 8-18 Total load at node 6 using fair, SOC-dependent proportional control

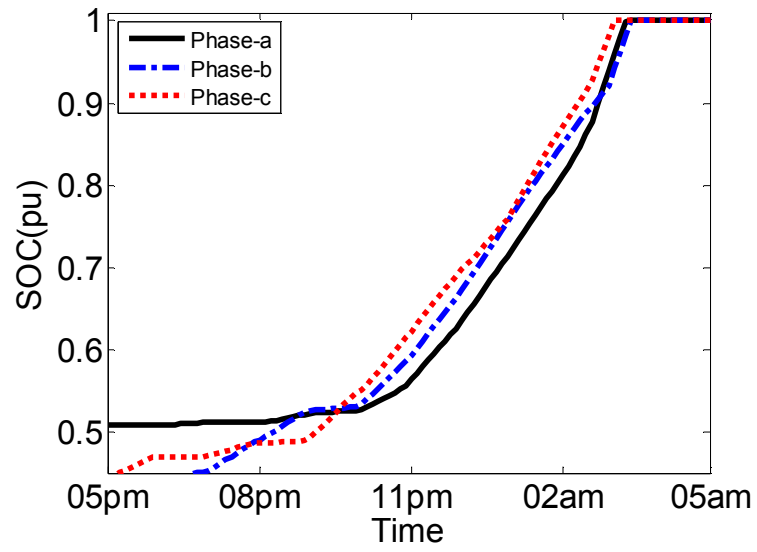


Figure 8-19 Average battery SOC at node 2, using fair, SOC-dependent proportional control

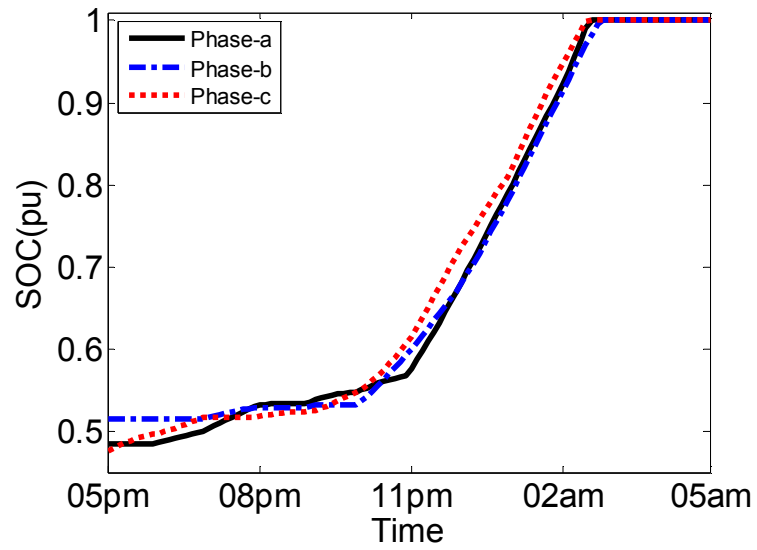


Figure 8-20 Average battery SOC at node 6, using fair, SOC-dependent proportional control

Table 8-2 Comparison in terms of average time to full charge

Control Scheme	Average time at Node 2 (hr)			Average time at Node 6 (hr)			Difference between earliest and latest (hr)
	Phase a	Phase b	Phase c	Phase a	Phase b	Phase c	
Flat V_{ref}	2.1	2.3	2.3	11	10.9	10.9	8.9
SOC-dependent	10.4	10.4	10.1	9.7	9.9	9.7	0.7

Figure 8-5 to Figure 8-20 have same trend and implications as already discussed in Simulink based simulations in Chapter-5. These results again prove that the proposed strategy has advantages of maintaining a flatter voltage profile along with ensuring fairness of charging among EVs connected to upstream nodes and those connected to downstream nodes.

Figure 8-21 and Figure 8-22 show that limiting the drop in power draw to 5% actually results in a flatter load profile and also charges the EVs more quickly as compare to 50%. The reduction in rate limit also attains a more stable voltage profile at the nodes which helps to stabilize the system.

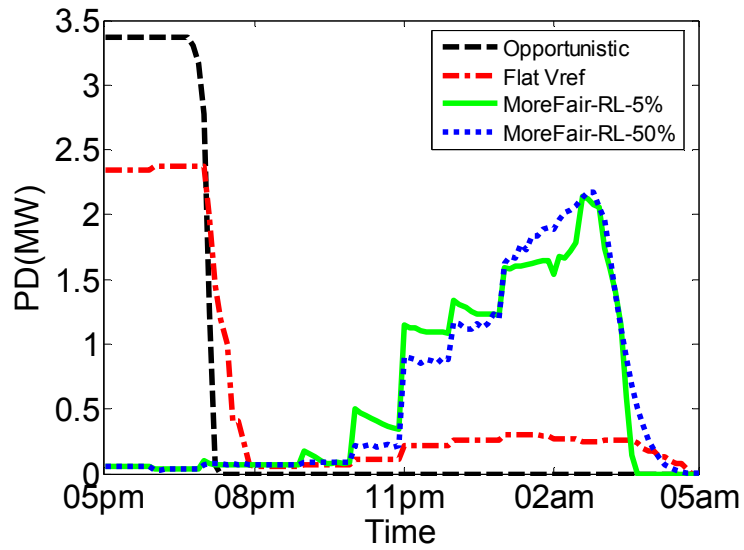


Figure 8-21 Aggregate EV charging load for the distribution system

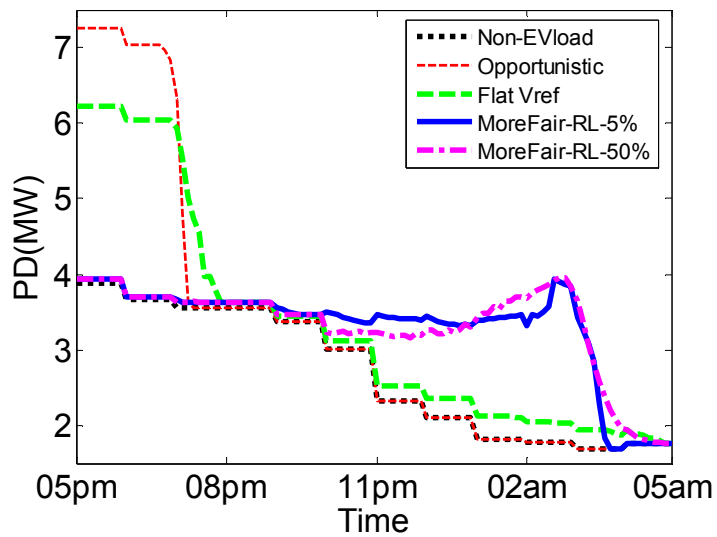


Figure 8-22 Total load (EV + non-EV) for the distribution system

CHAPTER 9

PROGRAM TO INCENTIVIZE EV OWNER

As far as the simulation results are concerned, the proposed EV charging strategy has proved to be beneficial to support the utility company in terms of voltage support, flattening load profile and charging the EVs in the allotted time window of 12 hours. This charging strategy focuses those electric vehicles which are charged at homes. These electric vehicles are available for more time as compared to the EVs which needs charging during travelling.

However, for the charging strategy proposed in this thesis, the EV owners usually have no such urgency, except for those who have low preferred ECT. The EV owners who reach their home after work will park their EVs in their garage and then most expectedly, they will re-drive them till the next morning. Thus, if an EV is idle for such long time interval of almost 12 hours then why the owner should pay the charges to charge it faster. Hence, this scheme seems to be very practical and friendly from both EV owner and distribution company. Moreover, this scheme is “aggregator-less” EV owner is directly associated with the distribution company, to make this scheme favorable and appreciable among EV owners certain basic incentives can be implemented.

The distribution company can incentivize the EV owners for their active participation in this program as this will lead to a more stable and more efficient distribution system. It is quite evident that distribution system has no obligations to promote the use of EVs but

incentivizing the EV owners will consequently lead to a well maintained distribution system.

The main focus of the distribution company is to maintain the nodal voltage profiles and equipment loading levels within permissible. Thus this work has devised an incentivizing scheme based on the impact of EV charging over overall voltage profile. Here again two extreme cases are considered; the most upstream node (Node # 2) and one of the most downstream nodes (Node # 6).

The system is tested by providing all EVs a fixed ECT and hence a value of minimum PD based on the rule defined in Section 4.5 (Equation 3 and 4). The system is tested with three different ECTs between 3 and 7 hours. The idea is to investigate how the ECT preference will affect the system's voltage profile. This analysis will be utilized to decide how the tariff will be altered to incentivize those owners which are utilizing ECT that is favorable to the system's voltage profile. Here, it is worth mentioning that TOU has already been incorporated in randomizing the EV plug-in time.

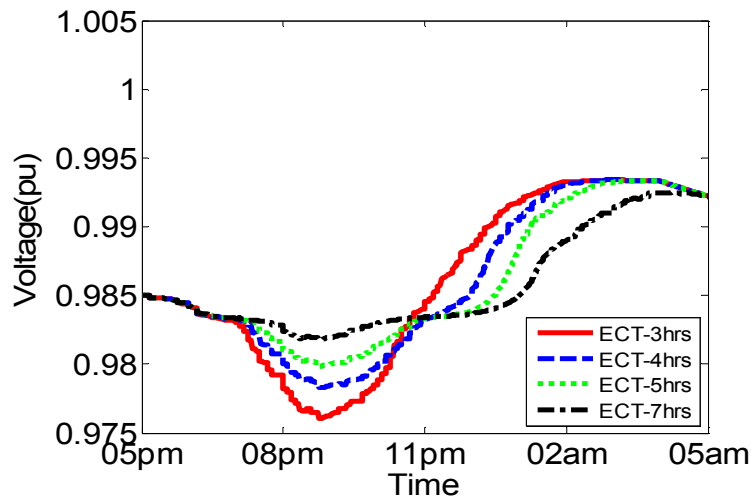


Figure 9-1 Voltages at Node-2 Phase-b for different ECT levels for all EVs

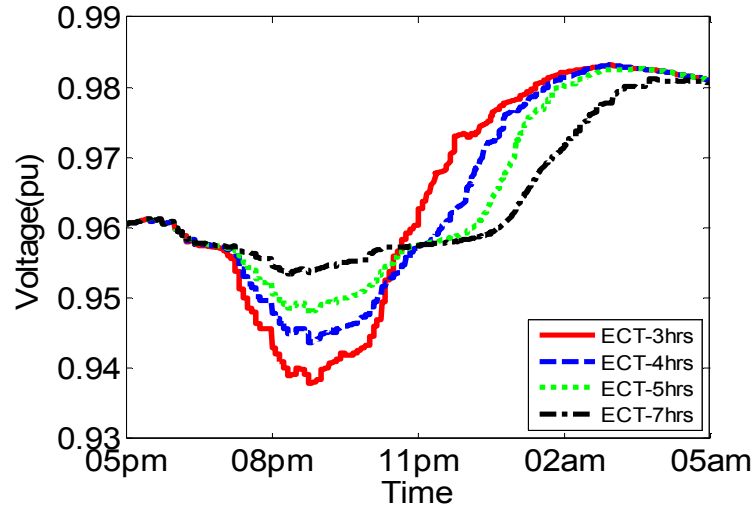


Figure 9-2 Voltages at Node-6 Phase-b for different ECT levels for all EVs

Figure 9-1 and Figure 9-2 show that the 5 hours is the minimum ECT at which the EV charging is still maintaining voltage lower permissible limit of 0.95 pu. By making use of the Table 5-4, the maximum ECT level is selected as 7 hours, as the average charging time is around 6 hours. And results related to 7 hours show that the voltage profile is well above the minimum level.

On the basis of these results and analysis, a generalized incentive plan is proposed as follows:

1. EVs with no preference will be given a 50% discount of the actual energy price.
2. EVs with preferred ECT of 7 hours will be given a 40% discount of the actual energy price.
3. EVs with preferred ECT of between 6 and 7 hours will be given a 30% discount of the actual energy price.
4. EVs with preferred ECT of between 5 and 6 hours will be given a 20% discount of the actual energy price.

5. EVs with preferred ECT below 5 hours will be charged actual energy price.

On the basis of the above mentioned incentive plan, an analysis was carried out to determine the income of the distribution system operator. The analysis carried out on node # 2 for total load i.e. both EV load and Non-EV load. This analysis took into consideration the TOU tariff from 7pm to 7am. The tariff was taken as 12.551 cents/kWh between 7am to 7pm and 10.830 cents/kWh between 7pm to 7am [70]. The total income for whole day, from node # 2, with and without discount, is found to be \$219,150 and \$240,000 respectively. It shows that by giving a 50% discount to EV owners, the decrease in the income is approximately 7%.

The actual amount of discount is not such straight forward but still it serves as a first step to begin with. Actually, the discount can be based upon several important factors such as scheduled maintenance cost of the system, cost of the voltage control devices, cost of the breakdown maintenance etc.

CHAPTER 10

CONCLUSION AND RECOMMENDATIONS

This thesis has proposed an effective, autonomous, voltage-based control scheme for charging electric vehicles. This control scheme, though requires no real-time communication, effectively coordinates charging among the EVs connected to the distribution nodes in a fair manner so that voltage violations are avoided. The new scheme also results in a flattened EV charging profile. In addition to the local voltage level, the proposed scheme takes into account the battery SOC and the EV owner's preference (if any) of end-of-charge time. The proposed scheme is tested for different contingencies that expected to occur, and the simulation results proved its robustness and stability. It is also noteworthy that this scheme efficiently coordinates with the voltage control devices and maintains the basic purpose of avoiding voltage violations and flat load profile along with fairness among EVs. The proposed scheme is validated through RTDS platform which makes it more reliable and favorable for real time implementation.

As it is evident that the proposed control strategy is robust and efficient to serve the specified purpose, there are two additional aspects that can serve as future research work in its continuation.

1. The existing strategy deals with uni-directional power flow from grid to EV. It can be extended to implement bi-directional V2G by allowing PD to be negative when measured voltage falls below the reference value contrary to the existing case when PD becomes zero when measured voltage is less than reference voltage.
2. The same strategy can be tested and modified, if needed, for a distribution system containing distributed generators.

References

- [1] “Navigant Research, ‘Electric Vehicle Market Forecasts’ 2013.”[Online]. Available: <http://www.navigantresearch.com/research/electric-vehicle-market-forecasts>. [Accessed: 08-Sep-2013].
- [2] S. W. Hadley and A. A. Tsvetkova, “Potential Impacts of Plug-in Hybrid Electric Vehicles on Regional Power Generation,” *Electr. J.*, vol. 22, no. 10, pp. 56–68, Dec. 2009.
- [3] W. Su, H. Eichi, W. Zeng, and M.-Y. Chow, “A Survey on the Electrification of Transportation in a Smart Grid Environment,” *IEEE Trans. Ind. Informatics*, vol. 8, no. 1, pp. 1–10, Feb. 2012.
- [4] J. A. P. Lopes, F. J. Soares, and P. M. R. Almeida, “Integration of Electric Vehicles in the Electric Power System,” *Proc. IEEE*, vol. 99, no. 1, pp. 168–183, Jan. 2011.
- [5] K. J. Dyke, N. Schofield, and M. Barnes, “The Impact of Transport Electrification on Electrical Networks,” *IEEE Trans. Ind. Electron.*, vol. 57, no. 12, pp. 3917–3926, Dec. 2010.
- [6] S. Blumsack, C. Samaras, and P. Hines, “Long-term electric system investments to support Plug-in Hybrid Electric Vehicles,” in *2008 IEEE Power and Energy Society General Meeting - Conversion and Delivery of Electrical Energy in the 21st Century*, 2008, pp. 1–6.
- [7] D. Wu and D. C. Aliprantis, “Potential impacts of aggregator-controlled plug-in electric vehicles on distribution systems,” in *2011 4th IEEE International Workshop on Computational Advances in Multi-Sensor Adaptive Processing (CAMSAP)*, 2011, pp. 105–108.
- [8] V. Tikka, J. Lassila, J. Haakana, and J. Partanen, “Case study of the effects of electric vehicle charging on grid loads in an urban area,” in *2011 2nd IEEE PES International Conference and Exhibition on Innovative Smart Grid Technologies*, 2011, pp. 1–7.
- [9] H. Turker, S. Bacha, D. Chatroux, and A. Hably, “Low-Voltage Transformer Loss-of-Life Assessments for a High Penetration of Plug-In Hybrid Electric Vehicles (PHEVs),” *IEEE Trans. Power Deliv.*, vol. 27, no. 3, pp. 1323–1331, Jul. 2012.
- [10] K. Schneider, C. Gerkenmeyer, M. Kintner-Meyer, and R. Fletcher, “Impact assessment of plug-in hybrid vehicles on pacific northwest distribution systems,”

in *2008 IEEE Power and Energy Society General Meeting - Conversion and Delivery of Electrical Energy in the 21st Century*, 2008, pp. 1–6.

- [11] C. Roe, J. Meisel, A. P. Meliopoulos, F. Evangelos, and T. Overbye, “Power System Level Impacts of PHEVs,” in *2009 42nd Hawaii International Conference on System Sciences*, 2009, pp. 1–10.
- [12] L. Pieltain Fernandez, T. Gomez San Roman, R. Cossent, C. Mateo Domingo, and P. Frias, “Assessment of the Impact of Plug-in Electric Vehicles on Distribution Networks,” *IEEE Trans. Power Syst.*, vol. 26, no. 1, pp. 206–213, Feb. 2011.
- [13] K. Clement-Nyns, E. Haesen, and J. Driesen, “The Impact of Charging Plug-In Hybrid Electric Vehicles on a Residential Distribution Grid,” *IEEE Trans. Power Syst.*, vol. 25, no. 1, pp. 371–380, Feb. 2010.
- [14] K. Clement, E. Haesen, and J. Driesen, “Coordinated charging of multiple plug-in hybrid electric vehicles in residential distribution grids,” in *2009 IEEE/PES Power Systems Conference and Exposition*, 2009, pp. 1–7.
- [15] M. A. S. Masoum, P. S. Moses, and S. Hajforoosh, “Distribution transformer stress in smart grid with coordinated charging of Plug-In Electric Vehicles,” in *2012 IEEE PES Innovative Smart Grid Technologies (ISGT)*, 2012, pp. 1–8.
- [16] P. Zhang, K. Qian, C. Zhou, B. G. Stewart, and D. M. Hepburn, “A Methodology for Optimization of Power Systems Demand Due to Electric Vehicle Charging Load,” *IEEE Trans. Power Syst.*, vol. 27, no. 3, pp. 1628–1636, Aug. 2012.
- [17] E. Sortomme, M. M. Hindi, S. D. J. MacPherson, and S. S. Venkata, “Coordinated Charging of Plug-In Hybrid Electric Vehicles to Minimize Distribution System Losses,” *IEEE Trans. Smart Grid*, vol. 2, no. 1, pp. 198–205, Mar. 2011.
- [18] D. Wu, D. C. Aliprantis, and L. Ying, “Load Scheduling and Dispatch for Aggregators of Plug-In Electric Vehicles,” *IEEE Trans. Smart Grid*, vol. 3, no. 1, pp. 368–376, Mar. 2012.
- [19] D. Steen, L. A. Tuan, O. Carlson, and L. Bertling, “Assessment of Electric Vehicle Charging Scenarios Based on Demographical Data,” *IEEE Trans. Smart Grid*, vol. 3, no. 3, pp. 1457–1468, Sep. 2012.
- [20] M. Gharbaoui, L. Valcarenghi, R. Bruno, B. Martini, M. Conti, and P. Castoldi, “An advanced smart management system for electric vehicle recharge,” in *2012 IEEE International Electric Vehicle Conference*, 2012, pp. 1–8.
- [21] M. Erol-Kantarci and H. T. Mouftah, “Supply and load management for the smart distribution grid using wireless networks,” in *2012 Japan-Egypt Conference on Electronics, Communications and Computers*, 2012, pp. 145–150.

- [22] M. Erol-Kantarci, J. H. Sarker, and H. T. Mouftah, "Communication-based Plug-In Hybrid Electrical Vehicle load management in the smart grid," in *2011 IEEE Symposium on Computers and Communications (ISCC)*, 2011, pp. 404–409.
- [23] M. Erol-Kantarci, J. H. Sarker, and H. T. Mouftah, "Quality of service in Plug-in Electric Vehicle charging infrastructure," in *2012 IEEE International Electric Vehicle Conference*, 2012, pp. 1–5.
- [24] W. Kempton and J. Tomić, "Vehicle-to-grid power implementation: From stabilizing the grid to supporting large-scale renewable energy," *J. Power Sources*, vol. 144, no. 1, pp. 280–294, Jun. 2005.
- [25] W. Kempton and J. Tomić, "Vehicle-to-grid power fundamentals: Calculating capacity and net revenue," *J. Power Sources*, vol. 144, no. 1, pp. 268–279, Jun. 2005.
- [26] J. Tomić and W. Kempton, "Using fleets of electric-drive vehicles for grid support," *J. Power Sources*, vol. 168, no. 2, pp. 459–468, Jun. 2007.
- [27] C. Guille and G. Gross, "A conceptual framework for the vehicle-to-grid (V2G) implementation," *Energy Policy*, vol. 37, no. 11, pp. 4379–4390, Nov. 2009.
- [28] C. Quinn, D. Zimmerle, and T. H. Bradley, "The effect of communication architecture on the availability, reliability, and economics of plug-in hybrid electric vehicle-to-grid ancillary services," *J. Power Sources*, vol. 195, no. 5, pp. 1500–1509, Mar. 2010.
- [29] A. Brooks, E. Lu, D. Reicher, C. Spirakis, and B. Wehl, "Demand Dispatch," *IEEE Power Energy Mag.*, vol. 8, no. 3, pp. 20–29, May 2010.
- [30] A. N. Brooks, "Vehicle-to-Grid Demonstration Project: Grid Regulation Ancillary Service with a Battery Electric Vehicle," 2002.
- [31] W. Kempton, V. Udo, K. Huber, K. Komara, S. Letendre, S. Baker, D. Brunner, and N. Pearre, "A Test of Vehicle-to-Grid (V2G) for Energy Storage and Frequency Regulation in the PJM System," 2009.
- [32] Y. Ota, H. Taniguchi, T. Nakajima, K. M. Liyanage, K. Shimizu, T. Masuta, J. Baba, and A. Yokoyama, "Autonomous Distributed Vehicle-to-Grid for Ubiquitous Power Grid and its Effect as a Spinning Reserve," *J. Int. Counc. Electr. Eng.*, vol. 1, no. 2, pp. 214–221, Apr. 2011.
- [33] J. R. Pillai and B. Bak-Jensen, "Integration of Vehicle-to-Grid in the Western Danish Power System," *IEEE Trans. Sustain. Energy*, vol. 2, no. 1, pp. 12–19, Jan. 2010.

- [34] Y. Hanai, K. Yoshimura, J. Matsuki, and Y. Hayashi, "Load Management using Heat-Pump Water Heater and Electric Vehicle Battery Charger in Distribution System with PV," *J. Int. Counc. Electr. Eng.*, vol. 1, no. 2, pp. 207–213, Apr. 2011.
- [35] K. Sezaki, "Development of an Optimal Vehicle-to-Grid Aggregator for Frequency Regulation," *IEEE Trans. Smart Grid*, vol. 1, no. 1, pp. 65–72, Jun. 2010.
- [36] N. Rotering and M. Ilic, "Optimal Charge Control of Plug-In Hybrid Electric Vehicles in Deregulated Electricity Markets," *IEEE Trans. Power Syst.*, vol. 26, no. 3, pp. 1021–1029, Aug. 2011.
- [37] E. Sortomme and M. A. El-Sharkawi, "Optimal Scheduling of Vehicle-to-Grid Energy and Ancillary Services," *IEEE Trans. Smart Grid*, vol. 3, no. 1, pp. 351–359, Mar. 2012.
- [38] Z. Ma, D. S. Callaway, and I. A. Hiskens, "Decentralized Charging Control of Large Populations of Plug-in Electric Vehicles," *IEEE Trans. Control Syst. Technol.*, vol. 21, no. 1, pp. 67–78, Jan. 2013.
- [39] Changsun Ahn, Chiao-Ting Li, and Huei Peng, "Decentralized charging algorithm for electrified vehicles connected to smart grid." pp. 3924–3929, 2011.
- [40] L. Gan, U. Topcu, and S. Low, "Optimal decentralized protocol for electric vehicle charging," in *IEEE Conference on Decision and Control and European Control Conference*, 2011, pp. 5798–5804.
- [41] W. Su and M.-Y. Chow, "Computational intelligence-based energy management for a large-scale PHEV/PEV enabled municipal parking deck," *Appl. Energy*, vol. 96, no. null, pp. 171–182, Aug. 2012.
- [42] T. Logenthiran and D. Srinivasan, "Multi-agent system for managing a power distribution system with Plug-in Hybrid Electrical vehicles in smart grid," in *ISGT2011-India*, 2011, pp. 346–351.
- [43] Changsun Ahn, Chiao-Ting Li, and Huei Peng, "Decentralized charging algorithm for electrified vehicles connected to smart grid." pp. 3924–3929, 2011.
- [44] H. Turker, A. Hably, S. Bacha, and D. Chatroux, "Rule based algorithm for Plug-in Hybrid Electric Vehicles (PHEVs) integration in residential electric grid areas," in *2012 IEEE PES Innovative Smart Grid Technologies (ISGT)*, 2012, pp. 1–7.
- [45] M. Singh, P. Kumar, and I. Kar, "Implementation of Vehicle to Grid Infrastructure Using Fuzzy Logic Controller," *IEEE Trans. Smart Grid*, vol. 3, no. 1, pp. 565–577, Mar. 2012.

- [46] J. A. Peças Lopes, S. A. Polenz, C. L. Moreira, and R. Cherkaoui, "Identification of control and management strategies for LV unbalanced microgrids with plugged-in electric vehicles," *Electr. Power Syst. Res.*, vol. 80, no. 8, pp. 898–906, Aug. 2010.
- [47] Y. Ota, H. Taniguchi, T. Nakajima, K. M. Liyanage, J. Baba, and A. Yokoyama, "Autonomous Distributed V2G (Vehicle-to-Grid) Satisfying Scheduled Charging," *IEEE Trans. Smart Grid*, vol. 3, no. 1, pp. 559–564, Mar. 2012.
- [48] A. Arancibia and K. Strunz, "Autonomous control of electric vehicles in grid-connected and islanded modes," in *2012 3rd IEEE PES Innovative Smart Grid Technologies Europe (ISGT Europe)*, 2012, pp. 1–7.
- [49] P. Richardson, D. Flynn, and A. Keane, "Local Versus Centralized Charging Strategies for Electric Vehicles in Low Voltage Distribution Systems," *IEEE Trans. Smart Grid*, vol. 3, no. 2, pp. 1020–1028, Jun. 2012.
- [50] A. T. Al-Awami and E. Sortomme, "Electric vehicle charging modulation using voltage feedback control," in *2013 IEEE Power & Energy Society General Meeting*, 2013, pp. 1–5.
- [51] J. T. Salihi, "Energy Requirements for Electric Cars and Their Impact on Electric Power Generation and Distribution Systems," *IEEE Trans. Ind. Appl.*, vol. IA-9, no. 5, pp. 516–532, Sep. 1973.
- [52] D. Okwii, "Smart Grid: How it can help improve on power distribution and utility consumption," *28th March*, 2013. [Online]. Available: <http://www.techpost.ug/1966/smart-grid-how-it-can-help-improve-on-power-distribution-and-utility-consumption/>. [Accessed: 05-May-2013].
- [53] "Electric Drive Transportation Association, 'Electric drive vehicle sales figures (U.S. Market)' 2013." [Online]. Available: <http://www.electricdrive.org/index.php?ht=d/sp/i/20952/pid/20952>.
- [54] "Global EV Outlook - Understanding the Electric Vehicle Landscape to 2020." [Online]. Available: http://www.iea.org/topics/transport/electricvehiclesinitiative/EVI_GEO_2013_Full_Report.pdf.
- [55] E. Sortomme, A. I. Negash, S. S. Venkata, and D. S. Kirschen, "Multistate voltage dependent load model of a charging electric vehicle," in *2012 IEEE Transportation Electrification Conference and Expo (ITEC)*, 2012, pp. 1–5.
- [56] A. Visioli, *Practical PID Control*. London, U.K: Springer-Verlag, 2006.

- [57] Cooper Industries, *Cooper Power Systems, Ed. 3, Electrical Distribution-System Protection.*, Third. Cooper Power Systems, 1990.
- [58] E. Sortomme, M. Venkata, and J. Mitra, “Microgrid protection using communication-assisted digital relays,” in *IEEE PES General Meeting*, 2010, pp. 1–1.
- [59] M. A. Zamani, A. Yazdani, and T. S. Sidhu, “A Communication-Assisted Protection Strategy for Inverter-Based Medium-Voltage Microgrids,” *IEEE Trans. Smart Grid*, vol. 3, no. 4, pp. 2088–2099, Dec. 2012.
- [60] “Electric Reliability Council of Texas, ‘Load Profiling,’ August 2010, [Online]. <http://www.ercot.com/mktinfo/loadprofile/> [Accessed: Aug. 20, 2010].”[Online]. Available: <http://www.ercot.com/mktinfo/loadprofile/>.
- [61] William H. Kersting, *Distribution System Modeling and Analysis*, Second Edi. CRC Press, 2007.
- [62] F. Lambert, “Secondary Distribution Impacts of Residential Electric Vehicle Charging,” 2000.
- [63] “Nissan USA, ‘2013 Nissan LEAF® Electric Car Specifications,’ 2013, [Online].,” 2013. [Online]. Available: <http://www.nissanusa.com/electric-cars/leaf/versions-specs/>. [Accessed: 05-May-2013].
- [64] “Step Voltage Regulator Utility,” 2011. [Online]. Available: <http://www.powerqualityworld.com/2011/04/step-voltage-regulator-utility.html>.
- [65] F. A. VIAWAN, “Voltage Control and Voltage Stability of Power Distribution Systems in the Presence of Distributed Generation,” Chalmers University of Technology, 2008.
- [66] J. Ostergaard and F. Mara, “A real-time simulation platform for power system operation,” in *2010 Conference Proceedings IPEC*, 2010, pp. 909–914.
- [67] R. Kuffel, J. Giesbrecht, T. Maguire, R. P. Wierckx, and P. McLaren, “RTDS-a fully digital power system simulator operating in real time,” in *IEEE WESCANEX 95. Communications, Power, and Computing. Conference Proceedings*, 1995, vol. 2, pp. 300–305.
- [68] A. Saran, S. K. Palla, A. K. Srivastava, and N. N. Schulz, “Real time power system simulation using RTDS and NI PXI,” in *2008 40th North American Power Symposium*, 2008, pp. 1–6.

- [69] C. A. Apostolopoulos and G. N. Korres, "Real-time implementation of digital relay models using MATLAB/SIMULINK and RTDS," *Eur. Trans. Electr. Power*, vol. 20, no. 3, pp. 290–305, Apr. 2010.
- [70] "Time-of-Use Rates for Residential Customers," 2013. [Online]. Available: <https://www.pplelectric.com/at-your-service/electric-rates-and-rules/time-of-use-option/rs-time-of-use-option.aspx>. [Accessed: 15-Dec-2013].

Vitae

Name: Ghous Muhammad Asim Akhtar

Date of Birth: December 15, 1986

Nationality: Pakistani

Present Address: P. O. Box 8601, King Fahd University of Petroleum & Minerals, Dhahran 31261, Saudi Arabia

Permanent Address: House # LS-6, ST-11, Sector # 8, North Karachi, Karachi, Pakistan

Email: asim.akhtar@live.com

Educational Qualification:

M.S. (Electrical Engineering)

November, 2013

King Fahd University of Petroleum & Minerals

Dhahran, Saudi Arabia

B.E. (Electrical Engineering)

November, 2008

NED University of Engineering & Technology

Karachi, Pakistan

Publications:

- G.M. Asim Akhtar and Ali T. Al-Awami, “Emission-Aware Energy Trading by Coordinating Wind and Thermal Power Generation,” in Power Engineering, Energy and Electrical Drives (POWERENG), 2013 Fourth International Conference, Istanbul, Turkey, 13-17 May, 2013.
- G.M. Asim Akhtar, Ali T. Al-Awami and M. Waqas Khalid “Coordinating Emission-Aware Energy Trading with V2G (Vehicle-to-Grid) Services,” in IEEE Eurocon, Zagreb, Croatia, 1-4 July, 2013.
- G.M. Asim Akhtar, Ali T. Al-Awami, Eric Sortomme, M.A. Abido and M. Waqar Ahmed, ”Autonomous Electric vehicle Charging Management over Real Time Digital Simulator”, submitted to IEEE General Meeting of Power & Energy Society, 2014.
- Ali T. Al-Awami, Eric Sortomme and G.M. Asim Akhtar, “Electric Vehicle Charging Management using Voltage Feedback Control”, third manuscript submitted to IEEE Transactions in Power Systems.